Abteilung für Experimentelle Neurologie an der Klinik für Neurologie
der Medizinischen Fakultät Charité – Universitätsmedizin Berlin

DISSERTATION

ESSENTIAL ROLE OF ACTIN FILAMENT DYNAMICS IN MICROGLIA ACTIVATION

zur Erlangung des akademischen Grades
Doctor of Philosophy (PhD)
im Rahmen des
International Graduate Program Medical Neurosciences

vorgelegt der Medizinischen Fakultät
Charité – Universitätsmedizin Berlin

von

Diplom-Biologin Ria Uhlemann

aus Mittweida, Deutschland

Datum der Promotion: 27.02.2015

TABLE OF CONTENTS

INDEX OF FIGURES

ABBREVIATIONS

ABP	Actin binding protein
AD	Alzheimer's disease
ADF	Actin depolymerizing factor
ADP	Adenosindiphosphate
ARP	Actin-Related Protein
ATP	Adenosintriphosphate
Aβ, oAβ	Amyloid β, oligomeric Aβ
BBB	Blood brain barrier
CFL	Cofilin
CFSE	Carboxyfluorescein succinimidyl ester
CNS	Central nervous system
CSF	Colony stimulating factor
DAMP	Damage-associated molecular patterns
DAPI	4',6-diamidino-2-phenylindole
DMEM	Dulbecco's Modified Eagle's Medium
dpm	Disintegrations per minute
F-actin	Filamentous actin
FCS	Fetal calf serum
FITC	Fluorescein isothiocyanate
G-actin	Globular actin
GAPDH	Glycerinaldehyd-3-phosphat-dehydrogenase
Gsn	Gelsolin
IBA1	Ionized calcium binding adaptor molecule 1
IGF-1	Insulin growth factor
IL	Interleukin
iNOS	Inducible nitric oxide synthase
kDa	Kilodalton
LDH	Lactate dehydrogenase
LPS	Lipopolysaccharide
MCAo	Middle cerebral artery occlusion

mRNA	Messenger RNA
MTT	3-[4,5-dimethylthiazol-2-yl]-2,5 diphenyl tetrazolium bromide
NADH	Nicotinamide adenine dinucleotid
NMDA	N-Methyl-D-aspartate
NO	Nitric oxide
Nox	NADPH oxidase
PAMP	Pathogen-associated molecular patterns
PBS	Phosphate puffered saline
PIP2	Phosphatidylinositol biphosphate
PLL	Poly-l-lysine
PRR	Pattern-recognition receptor
RNS	Reactive nitrogen species
ROS	Reactive oxygen species
SRF	Serum response factor
SRF	Serum response factor
Stat6	Signal transducer and activator of transcription 6
TGF-1	Transforming growth factor beta
TNF-α	Tumor necrosis factor alpha
UTP	Uridine-5'-triphosphate
VDCC	Voltage-dependent calcium channels
Wt	Wildtype

1. ABSTRACT

Disturbed actin dynamics have been associated with aging, neurodegenerative conditions and cell death. The current thesis investigates the interplay between microglia activation and the state of the actin cytoskeleton. Models of actin stabilization included microglia from gelsolin-deficient (*Gsn*$^{-/-}$) mice as well as treatment with actin polymerization agent jasplakinolide. Cytochalasin D served as a blocker of actin polymerization. Disruption of actin dynamics did not affect transcription of genes involved in the LPS-triggered classical inflammatory response. However, genes involved in IL-4 induced alternative activation were strongly transcriptionally downregulated by disturbed actin dynamics, which was related to impaired nuclear translocation of phospho-Stat6. Functionally, disturbed actin dynamics resulted in reduced NO secretion and reduced release of TNF-α and IL-6 from LPS-stimulated microglia and of IGF-1 from IL-4 stimulated microglia. Reduced NO secretion was associated with reduced cytoplasmic iNOS protein expression and reduced arginine uptake. However, stabilization of the actin cytoskeleton increased LPS-induced release of IL-1β, which belongs to a non-classical release pathway. Furthermore, disruption of actin dynamics resulted in reduced microglia migration, proliferation and phagocytosis *in vitro*. Similarly, proliferation of IBA1-expressing cells was reduced in *Gsn*$^{-/-}$ mice after facial nerve axotomy as well as in a model of mild brain ischemia. Finally, baseline and ATP-induced intracellular calcium levels were significantly increased in *Gsn*$^{-/-}$ microglia. Together, disruption of actin dynamics attenuates both classical and alternative microglia activation. While alternative activation is strongly downregulated at the level of gene transcription, the mechanisms operating in classical activation are post-transcriptional and primarily relate to impaired uptake, transport and release.

1. ZUSAMMENFASSUNG

Neurodegenerative Pathologien, Alterungsprozesse und Zelltod gehen oft mit einer Dysfunktion des Aktinzytoskeletts einher. Ziel vorliegender Arbeit war es, den Einfluss des Aktinzytoskeletts auf den Prozess der Mikrogliaaktivierung näher zu erforschen und zu charakterisieren. Das Modell zur Untersuchung dieser Aktinstabilisierungsprozesse basiert auf der gelsolindefizienten Mauslinie (*Gsn*$^{-/-}$) und dem Einsatz pharmazeutischer Interventionen mit Jasplakinolid und Cytochalasin D. Während Jasplakinolid zur Stabilisierung (Polymerisation) des Aktinfilamentes führt, resultieren Interventionen mit Cytochalsin D in einer Destabilisierung (Depolymerisation). Die Arbeit zeigt, dass gezielte Störungen des Auf- und Abbaus von Aktinfilamenten in klassisch aktivierter Mikroglia (mittels LPS) keinen Einfluss auf die Transkription von typischen „M1" Genen haben. Unterdessen resultierten Eingriffe in die Aktinfilamentstabilität bei alternativer Aktivierung von Mikroglia (mittels IL-4) in einer deutlichen Herabregulierung der Transkriptionsrate typischer „M2" Gene, was auf einen verminderten Transport des Transkriptionsaktivators pStat6 in den Nukleus zurückzuführen ist. Auf funktionaler Ebene führen Veränderungen der Aktindynamik zu reduzierter Freisetzung von Stickstoffmonoxid, TNF-α, IL-6 und IGF-1. Als Grund für die verringerte NO-Sekretion konnte eine reduzierte iNOS-Proteinexpressionsrate im Zytoplasma und eine verminderte Aufnahme von Arginin gezeigt werden. Dagegen ist die LPS-induzierte Freisetzung von IL-1β, das dem „nicht-klassischen" Freisetzungsmechanismus über Golgi-Apparat und ER folgt, unter Stabilisierung des Aktinzytoskeletts erhöht. Die *in vitro* Experimente vorliegender Arbeit zeigen, dass Störungen der Aktindynamik zu deutlich herabgesetzter Migration, Proliferation und Phagozytose von Mikrogliazellen führen. Zudem konnte bei der *Gsn*$^{-/-}$ Mauslinie eine verringerte Proliferationsrate IBA-1-expremierender Zellen nach Hirnischämie und ein verringerter Anstieg an IBA-1^{+} Zellen im *Nucleus facialis* nach Axotomie des *Nervus facialis* festgestellt werden. Desweiteren beweist die Arbeit, dass das intrazelluläre Calciumniveau (Basislinie und ATP-induziert) in *Gsn*$^{-/-}$ Mikroglia signifikant erhöht ist. Zusammenfassend kann festgehalten werden, dass gezielte Störungen der Aktindynamik sowohl klassische als auch alternative Mikrogliaaktivierungsprozesse abschwächen. Während alternative (IL-4 vermittelte) Mikrogliaaktivierung mit einer deutlichen Herabregulierungen auf Gentranskriptionsebene assoziiert ist, finden die klassischen (LPS vermittelten) Aktivierungsprozesse auf post-transkriptionaler Ebene statt und führen zu Beeinträchtigungen von Substrataufnahme-, Transport- und Freisetzungsmechanismen.

2. INTRODUCTION

2.1 The eukaryotic cytoskeleton

Every prokaryotic or eukaryotic cell possesses a cytosolic scaffold, the cytoskeleton. In eukaryotes, the cytoskeleton consists of filamentous protein structures that, according to filament diameter, can be distinguished into microfilaments (6 nm), intermediate filaments (10 nm) and microtubules (25 nm). Microfilaments are mainly made up of actin. Microtubules are mostly composed of a protein called tubulin. Intermediate filaments are constructed from a number of different subunit proteins. Recently, a fourth component of the cytoskeleton has been discovered, the so called septins (1). It seems likely that there are some more, maybe unknown eukaryotic cytoskeleton components that need to be investigated and clearly defined (2). However, the interplay between these filament subtypes, as well as the dynamic structural changes within each filament type, regulate fundamental cellular properties, such as cell division, motility, intracellular transport, cellular compartmentalization and cell shape and rigidity.

2.1.1 Microfilaments and actin dynamics

Microfilaments are actin protein polymers. Actin is one of the most abundant proteins that can be found in every cell. It is highly conserved from birds to mammals (3).

In the brain two isoforms of nonmuscular actin, β-actin and γ-actin, are expressed and encoded by *Actb* and *Actg1*, respectively (3, 4). Recently, it could be shown that differential biochemical properties between the two isoforms pertain to actin polymertization and G/F-actin ratio regulation (4, 5). In mice, γ-actin–null individuals are viable whereas β-actin mutants die during development (6, 7). In humans, severe forms of Baraitser–Winter syndrome (a developmental disorder characterized by the combination of congenital ptosis, high-arched eyebrows, hypertelorism, ocular colobomata and a brain malformation consisting of anterior predominant lissencephaly) are caused by ACTB (β-actin) mutations rather than ACTG1 (γ-actin) mutations (8).

Inside the cell, actin is present in two forms: i) monomeric (G)-actin and ii) filamentous (F)-actin. The actin filaments are thin and flexible fibers appearing in helices that can be further organized in higher-order structures like bundles or networks. Basically, actin filaments are highly dynamic structures characterized by depolymerization and polymerization of the actin

strand. Polymerization of the actin strand occurs via ATP-actin at the barbed (+) end, loss of ADP-actin occurs at the pointed (–) end (Figure 1) (9). The "treadmilling phenomena" describe the maintenance of the actin filament length via equilibrated ATP-actin association and simultaneous ADP-actin loss (10, 11). Further actin dynamics, such as cross-linking, severing, branching and capping, are organized and regulated by actin binding proteins (see chapter 2.1.2). Drugs such as cytochalasin D and jasplakinolide are toxins influencing actin filament remodeling (see chapter 2.1.3).

The brain consists of diverse types of cells with complex interactions. It is virtually impossible to study all these interrelations at once and reductionist approaches are needed. Thus, an effective method is to focus on one specific brain cell type (e.g. microglia). As a starting point it seems appealing to investigate the role of microglia function (migration, phagocytosis, proliferation and inflammatory responses) in order to better understand their contribution to neurodegenerative diseases. Although actin dynamics have been marginally investigated in studies concerning microglia motility, migration, phagocytosis, proliferation and shaping of cell morphology, still little is known about exact mechanisms regarding the influence of actin remodeling on the priming of neuro-protective or -toxic microglia during neurodegenerative diseases (12-15).

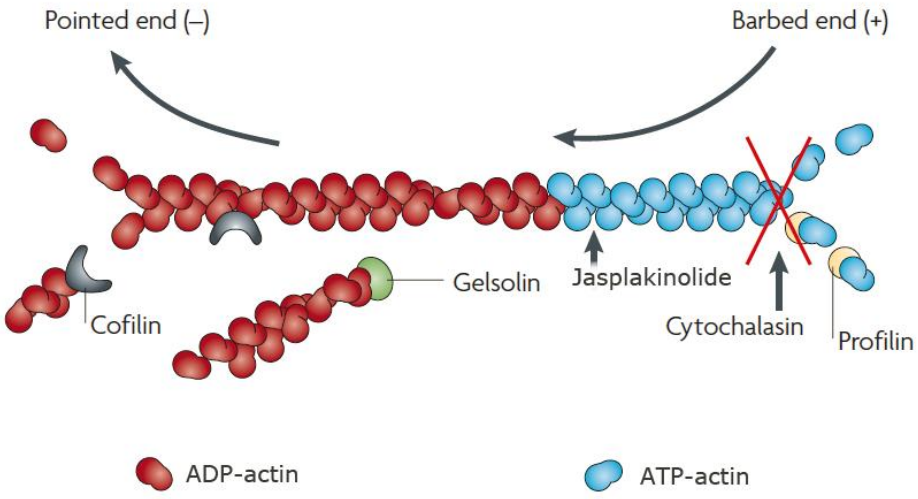

Figure 1 Actin filament dynamics, actin binding proteins and actin disrupting drugs. The actin filament (F-actin) consists of monomeric globular actin (G-actin). Polymerization of the actin strand occurs via ATP-actin at the barbed (+) end, loss of ADP-actin occurs at the pointed (–) end. Actin binding proteins (such as cofilin, profilin, gelsolin) may modulate the filament architecture and actin filament dynamics. Drugs (such as jasplakinolide and cytochalasin D) can interfere with actin filament remodeling. Jasplakinolide induces actin filament polymerization whereas cytochalasin D inhibits actin filament polymerization. Modified after Cingolani and Goda (2009) (9).

2.1.2 Actin binding proteins (ABPs)

Actin binding proteins (ABPs) are important to generate a variety of architectures out of actin filaments, such as branched or cross-linked networks in the lamellipodium, parallel bundles in filopodia, and antiparallel structures in contractile fibers (16). Most ABPs are effector targets of Rho family small GTPases (17). According to Winder and Ayscough, ABPs can be classified into the following ten categories (18):

a) Monomer binders
b) Bundlers and crosslinker
c) Crosslinkers
d) Cytoskeletal linkers
e) Capping and severing proteins
f) Rulers and stabilizers
g) Myosins
h) Anchors to membranes and membrane proteins
i) Sidebinders and signalers
j) Branch formation proteins

The current thesis partly deals with ABPs grouped in a) and e). These proteins are involved in nucleotide exchange (profilin), nucleation & polymerization (arp2/3) and capping and severing (gelsolin, cofilin).

Gelsolin

Gelsolin is an eponym for a conserved class of ABPs, where all members contain the homologous gelsolin-like (G) domain. Besides gelsolin, the family includes villin, adseverin, capG, advillin, supervillin and flightless I (19).

Gelsolin is a potent 80-83 kDa actin filament severing protein (20), first described by studying “gel” to “sol” transitions in macrophages (21). It exists in mammals as extracellular, secreted isoform found in plasma (pGSN) and intracellular as cytoplasmic (cGSN) isoform (22). Both, pGSN and cGSN, are encoded by a single gene on chromosome 9 in humans and chromosome 2 in mice (22). It executes multimodal activities like actin severing, capping and promotion of actin nucleation (Figure 2). Increasing intracellular micromolar calcium levels lead to a confirmation change and activation of gelsolin with subsequent binding to filamentous actin, thereby severing the actin strand. Gelsolin remains bound at the barbed (+) end and maintains the capping activity until calcium levels decrease and available

phosphoinositides (PIP_2) release the protein (23). Calcium also facilitates the nucleation promoting activity, in which gelsolin binds two G-actin molecules, forming a nucleus for elongation (24). The consequence of the multimodal activities of the activated gelsolin is the formation of a large number of short F-actin filaments important for increased actin dynamics (18). Besides actin binding, gelsolin has been found be a substrate for caspase 3, and a function during apoptosis has been suggested (25). Further research revealed a neuroprotective role of gelsolin during murine stroke, regulated by calcium influx and mediated by actin dynamics and VDCC and NMDA channel rundown (26). Gelsolin probably also plays a role in Alzheimer's disease, as it reduces amyloid-ß levels in the APP/Ps1 transgenic mouse (27). Interestingly (because AD and stroke are age-related diseases), gelsolin levels increase in brain tissue with age, maybe to antagonize apoptosis (28).

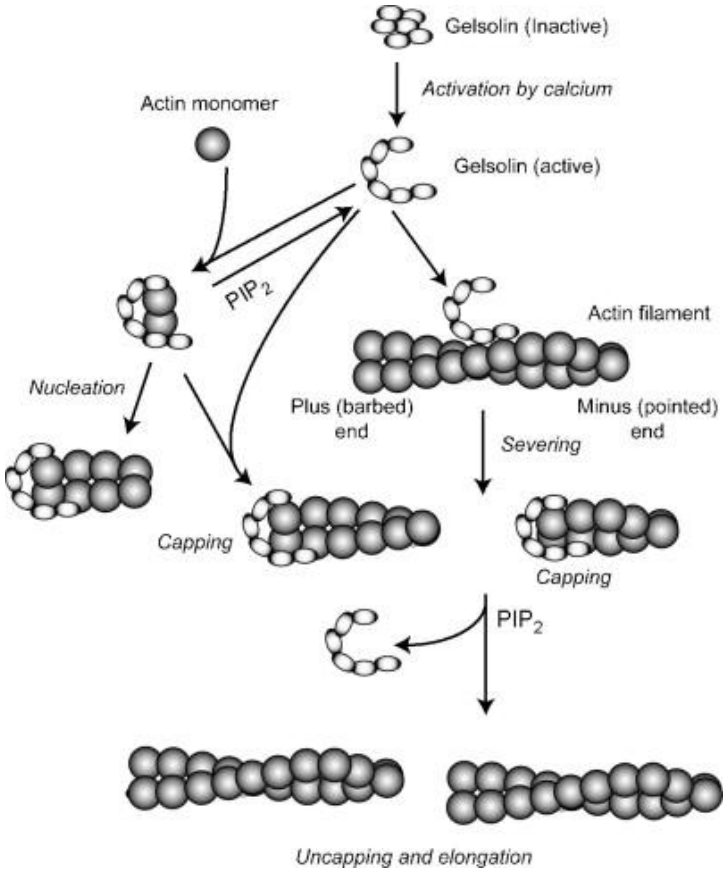

Figure 2 Mode of action for gelsolin.
Increasing intracellular calcium levels lead to conformational changes of the gelsolin protein and increase its accessibility to actin. Once bound to actin, gelsolin severs actin filaments and caps the resulting barbed (+) ends. Calcium also facilitates the nucleation promoting activity, in which gelsolin binds two G-actin molecules, forming a nucleus for elongation. Rising phosphoinositide (PIP_2) levels promote the release of gelsolin from actin sides and inhibit the severing activity of gelsolin. Adapted from Ono (2007) (29).

Cofilin

A special role for cofilin in microglia mediated phagocytosis and migration with implication for multiple sclerosis and Huntington's disease has been described (30, 31). Cofilin belongs to the AC (ADF/cofilin) family that mainly controls F-actin remodeling (32). Cofilin can sever actin filaments, thereby generating free actin filament ends that are accessible for F-actin polymerization and depolymerization without changing the rate of G-actin association and dissociation at either filament end (33). Three different ADF/cofilins have been found in the human and in the mouse: cofilin-1, cofilin-2, and ADF. Cofilin-1 is expressed in most cells, cofilin-2 is expressed predominantly in muscle cells, and ADF mostly occurs in epithelial and endothelial cells (34). The activity of cofilin can be regulated by phosphorylation, pH and phosphoinositides. Phosphorylation of cofilin at amino acid ser-3 by LIM kinase leads to abolished actin-binding activity (35). Dephosphorylation of cofilin leads to activation and is executed by phosphatases like slingshot and chronophin (36). Similar to phosphorylation, binding to PIP_2 leads to cofilin inactivation (37).

Profilin

Profilin is involved in many fundamental cellular processes in the brain. Particularly radial migration of neurons is dependent on profilin 1 function. When profilin is diminished in mouse brains, this results in cerebellar hypoplasia, aberrant organization of cerebellar cortex layers and ectopic cerebellar granule neurons (38). Microglia cells also express profilin and upregulate its expression after nerve injury (39). In the mammalian brain two out of four profilins are expressed: profilin 1 and profilin 2. Profilin is responsible for maintaining the intracellular G-actin pool, and it binds with high affinity to monomeric actin (40). Moreover, it catalyzes the exchange of actin-bound ADP to ATP and thereby promotes F-actin polymerization (41).

Actin-related proteins 2 and 3 (Arp2/3)

Arp2/3 is a seven component molecular "machine" acting as actin nucleator complex that generates branched actin networks. Arp2/3 is activated by the WASp/Scar/WAVE protein family that has the function to bring Arp2/3 complex close to F-actin. Arp2/3 can build crosslinked actin networks by binding to the sides of ATP-F-actin near the growing barbed end of the filament and nucleates growth of new filament branches, resulting in a dendritic filament array. According to the current knowledge, the arp2/3 complex is involved in microglial podosome formation and migration (13).

SRF serum response factor - regulation of ABPs via transcriptional control

The serum response factor is a highly conserved and widely expressed transcription factor. It controls transcription of genes containing a "CArG box" (SRF binding element). This box has been found in the promoter of a plethora of genes involved in proliferation, growth and migration. Therefore, it is not surprising that SRF binding elements are found in many genes encoding ABPs, such as gelsolin, profilin, cofilin and arp2/3 (42). SRF depletion in mice is lethal, underlining the important role of this transcription factor during developmental processes (43). Increased activity of SRF via Rho-GTPase depletes the G-actin pool in the nucleus during F-actin polymerization. The activity of SRF can be modulated by cofactors such as MRTF (myocardin-related transcription factor). Depleted G-actin pools trigger MRTF binding to SRF in the nucleus and this complex activates context-dependent gene transcription (44).

2.1.3 Disruption of actin dynamics as a model to study the role of the actin cytoskeleton in microglia cells

Exogenous and endogenous modulations of actin structures display helpful tools to study and understand the role of actin filament stabilization in different aspects of microglia function.

Exogenous modulation of actin dynamics

Cytochalasin D is a naturally occurring fungal toxin (45). It can permeate cell membranes and bind to the barbed end of actin filaments, sever F-actin and thereby inhibit actin polymerization (Figure 1) (46-48).

The drug jasplakinolide used throughout the experiments is a toxin isolated from the marine sponge *Jaspis johnstoni* (49). Like cytochalasin D, it is membrane permeable. Jasplakinolide induces stabilization and polymerization of actin filaments (Figure 1) (50).

Endogenous modulation of actin dynamics

The Gelsolin knock out mouse model ($Gsn^{-/-}$) has been generated and established in 1995, and shows normal embryonic development and longevity (51). Work in our group on this mouse model showed that gelsolin plays an important protective role in neurodegenerative paradigm like murine stroke and has anti- apoptotic properties in neurons (26, 52, 53). The protective action of gelsolin in neurons is associated with the maintenance of the intracellular Ca^{++} homeostasis by modulation of calcium channel and NMDA receptor activities (54).

2.2 Microglia

Microglia are the resident immune cells of the central nervous system. They were first described in the early 20th century by the Spanish neuroanatomist Pio del Rio-Hortega. Based on observations of brain slices stained by silver carbonate he described microglia as nonneuronal cells with mesodermal origin that enter the brain during development and are capable to change their morphology in response to certain stimuli. Furthermore, he observed that they are capable to migrate, phagocytose and proliferate [reviewed in Kettenmann et al. (2011)] (55). Current knowledge on microglia is largely based on the early descriptions of Rio-Hortega and colleagues. State of the art staining, imaging and molecular methods have provided additional insights into microglia biology. Microglia are currently defined as permanent resident tissue macrophages of the immune-privileged central nervous system, taking over two important functions:

1) Homeostatic maintenance functions during development and under physiological conditions by constantly surveying their environment with motile processes. To support healthy tissue function they, if required, phagocytose cell debris or apoptotic cells, release trophic factors, regulate myelin turnover and are involved in synapse remodeling (55-57).

2) Triggering an immune response as "first line of defense guardians" under pathophysiological conditions, microglia can develop diverse stimuli-dependent phenotypes that additionally differ in a spatial-temporal manner (Figure 3). This can lead to either detrimental or protective effects on nervous tissue (58). For administrating immune functions, microglia express a plethora of pattern recognition receptors (PRRs) on their surface to recognize two kind of signals for activation, classified as DAMPs (damage associated pattern) or PAMPs (pathogen associated pattern) (59).

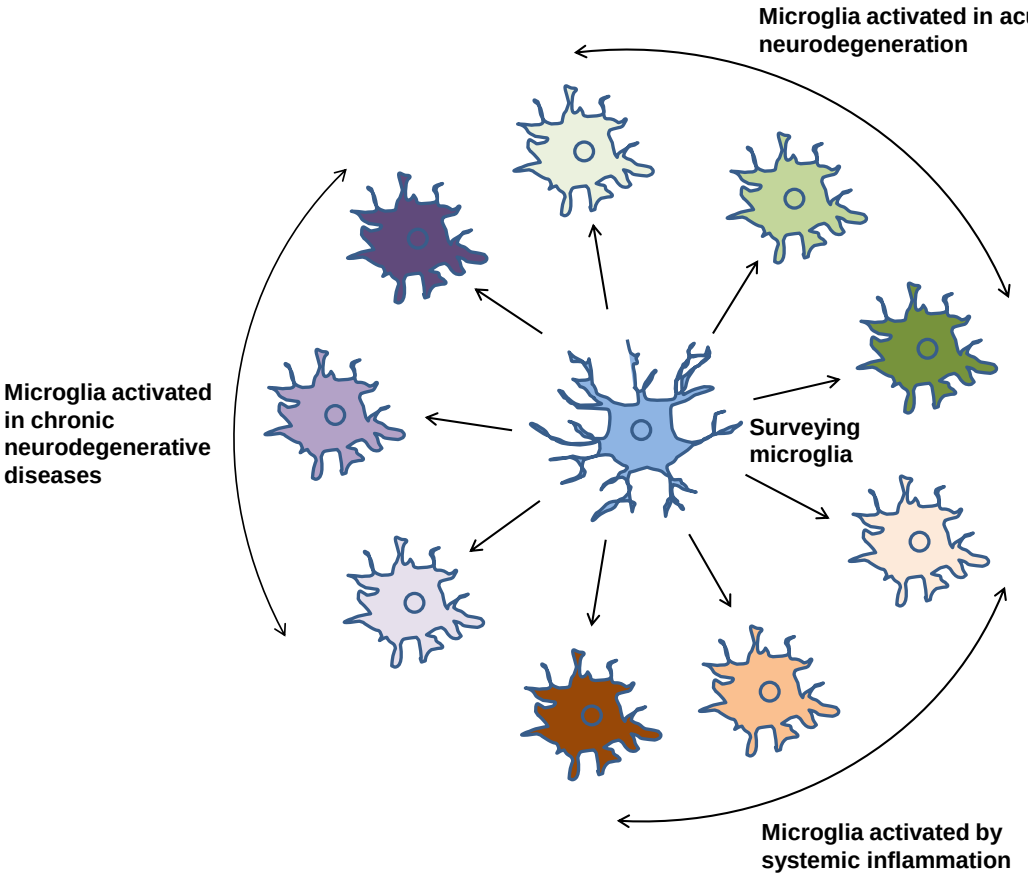

Figure 3 Diverse phenotypes of activated microglia *in vivo*.
Differing colors display diverse phenotypes depending on the extent and type of the activation stimuli, time of examination after microglia activation and age of the individual. Modified after Perry et al. (2010) (58).

2.2.1 Origin of microglia

Despite being the innate immune cells of the CNS that mount an immune response under pathological conditions, the main function of microglia is to maintain the homeostatic balance of the healthy brain. In this respect, microglia differ from the immune system outside the immune-privileged CNS, with its defense function as first priority. Thus, it is noteworthy to bring up the origin of these cells. It has been shown in mice that microglia arise early in development from the primitive hematopoiesis within the yolk sac and infiltrate the neuroepithelium at E9.5 probably via migration through ventricles, meningeal tissue, or vasculature (60-62). It has been proposed that throughout life, adult microglia are capable of self-renewal and do not require replenishment by circulating monocytic precursors (63). But it is still under discussion, if and how during neurodegenerative diseases, resident microglia function independently and differently of invading bone marrow derived macrophages that enter the brain because of active recruitment through a leaky blood brain barrier (64).

2.2.2 Diverse activated microglia phenotypes *in vivo* - concept of classical LPS and alternative IL-4 activation *in vitro*

Microglia activation *in vivo* presents a histological hallmark in nearly all neurodegenerative diseases. The influence on disease progression and outcome is not fully understood yet, and it is still debated, whether microglia activation worsens or increases recovery from brain disease. Our current lack of understanding results, on the one hand, from an unclear distinguishable marker between different *in vivo* microglia phenotypes, intermediate states and the temporal-spatial distribution of differently activated cells. On the other hand, different animal disease models have led to contradictory results. Activation can (but does not need to) be accompanied by changes in morphology, such as transformation into process retracted amoeboid ("fried egg") or rod-like shapes, or upregulation of surface markers (such as CD11b, CD45, iba-1, F4/80, CD16/32, CD68, CD86, CD204, CD 206) (65-67).

A possible way to categorize activated microglia cells is based on their released or secreted factors, whether microglia are considered to be detrimental or protective to neurons. A simplified activation paradigm can be executed *in vitro* and serves as model to study different microglia phenotypes. The concept has evolved from classification of T-cell responses into Th1 and Th2, and reflects the "Janus-like" behavior of microglia by functionally differentiating between M1 and M2 phenotypes. M1 is considered to be neurotoxic, whereas M2 is considered to be neuroprotective (Figure 4) (65, 68, 69). This model should be cautiously interpreted, as it represents only extreme *in vivo* activation and excludes intermediate states. Furthermore, the M1 phenotype is important for the defense from microorganisms and can secrete also anti-inflammatory cytokine IL-10 (70). IFN-γ and lipopolysaccharide (LPS) are elicitors priming microglia towards the M1 state and induce the expression and release of pro-inflammatory interleukin- (IL-) 1, 6, 12 and TNF-α (65, 68, 69). Furthermore, cells synthesize nitric oxide via iNOS (nitric oxide synthase) pathway by using arginine as substrate (71). Also the production of ROS (reactive oxygen species) via Nox2 has been observed after LPS activation (72). Treatment with IL-4 or IL-13 turns microglia into M2 phenotype, which can be characterized by the production of growth factors such as IGF-1, TGF-β and upregulated expression of genes involved in tissue remodeling and repair such as arginase 1 (Arg1), mannose receptor (Mrc1), found in inflammatory zone 1 (Fizz1), and chitinase 3-like protein 3 (Ym1) (65, 68, 69, 73-76).

Besides the release of pro- and anti-inflammatory factors, activated microglia are able to migrate, phagocytose and proliferate in response to certain stimuli.

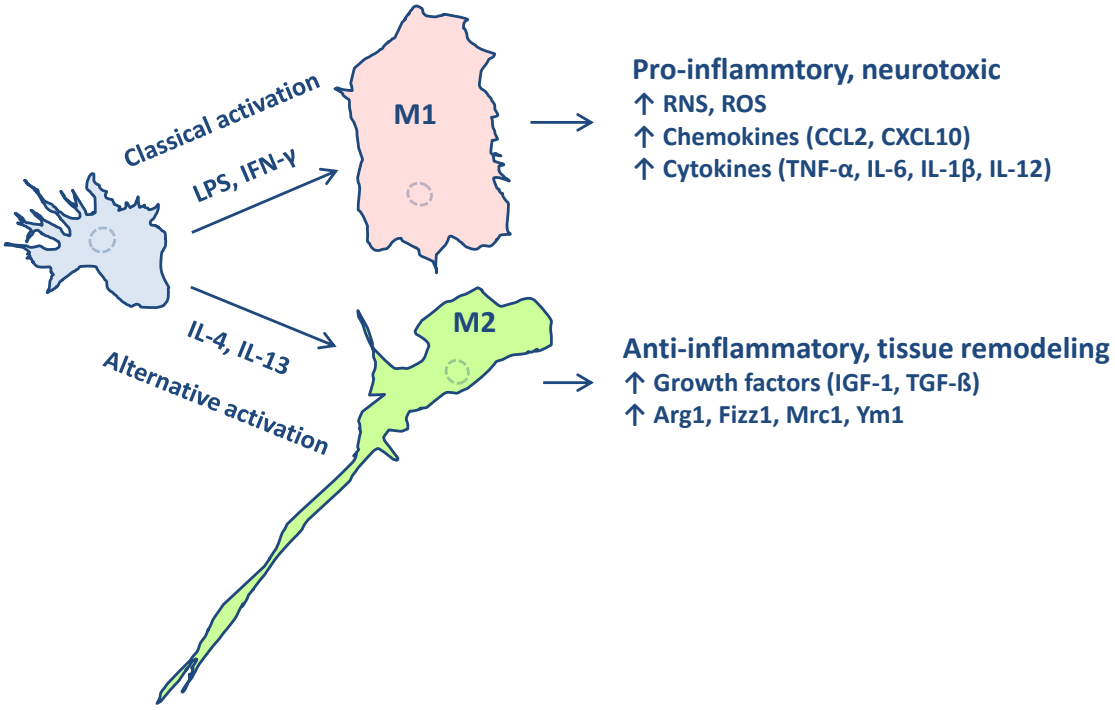

Figure 4 Conceptual framework of microglia polarization.
Microglia activation by diverse stimuli leads to polarization of the cell towards different phenotypes. Application of LPS or IFN-γ triggers classical activation with pro-inflammatory (M1) phenotype. Alternative activation by IL-4 or IL-13 primes the cell towards anti-inflammatory (M2) phenotype. RNS (reactive nitrogen species), ROS (reactive oxygen species), CCL2 (chemokine (C-C motif) ligand 2), CXCL10 (chemokine (C-X-C motif) ligand 10), TNF-α (tumor necrosis factor alpha), IL-1,-6,-12 (interleukin-1,-6,-12), IGF-1 (insulin-like growth factor 1), TGF-β (transforming growth factor beta), Arg1 (arginase 1), Mrc1 (mannose receptor 1), Fizz1 (found in inflammatory zone 1), Ym1 (chitinase 3-like protein 3)

2.2.3 Migration

Microglia are highly motile and migratory cells. Motility refers to the cells' rapid movement of their branched processes to constantly survey the environment. In contrast to motility, microglial migration is characterized by translocation of the whole cell body. Both mechanisms are important for developmental, physiological and pathophysiological functioning (77-79). Under developmental aspects, microglia migration occurs during embryogenesis, when yolk sac derived cells enter the brain (60). Under pathophysiological aspects, microglia are migrating in response to a "danger" signal towards the site of injury, accompanied by a transformation from a ramified into an amoeboid microglia phenotype (55). This phenomenon is also observed after ischemic stroke (80). "Danger" signals after stroke

are released from cells of the injured region and can be of diversified nature, examples are extracellular nucleotides (ATP, ADP, UDP), cannabinoids, galanine or bradykinin (81-85). Although all these chemoattractants have the capability to increase microglia migration, the signal cascades controlling migratory behavior and underlying actin cytoskeleton reorganizations are highly complex and diverse. This diversity underlines the different functions of danger signals to microglia polarization under pathological conditions and is one piece of a puzzle in the diversity of microglia phenotypes.

2.2.4 Phagocytosis

As being part of the vertebrate immune system, microglia is not only the key player driving inflammatory reactions within the central nervous system, but also being qualified of doing phagocytosis and thereby helping to maintain homeostasis of the brain. Phagocytosis, per definition, is the process of recognition ("find me"), engulfment ("eat me") and degradation ("digest me") of particles or organisms (86). Microglia phagocytosis involves a broad spectrum of different targets, ranging from the engulfment of bacteria, spines, axonal and myelin debris, protein aggregates (Aß) to dead or dying cells (87). Recently the term phagoptosis was introduced, as it was found that microglia can induce neurodegeneration by phagocytosis of stressed but still viable neurons (88). Dependent on the brain's pathophysiological condition and the engulfed target, phagocytosis can on the one hand result in respiratory burst and inflammatory occurrences, as it is known for microbe uptake (PAMPs). On the other hand, as it is known for the uptake of apoptotic cells (DAMPs), phagocytosis can be executed without inflammation but is related to the release of anti-inflammatory signals like TGF-ß or IL-10 (89). A number of receptors and intracellular pathways are involved in the execution of phagocytosis. As "find me" signals, released from the targets itself, may serve extracellular nucleotides (ATP, UTP) or fractalkine. Since microglia cells are constantly surveying their environment, they sense these chemoattractants and migrate towards the target site. Along the way, microglial receptors, such as $P2Y_6$ or fractalkine are able to adapt the cell to mediate phagocytosis (90, 91). Once microglia find their target, the target features "eat me" or "don´t eat me" signals to initiate or refuse the phagocytosis process. "Eat me" signals include a great number of members belonging to the phosphatidylserine-, integrin-, Ig superfamily- and scavenger-receptor family. Once the phagocyte finds its target, a short lived "phagocytic synapse" is formed (92), which triggers complex intracellular signaling pathways resulting in cytoskeletal remodeling and formation of a phagocytic cup that surrounds the target and develops the phagosome (phagocytic

vesicle). This phagosome is defined as a membrane bound compartment containing the phagocytosed target. By further fusion of the phagosome with lysosomes (derived from the Golgi apparatus, filled up with digestive proteins), the target is degraded within the newly formed phagolysosome in an acidic environment. The acidic environment is maintained by the activity of proton pumps. Dependent on the internalized target, it is digested into basic cellular building blocks including nucleotides, fats, sterols and peptides/amino acids. Also dependent on the engulfed target is the response of the microglia cell, whether it polarizes towards a pro- or anti-inflammatory phenotype, or both.

2.2.5 Proliferation

Surveillant microglia account for approximately 5% to 12% of the total cell population in the healthy adult mouse brain (93). However, a massive proliferative activity of microglia cells is found as an epiphenomenon of microglial activation in animal models of stroke, AD, MS or prion disease (94-98). Main drivers of microglial proliferation are macrophage colony-stimulating factor (CSF1) and the expression of its receptor (CSF1R) (99, 100). On the transcriptional level, CFS1R expression is regulated via transcription factors PU.1 and C/EBPα, which are considered to be involved in regulating the molecular M1/M2 phenotype switch (94). The transection of the facial nerve in rodents provides a unique model to selectively assess resident microglia proliferation *in vivo.* The axotomy paradigm leads to a microglial response within its central nucleus of origin and restricts infiltration of peripheral macrophages because of the intact BBB (blood brain barrier) (101, 102). Thus, the application of the facial nerve axotomy to *Gsn*$^{+/+}$ and *Gsn* $^{-/-}$ mice provides an excellent model to study the impact of actin filament remodeling on proliferation in microglia cells.

2.2.6 The role for microglia in neurodegenerative diseases like stroke, Alzheimer's disease and its relation to age

With the advance of knowledge on the cellular and molecular pathomechanisms involved in neurodegeneration, nonneuronal cells and, in particular microglia, have begun to take center stage. Microglia, the "garbage men" of the central nervous system (103), fulfill crucial functions in the brain by continuously surveying their microenvironment and mounting an immune response in case of disease or tissue injury (104, 105). Research has moved beyond the simplistic notion of "wholesale good" or "wholesale bad" effects of microglia and instead

suggests that these cells may be beneficial, pernicious or both, depending on the precise temporal-spatial disease context.

For example, in Alzheimer's disease, microglia is hypothesized to be helpful as long as they are able to keep up with Aβ aggregate accumulation. However, once Aβ deposits exceed a critical size, microglial functions may be impaired and their phenotype may shift toward neurotoxicity (106, 107).

Following cerebral ischemia, resident microglia immediately respond by inflammatory activation and accumulate at the lesion site and in the penumbra (96). Further immune modulatory actions, greatly influenced by DAMPs released from the injured region, can be achieved even after several days and months. Temporal-spatial dynamics of microglia phenotypes lead to a release of beneficial and detrimental substances (108).

Since neurodegenerative diseases such as stroke or AD have the tendency to occur more often in elderly individuals (109-111), the question remains how "aged" microglia contribute to the progress of these diseases. Aging, and especially human aging, is associated with increased rigidity of cytoskeletal structures. With increasing cellular senescence, the equilibrium between monomeric, non-aggregated G-actin ("globular actin") and fibrillar F-actin shifts toward the filamentous state (112-115). It has been proposed that in the aged brain, dystrophic (senescent) microglia has a reduced capability to maintain their homeostatic and neuroprotective functions and contribute to neurodegenerative processes (116-118). Moreover, if "aged" microglia cells are challenged with diseases, they are proposed to have a decreased ability to mount a beneficial response to injury (119-121). Hence, a comparison between gelsolin deficient and wildtype microglia and an additional comparison between adult and aged microglia could give more insights into the effects of pathological actin filament stabilization as a mediator of the detrimental effects of aging.

2.3 Hypothesis

Core aspects of microglia function including the response to challenges are highly dependent on actin cytoskeleton dynamics. In particular, modulation of actin dynamics differentially affects classical and alternative microglia activation. Furthermore, the state of the actin cytoskeleton impacts fundamental microglia processes such as proliferation, migration and phagocytosis *in vitro* and *in vivo*.

This hypothesis leads to the following specific research questions:

1. Does modulation of actin dynamics and microglia activation affect intracellular levels of actin binding proteins and the G/F-actin ratio?
2. Does (if yes, how does) modulation of actin dynamics affect the response to classical microglia activation?
3. Does (if yes, how does) modulation of actin dynamics affects the response to alternative microglia activation?
4. Does modulation of actin dynamics affect microglia proliferation, migration and phagocytosis and are there differences between microglia from "adult" animals (<6 months) compared to "aged" animals (>16 months of age)?

In order to answer these questions and test the overall hypothesis, the following two experimental approaches were applied:

1. Exogenous approach
   In order to influence actin polymerization and depolymerization in Wt (BL6/N) postnatal and BV-2 microglial cells, pharmacological intervention with jasplakinolide and cytochalasin D was applied.

2. Endogenous approach
   The goal was to study differences of Gelsolin$^{+/+}$ and Gelsolin$^{-/-}$ microglial cells *in vitro* and *in vivo* and additionally test interaction with age (adult vs. aged) using a 2 x 2 design.

3. MATERIALS AND METHODS

3.1 Materials

3.1.1 Cell culture media, supplements and enzymes

Product	**Supplier**
Deoxyribonuclease I	Worthington (Lakewood, NJ, USA)
Dulbecco's MEM (DMEM)	Merck KGaA (Darmstadt, Germany)
Fetal Bovine Serum (FBS)	Merck KGaA (Darmstadt, Germany)
Hank's Balanced Salt Solution (HBSS) Ca, Mg	Invitrogen (Darmstadt, Germany)
Hank's Balanced Salt Solution (HBSS) w/o Ca, Mg	Invitrogen (Darmstadt, Germany)
Mouse CSF-1 Recombinant Protein	eBioscience (San Diego, CA, USA)
Mouse GM-CSF Recombinant Protein	eBioscience (San Diego, CA, USA)
Penicillin/ Streptomycin	Merck KGaA (Darmstadt, Germany)
Phosphate buffered saline (PBS)	Invitrogen (Darmstadt, Germany)
Polylysine (PLL)	Merck KGaA (Darmstadt, Germany)
Sodium Pyruvate	Merck KGaA (Darmstadt, Germany)
Trypsin/ EDTA solution	Merck KGaA (Darmstadt, Germany)

3.1.2 Chemicals

Product	**Supplier**
4’,6-Diamidino-2-phenylindole dihydrochloride (DAPI)	Sigma-Aldrich (Saint Louis, MO, USA)
4’,6-Diamidino-2-phenylindole dihydrochloride (DAPI)	Sigma-Aldrich (Saint Louis, MO, USA)
5-Bromo-2′-deoxyuridine (BrdU)	Sigma-Aldrich (Saint Louis, MO, USA)
Adenosine 5’-diphosphate Sodium Salt (ADP)	Sigma-Aldrich (Saint Louis, MO, USA)
Adenosine 5′-triphosphate Magnesium Salt (ATP)	Sigma-Aldrich (Saint Louis, MO, USA)
Ammonium acetate	Sigma-Aldrich (Saint Louis, MO, USA)
Calcium chloride $CaCl_2$)	Merck KGaA (Darmstadt, Germany)
Carboxyfluorescein Diacetate, Succinimidyl Ester (CFSE)	Invitrogen (Darmstadt, Germany)
Chloroform	Sigma-Aldrich (Saint Louis, MO, USA)
Clodronate, Disodium Salt	Merck KGaA (Darmstadt, Germany)
Cytochalasin D	Sigma-Aldrich (Saint Louis, MO, USA)
D-(+)-Glucose	Carl Roth (Karlsruhe, Germany)
D-(+)-Saccharose	Carl Roth (Karlsruhe, Germany)

Dimethylsulfoxid (DMSO)	Sigma-Aldrich (Saint Louis, MO, USA)
Ethanol, Absolute	Merck KGaA (Darmstadt, Germany)
Ethylene Glycol,	Sigma-Aldrich (Saint Louis, MO, USA)
FORENE® (Isoflurane)	Abbott (Wiesbaden, Germany)
Fura-2 Calcium Indicator	Invitrogen (Darmstadt, Germany)
Glycerin	Sigma-Aldrich (Saint Louis, MO, USA)
HEPES	Carl Roth (Karlsruhe, Germany)
Hexafluoroisopropanol (HFIP)	Sigma-Aldrich (Saint Louis, MO, USA)
Hydrochloric acid (HCl)	Sigma-Aldrich (Saint Louis, MO, USA)
Ionomycin	Invitrogen (Darmstadt, Germany)
Isopropyl alcohol	Sigma-Aldrich (Saint Louis, MO, USA)
Jasplakinolide (InSolution^{Tm})	Merck KGaA (Darmstadt, Germany)
L-[^{14}C(U)]-Arginine	PerkinElmer (Turku, Finland)
L-Arginine	Sigma-Aldrich (Saint Louis, MO, USA)
Lipopolysaccharide (LPS) *E.coli* 055:B5	Sigma-Aldrich (Saint Louis, MO, USA)
Liquid Scintillation Cocktail (Opti-Fluor)	PerkinElmer (Shelton, Ct, USA)
L-Leucine	Sigma-Aldrich (Saint Louis, MO, USA)
Magnesium sulfate ($MgSO_4$)	Merck KGaA (Darmstadt, Germany)
Monobasic potassium phosphate (KH_2PO_4)	Merck KGaA (Darmstadt, Germany)
Paraformaldehyde	Sigma-Aldrich (Saint Louis, MO, USA)
Phenol:Chloroform:Isoamyl Alcohol (UltraPure™)	Invitrogen (Darmstadt, Germany)
Pluronic® F-127 (20% Solution in DMSO)	Invitrogen (Darmstadt, Germany)
Potassium chloride (KCl)	Merck KGaA (Darmstadt, Germany)
Pyruvic Acid	Sigma-Aldrich (Saint Louis, MO, USA)
Recombinant Murine IL-4	PeproTech (Rocky Hill, NJ, USA)
Saline (0.9%)	Fresenius Kabi (Bad Homburg, Germany)
Sodium dodecyl sulfate (SDS)	Sigma-Aldrich (Saint Louis, MO, USA)
Sodium nitrite (NaCl)	Sigma-Aldrich (Saint Louis, MO, USA)
Thiazolyl Blue Tetrazolium Bromide (MTT)	Sigma-Aldrich (Saint Louis, MO, USA)
Tris	Carl Roth (Karlsruhe, Germany)
Triton™ X-100 solution	Sigma-Aldrich (Saint Louis, MO, USA)
TRIzol®	Invitrogen (Darmstadt, Germany)
Trypan Blue Stain (0.4%)	Invitrogen (Darmstadt, Germany)
β-Nicotinamide Adenine Dinucleotide, Reduced Disodium Salt Hydrate (ß-NADH)	Sigma-Aldrich (Saint Louis, MO, USA)

3.1.3 Antibodies, reagents and kits

10% SDS–polyacrylamide gel	Pierce (Rockford, lL, USA)
ABC Elite reagent	Vector Laboratories (Burlingame, CA,

	USA)
Amyloid β-Protein (1-42)	Bachem (Bubendorf, Switzerland)
APC Rat Anti-Mouse CD11b	BD Pharmingen (Heidelberg, Germany)
autoMACS® Rinsing Solution	Miltenyi (Bergisch Gladbach, Germany)
BCA Protein Assay	Pierce (Rockford, lL, USA)
CD11b MicroBeads	Miltenyi (Bergisch Gladbach, Germany)
Diaminobenzidine (DAB)	Sigma-Aldrich (Saint Louis, MO, USA)
FITC or RhodX conjugated secondary antibodies	Jackson ImmunoResearch Laboratories (West Grove, PA, USA)
FITC-β-Ala-Amyloid β-Protein (1-42) ammonium salt	Bachem (Bubendorf, Switzerland)
Griess' reagent for nitrite	Sigma-Aldrich (Saint Louis, MO, USA)
Horseradish Peroxidase-conjugated Goat Anti-Mouse IgG	Pierce (Rockford, lL, USA)
Horseradish Peroxidase-conjugated Goat Anti-Rabbit IgG	Pierce (Rockford, lL, USA)
LDH Enzyme (TruCal U)	DiaSys Greiner (Flacht, Germany)
Light Cycler® 480 SYBR Green I Master	Roche Diagnostics (Mannheim, Germany)
Live Cell Imaging Solution	Invitrogen (Darmstadt, Germany)
MACS® BSA Stock Solution	Miltenyi (Bergisch Gladbach, Germany)
M-MLV Reverse Transcriptase	Promega (Mannheim, Germany)
Mouse Anti-GAPDH	Merck KGaA, Darmstadt, Germany
Mouse IGF-I Immunoassay	R&D Systems (Minneapolis, MN, USA)
Mouse IL-1ß Immunoassay	R&D Systems (Minneapolis, MN, USA)
Mouse IL-6 Immunoassay	R&D Systems (Minneapolis, MN, USA)
Mouse TNF-alpha Platinum ELISA	eBioscience (San Diego, CA, USA)
Myelin Removal Beads II	Miltenyi (Bergisch Gladbach, Germany)
Neural Tissue Dissociation Kit (P)	Miltenyi (Bergisch Gladbach, Germany)
NucleoSpin® Tissue XS kit	Machery-Nagel (Düren, Germany)
PE Rat Anti-Mouse CD45	BD Pharmingen (Heidelberg, Germany)
pHrodo *S.aureus* BioParticles® Conjugate	Invitrogen (Darmstadt, Germany)
Rabbit Anti-Cofilin	Cell Signaling (Danvers, MA, USA)
Rabbit Anti-Gelsolin	Abcam (Cambridge, UK)
Rabbit Anti-HDAC1	Cell Signaling (Danvers, MA, USA)
Rabbit Anti-Iba1	Wako Chemicals (Neuss, Germany)
Rabbit Anti-iNOS (M19)	Santa Cruz (Dallas, TX, USA)
Rabbit Anti-Ki67	Abcam (Cambridge, UK)
Rabbit Anti-Phospho-Cofilin	Cell Signaling (Danvers, MA, USA)
Rabbit Anti-Phospho-STAT6	Cell Signaling (Danvers, MA, USA)
Rabbit Anti-SRF	Abcam (Cambridge, UK)
Rabbit Anti-STAT6	Cell Signaling (Danvers, MA, USA)

Rabbit Anti-β-Actin	Cell Signaling (Danvers, MA, USA)
Random Hexamer Primers	Roche Diagnostics (Mannheim, Germany)
Rat Anti-BrdU	Harlan Seralab (Indianapolis, IN, USA)
RNasin® RNase Inhibitor	Promega (Mannheim, Germany)
RQ1 RNase-Free DNase	Promega (Mannheim, Germany)
Subcellular Protein Fractionation Kit for Cultured Cells	Pierce (Rockford, lL, USA)
Super Signal West Dura Chemiluminescent Substrate	Pierce (Rockford, lL, USA)

3.1.4 Tools and equipment

µ-Slide (8 Well)	Ibidi (Martinsried, Germany)
CCD Camera	ORCA, Hamamatsu, (Herrsching am Ammersee, Germany).
Centrifuge, Eppendorf 5804R	Eppendorf (Hamburg, Germany)
Centrifuge, Hettich Universal 30RF	Andreas Hettich (Tuttlingen, Germany)
CO2 Incubator	BINDER (Tuttlingen, Germany)
Confocal Microscope Leica LFSA	Leica Mikrosysteme (Wetzlar, Germany)
Countess™ Automated Cell Counter and Slides	Invitrogen (Darmstadt, Germany)
Electrophoresis Chamber	PEQLAB (Erlangen, Germany)
Eppendorf Concentrator 5301	Eppendorf (Hamburg, Germany)
Falcon® HTS FluoroBlok™ Inserts	Becton Dickinson Labware (Franklin Lakes, NJ, USA)
Inverted Microscope Leica DMI3000	Leica Mikrosysteme Vertrieb (Wetzlar, Germany)
Inverted Microscope Olympus IX71; UPLSAPO X2 40x/0.95 objective	Olympus Deutschland (Hamburg, Germany)
Isofluorane Vaporizer 19.3	Drägerwerk (Lübeck, Germany)
MACS Separation Columns	Miltenyi (Bergisch Gladbach, Germany)
Multi-Purpose Shaker KL 2	Edmund Bühler (Hechingen, Germany)
Nanodrop® ND-2000 Spectrophotometer	Thermo Fisher Scientific (Wilmington, DE, USA)
pH Meter (pH 522)	WTW (Weilheim, Germany)
Plate Reader MRX	Dynatech (Denkendorf, Germany)
Plate Reader TriStar LB941	Berthold Tech. (Bad Wildbad, Germany)
Power Supply (Power Pac 200)	Bio-Rad (München, Germany)
QuadroMACS™, OctoMACS™ Separator	Miltenyi (Bergisch Gladbach, Germany)
Sliding Microtome	Leica Mikrosysteme (Wetzlar, Germany)
Sonicator, Sonorex Super 10P	BANDELIN electronic (Berlin, Germany)

Trans-Blot® SD Semi-Dry Transfer Cell	Bio-Rad (München, Germany)
Wallac Liquid Scintillation Counter 1409	PerkinElmer (Turku, Finland)

3.1.5 Primer

Primers have been purchased from Eurofins MWG Operon (Ebersberg, Germany).

Gsn	Gsn_ for	CTC CGT ACC GCT CTT CAC TG	Gsn_rev	CTC ATC CTG GCT GCA TTC ATT G
SRF	SRF_for	GCT ACA CGA CCT TCA GCA AGA G	SRF_rev	CAG GTA GTT GGT GAT GGG GAA G
Cfl1	Cfl1_for	TCT GTC TCC CTT TCG TTT CC	Cfl1_rev	ACC GCC TTC TTG CGT TTC TT
Vil1	Vil1_for	AGG CTC TCT CAA CAT CAC CAC	Vil1_rev	GTC CTG GCC AAT CCA GTA GT
Pfn1	Pfn1_for	TGG AAC GCC TAC ATC GAC AG	Pfn1_rev	TTG CCT ACC AGG ACA CCA AC
Arpc5	Arpc5_for	TCT GGA CAA GAA CGG TGT GG	Arpc5_rev	GTG AAC GGT GTC CAG TTC CA
iNos	iNOS_for	GCT CGC TTT GCC ACG GAC GA	iNOS_rev	AAG GCA GCG GGC ACA TGC AA
Cat1	Cat-1_for	CTC TCT CTG CGC ACT TTC CA	Cat-1_rev	CTG AGG TCA CAG TGG CGA TT
Cat2	Cat2_for	ACA ACG GGT GAA GAG GTT CG	Cat2_rev	CCA TCC TCC GCC ATA GCA TA
Cat3	Cat-3_for	CCT ACG TCA TTG GTA CAG CCA G	Cat-3_rev	CAG CAA TCC AGT GAG CAG CAA C
Asl	Asl_for	TAC ACA CAG GAC GAA GTC GC	Asl_rev	TGA ATC TCG TGT CAG CGC AA
Arg1	Arg1_for	ATG TGC CCT CTG TCT TTT AGG G	Arg1_rev	GGT CTC TCA CGT CAT ACT CTG T
Nfkb1	Nfkb1_for	GTC AAC AGA TGG CCC ATA CCT TC	Nfkb1_rev	GTC CTG CTG TTA CGG TGC ATA C
Tnfa	TNFa-1_for	CCA CCA CGC TCT TCT GTC TA	TNFa-1_rev	AGG GTC TGG GCC ATA GAA CT
IL6	IL6_for	GAG GAT ACC ACT CCC AAC AGA CC	IL6_rev	AAG TGC ATC ATC GTT GTT CAT ACA
IL12	IL12b_for	CCG GAC GGT TCAC GTG CTCA	IL12b_rev	CAC TGC CCG AGA GTC AGG GGA
IL1b	IL1b_for	CAA CCA ACA AGT GAT ATT CTC CAT G	IL1b_rev	GAT CCA CAC TCT CCA GCT GCA
Igf1	Igf1_for	GTC TTC ACA CCT CTT CTA CCT G	Igf1_rev	GCT GCT TTT GTA GGC TTC AGT G
Ym1	Ym1_for	CTC TAC TCC TCA GAA CCG TCA G	Ym1_rev	GCA GCC TTG GAA TGT CTT TCT CC
Fizz1	Fizz1_for	GTC CCA GTG AAT ACT GAT GAG AC	Fizz1_rev	GTT GCA AGT ATC TCC ACT CTG G
Mrc1	Mrc1_for	GTC AGA ACA GAC TGC GTG GA	Mrc1_rev	AGG GAT CGC CTG TTT TCC AG
Adam17	Adam17_for	CTC ATC CTG ACC ACT TTG GTG C	Adam17_rev	GTG TGT CGC AGA CTG TAG ATC C
P230	p230_for	GAC CAG CTT GAT GAC GTG ACA C	p230_rev	CCT CGC TCT CCA TAT CAG AAG G
Tpp2	Tpp2_for	CTT CTA TCC AAA GGC TCT CAA GG	Tpp2_rev	CTC TCC AGG TCT CAC CAT CAT G

3.1.6 Animals and Cell lines

C57/BL6 N mouse	FEM (Berlin, Germany)
Gsn $^{-/-}$ mouse	FEM-Bayer (Berlin, Germany)
Gsn $^{+/+}$ mouse	FEM-Bayer (Berlin, Germany)
BV-2 murine microglia cell line	H. Kettenmann (MDC Berlin-Buch, Germany)

3.1.7 Software

GraphPad Prism Version 6, GraphPad Software, Inc. (La Jolla, CA, USA)

Stereo Investigator, MBF Bioscience (Williston, VT, USA)

xcellence Software Olympus Deutschland GmbH (Hamburg, Germany)

Light Cycler 480 Version 1.5.0 F. Hoffmann-La Roche Ltd (Basel, Switzerland)

3.2 Methods

3.2.1 Animals and drug treatment

All procedures conformed to national and institutional guidelines and were approved by an official committee.

Mice lacking gelsolin (*Gsn*$^{-/-}$) have been described in detail previously (26, 51, 122). "Adult" *Gsn* $^{+/+}$ and *Gsn* $^{-/-}$ individuals refer to mice on average below 6 months of age, whereas "aged" animals have been on average older than 16 months of age.

Bromodeoxyuridine (BrdU) was administered intraperitoneally at a dose of 50 g/kg body weight.

3.2.2 Primary postnatal microglia cultures

Cultures of primary mouse microglia were prepared from newborn mice as described in detail previously (123). Briefly, microglial cells were harvested by gentle shake off and seeded at an initial density of 10^6 cells/ml. Cells remained in culture for an additional 24 h before use. The purity of cultures exceeded 98% as verified by regular flow cytometry analyses with CD11b and CD45 staining (rat anti-mouse CD11b and rat anti-mouse CD45). All experiments were performed in DMEM containing 10% fetal calf serum, 1% Pen/Strep and 1% Na-Pyruvate ("complete medium"). LPS was applied at a concentration of 1 µg/ml (123). Recombinant murine IL-4 was used at a concentration of 10 µg/ml. Unless indicated otherwise, 45 min prior LPS or IL-4 stimulation, jasplakinolide was applied at a concentration of 250 nM and cytochalasin D at a concentration of 2 µM.

3.2.3 Cultures of primary adult microglia

The procedure for the cultivation of adult-derived microglia has been described in detail recently (124). Cell suspensions of adult (< 6 months) and aged (> 16 months) mouse brains were seeded into PLL-coated 75-cm^2 cell culture flasks containing a monolayer of neonatal astrocytes. This so-called "substrate culture" was derived from neonatal mixed glial cultures of wildtype mice. After the astrocytic monolayer of the neonatal mixed glial culture had reached confluence, loosely attached microglia were gently shaken off and discarded with the medium. Cultures were then washed once with complete medium, incubated with clodronate (200 µg/ml) in complete medium (48 h, 37°C, 5% CO_2), and vigorously shaken (250 rpm,

37°C, overnight) to deplete any residual neonatal microglia (Figure 5A). Cultures were washed once with phosphate-buffered saline (PBS) and once with complete medium and kept in an incubator (37°C, 5% CO_2) until further use (within 24 to 48 h). Before the addition of the adult cell suspension (Figure 5B), the astrocytic culture received another medium exchange. 24 h after seeding, postnatal mixed glial cultures were washed (3× PBS) and received fresh complete medium. After 7 days, cultures received complete medium with growth factors GM-CSF (5 ng/ml) and CSF-1 (10 ng/ml) to stimulate microglia proliferation. Microglia cells were harvested after 5 days by gentle shake off and seeded at an initial density of 10^6 cells/ml. PCR analysis of DNA isolated from adult microglia cultures showed only one band with the typical length of DNA fragments for both genotypes, confirming the purity of cultures (i.e. no spillover of neonatal cells into adult cultures) (Figure 5C).

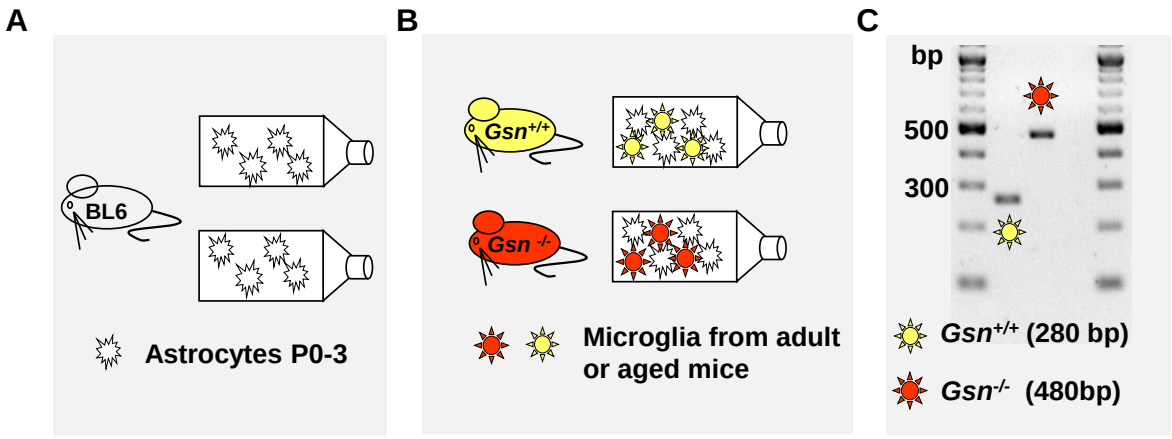

Figure 5 Overview of the "primary adult microglia culture" technique.
Clodronate treatment depletes microglia and leaves a monolayer of postnatal astrocytes (A). Brain suspensions of adult or aged *Gsn*$^{-/-}$ and *Gsn*$^{+/+}$ mice were seeded onto the monolayer of postnatal astrocytes. After 7 days of culture, proliferation was stimulated to obtain microglia cells (B). After harvest of cells from *Gsn*$^{-/-}$ and *Gsn*$^{+/+}$ cultures, purity was tested by DNA isolation and genotyping PCR (C).

3.2.4 *Ex vivo* isolation of adult microglia

Brains of adult *Gsn*$^{+/+}$ and *Gsn*$^{-/-}$ mice were perfused transcardially with 0.9 % saline. Brains were dissociated using the Neural Tissue Dissociation Kit (P) according to the manufacturer's protocol. After dissociation myelin was removed using Myelin Removal Beads. Finally, for magnetic cell sorting ("MACS") via columns, the cell suspension was incubated with CD11b MicroBeads. For calcium measurements, CD11b$^+$ cells were seeded onto 8-well chambered coverslips 24 h before imaging. For migration assay, cells have been seeded immediately on FluoroBlok™ Inserts.

3.2.5 Preparation of oligomeric β-amyloid$_{1-42}$

Amyloid-β (Aβ) protein (1-42) or FITC Aβ (1-42) was dissolved in ice-cold hexafluoro-2-propanol (HFIP) at a concentration of 1 mM. The solution was then incubated at room temperature for 2 h to allow monomerization and randomization of structure (125). The HFIP was removed by vacuum centrifugation using the Eppendorf concentrator until a clear peptide film appeared (126). The film was stored at -80°C. One day before the cell culture experiment, the peptide film was dissolved in DMSO at a concentration of 10 mM with further dilution to 100 µM in PBS and stored at 4°C.

3.2.6 MTT assay

Microglia cell viability was assayed by measuring intracellular reduction of the tetrazolium salt 3-(4,5-dimethylthiazol-2-yl)2,5-diphenyl tetrazolium bromide (MTT) to formazan. The MTT labeling agent was added to the cells at a final concentration of 0.5 mg/ml. The converted dye was solubilized in 10 % SDS in 0.01 M HCl and measured at 550 nm with a plate reader.

3.2.7 LDH assay

Aliquots of the cell culture medium were collected for analysis of lactate dehydrogenase (LDH) activity as described previously (127). Briefly, 50 µl cell culture supernatant or 25 µl standard LDH enzyme was mixed with 200 µl of 212 µM ß-NADH and 25 µl of 22,7 mM Pyruvat, both in 0.1 M KPO_4 buffer. Immediately, absorbance of the reaction was measured 10 times at a wavelength of 340 nm in a plate reader, with 30 s intervall and 10 s shaking in between. LDH concentration was calculated from the slope of the absorbance curve.

3.2.8 NO measurements

Nitric oxide (NO) production was quantified as nitrite accumulation using the Griess' reagent for nitrite as described previously (123). 100 µl of cell culture supernatant was incubated with 100 µl Griess reagent. Absorption was measured at 550 nm with a microplate spectrophotometer. The concentration of nitrite in samples was calculated using a standard curve ranging from 0 µM to 80 µM Sodium-Nitrite.

3.2.9 Cytokine measurements

The concentrations of IL-6 (R&D Systems), IL-1β (R&D Systems), TNF-α (eBioscience) and IGF-1 (R&D Systems) were measured in the cell culture supernatant by ELISA. After pre-dilution of cell culture supernatant samples, the ELISA protocol followed exactly the manufacturer´s instructions.

3.2.10 Messenger RNA isolation, cDNA synthesis and quantitative polymerase chain reactions

Total RNA was extracted using the NucleoSpin® Tissue XS kit according to the protocol. Contaminating DNA was removed by 20 min incubation at 37°C with RQ1 DNase that produces 3´-hydroxyl oligonucleotides. RNA degradation was inhibited by adding 4U/µl RNasin® Inhibitor to the Mastermix. Enzymes were removed afterwards by Phenol/Chloroform extraction followed by ethanol precipitation (128). RNA conconcentration has been measured with Nanodrop® Spectrophotometer and was used for cDNA synthesis which was set up with random hexamer primers and M-MLV reverse transcriptase. For polymerase chain reaction amplification, we used gene-specific primers (listed in chapter 3.1.5) and Light Cycler® 480 SYBR Green I Master. Polymerase chain reaction conditions were as follows: preincubation 95°C, 10 min; 95°C, 10 s, primer-specific annealing temperature, 10 s, 72°C, 15 s (45 cycles). Crossing points of amplified products were determined using the Second Derivative Maximum Method (Light Cycler 480 Version 1.5.0, Roche). Quantification of messenger RNA expression was relative to tripeptidyl peptidase (Tpp) 2 (129). Specificity of polymerase chain reaction products was checked using melting curve analysis and electrophoresis in a 1.5% agarose gel.

3.2.11 Western blotting

Cells were fractionated into cytosolic, membrane and cytoskeletal (pellet) fractions using the Subcellular Protein Fractionation Kit for Cultured Cells according to the manufacturer's protocol. Protein concentration was determined by BCA Protein Assay. Equal amounts of protein were loaded on 10% SDS–polyacrylamide gels and blotted onto polyvinylidene fluoride membranes. Blots were probed with primary and secondary antibodies and developed by an enhanced chemiluminescent detection method. Antibodies were used in the following dilutions: rabbit anti-beta-Actin 1:5000, mouse anti-GAPDH 1:5000, rabbit anti-iNOS 1:200,

rabbit anti-Gelsolin 1:1000, rabbit anti-SRF 1:200, rabbit anti-Cofilin 1:800, rabbit anti-Phospho-Cofilin 1:500, rabbit anti-STAT6 1:500, rabbit anti-Phospho-STAT6 1:500, rabbit anti-HDAC1 1:500, horseradish peroxidase-conjugated goat anti-rabbit IgG 1:2000 and horseradish peroxidase-conjugated goat anti-mouse IgG 1:2000.

3.2.12 ^{14}C-labeled L-arginine uptake studies

Arginine uptake into microglia was measured after 45 min preincubation with 250 nM jasplakinolide or 2 µM cytochalasin D followed by 6 h cotreatment with LPS. Cells were washed twice with 500 µl prewarmed (37° C) wash buffer (137 mM NaCl, 5.4 mM KCl, 1.2 mM $MgSO_4 \cdot 7H_2O$, 2.8 mM $CaCl_2 \cdot 2H_2O$, 10 mM HEPES, and 1 mM KH_2PO_4 [pH 7.4]). Cells were then resuspended in 250 µl of 50 µM L-[^{14}C(U)]arginine] prewarmed wash buffer supplemented with 5 mM L-leucine. The reaction was stopped after 10 min. Samples were washed three times with ice-cold stop solution (10 mM HEPES, 10 mM Tris, 137 mM NaCl, 10 mM nonradioactive l-arginine [pH 7.4]). Cells were then lysed with 0.1% Triton in PBS, and radioactivity was counted in a liquid scintillation counter.

3.2.13 Microglial phagocytosis

Phagocytosis of bacterial particles was assessed using the pHrodo™ Red *S. aureus* Bioparticles® Conjugate for Phagocytosis according to the manufacturer's manual. Postnatal microglia were pretreated with cytoskeletal drugs for 45 min before experimentation.

For the Aβ phagocytosis studies, 5 µM FITC-coupled oligomeric Aβ was added to the microglia cultures. After incubation for 2 h at 37°C, cultures were stained with Hoechst 33342 for 20 min at room temperature. After washing with live cell imaging solution, extracellular fluorescence was quenched by addition of 0.4% trypan blue solution. FITC and Hoechst fluorescence were measured at wavelengths of 485(ex)/535(em) and 340(ex)/460(em), respectively.

3.2.14 Modified Boyden chamber assay

Cells were seeded on BD Falcon™ HTS FluoroBlok™ Inserts (8 µm pore size) at a density of 15 x 10^3 cells/ transwell insert. 100 µM ADP was added to the well below the insert. After 6 h of incubation at 37°C and 5% CO_2, the membranes of the inserts were stained with 10 µm CFSE dye, and then fixed with 4% paraformaldehyde (PFA) and counterstained with 2 µm 4′,6′-diamidino-2-phenylindole (DAPI). Migrated cells below the FluoroBlok membranes

were visualized using an inverted fluorescence microscope. The rate of microglia migration was calculated by counting cells in four different microscope fields of each membrane (at 20x objective magnification). In order to consider basal microglia migration, data is presented as the ratio of microglia migration to ADP / microglia migration without ADP.

3.2.15 Calcium imaging

Ex vivo-isolated microglia were seeded onto Ibidi µ-Slides at a density of 3 x 10^4 cells/well. 24 h after seeding, experiments were performed in HEPES buffer (130 mM NaCl, 4.7 mM KCl, 1 mM $MgSO_4$, 1.2 mM KH_2PO_4, 1.3 mM CaCl2, 20 mM Hepes, 5 mM glucose, pH 7.4). Cells were loaded with Fura-2/AM (5 µM; stock solution dissolved in 20% pluronic F-127) by incubation in HEPES buffer at 37°C for 30 min. After loading, Fura-2 was allowed to de-esterify for at least 10 min at room temperature in standard solution. Cells were monitored with an inverted Olympus IX71 stage equipped with an UPLSAPO X2 40x/0.95 objective. Fluorescence data was acquired on a PC running xcellence software via a cooled CCD camera. For stimulation experiments, 100 µM freshly prepared ATP was applied. Intracellular free Ca^{2+} concentration [$(Ca^{2+})_{int}$] was derived from background-subtracted F340/F380 fluorescent ratios (*R*) after *in situ* calibration according to the following equation: $[Ca^{2+}]_{int}$ (nM) = $K_d \cdot Q \cdot (R - R_{min})/(R_{max} - R)$, where K_d is the dissociation constant of Fura-2 for Ca^{2+} at room temperature (225 nM); Q is the fluorescence ratio of the emission intensity excited by 380 nm in the absence of Ca^{2+} to that during the presence of saturating Ca^{2+}; and R_{min} and R_{max} are the minimal or maximal fluorescence ratios, respectively. R_{min} was measured by perfusion with Ca^{2+}-free HEPES buffer (as described above) containing 10 µM ionomycin. R_{max} was obtained by perfusion with standard solution containing 10 mM $CaCl_2$/10 µM ionomycin. Released Ca^{2+} was calculated by subtracting baseline Ca^{2+} and plotted over time. Ionomycin (viability control after ATP measurements) was applied at 10 µM.

3.2.16 Facial nerve axotomy

For facial nerve axotomy we used 6- to 8-week-old $Gsn^{+/+}$ and $Gsn^{-/-}$ mice. The experimental procedures including subsequent histological analyses have been described in detail previously (130).

3.2.17 Induction of cerebral ischemia

Mice were anesthetized with 1.5% isofluorane and maintained in 1% isofluorane in 69% N_20 and 30% O_2 using a vaporizer. Ischemia was induced by 30 min filamentous middle cerebral artery occlusion (MCAo)/reperfusion as described in detail previously (131).

3.2.18 Histological procedures and imaging

After transcardial perfusion with 0.9% saline followed by 4% paraformaldehyde in 0.1 mol/L phosphate buffer, brains were stored in the fixative for 48 h and then transferred into 30% sucrose in 0.1 mol/L phosphate buffer for 24 h. Coronal sections of 40 µm or 20µm thickness were cut from a dry ice-cooled block on a sliding microtome. Sections were stored at -20°C in cryoprotectant solution containing 25% ethylene glycol, 25% glycerin, and 0.05 mol/L phosphate buffer. All antibodies were diluted in Tris-buffered saline containing 0.1% Triton X-100 and 3% donkey serum. Primary antibodies were rat anti-BrdU 1:500, rabbit anti-Iba1 1:500. FITC- or RhodX-conjugated secondary antibodies were all used at a concentration of 1:250. Immunohistochemistry followed the peroxidase method with biotinylated secondary antibodies, ABC Elite reagent, and diaminobenzidine (DAB) as chromogen.

Confocal microscopy was performed using a spectral confocal microscope (TCS SP5; Leica). Appropriate gain and black level settings were determined on control slices stained with secondary antibodies alone.

The number of $Iba1^+$ cells per volume (Microglia density) was assessed using StereoInvestigator® software. Hippocampal, striatal and facialis nucleus region of the right and left hemisphere were delineated at ×100 magnification and cells counted at ×200 magnification.

3.2.19 DNA isolation and genotyping

DNA was isolated using TRIzol® method according to the manual supplied by the manufacturer. The $Gsn^{+/+}$ gene (280bp) was amplified using the forward 5'-gtggagcaccccgaatt-3' and reverese 5'-ctcagttcaggtatatccatatccatacag-3' primers. The $Gsn^{-/-}$ gene (480 bp) was amplified using forward 5'-attgaacaagatggattgcac-3' and reverese 5'-cgtccagatcatcctgat-3' primers. PCR mastermix was prepared with both, $Gsn^{+/+}$ and $Gsn^{-/-}$ primer pairs. PCR products have been loaded on a 1.5% agarose gel.

4. RESULTS

4.1 Cytotoxicity of the actin toxins

In order to test the effects of different concentrations of the actin filament destabilizer cytochalasin D and the actin filament stabilizer jasplakinolide, two assays were performed. The viability of primary mouse microglia was assessed using the MTT dye assay (Figure 6A) as well as by measuring LDH release (Figure 6B). The concentrations used in subsequent experiments are highlighted by grey bars (Figure 6). Neither 24 hour treatment with cytochalasin D (0.25 µM, 0.5 µM, 1 µM, 2 µM), nor jasplakinolide (63 nM, 125 nM, 250 nM), had an effect on the viability of postnatal primary microglia cells. With higher cytochalasin D concentrations (4 µM, 8 µM), a significant increase in LDH release was observed. Higher dosages of jasplakinolide (500 nM, 1000 nM, 2000 nM) also reduced the MTT signal after cotreatment for 24 hours with 1 µg/ml LPS and significantly increased LDH release with and without LPS challenge. *$p<0.05$ relative to respective controls (i.e. cells not treated with cytochalasin D or jasplakinolide). N=3-5 independent measurements per data point.

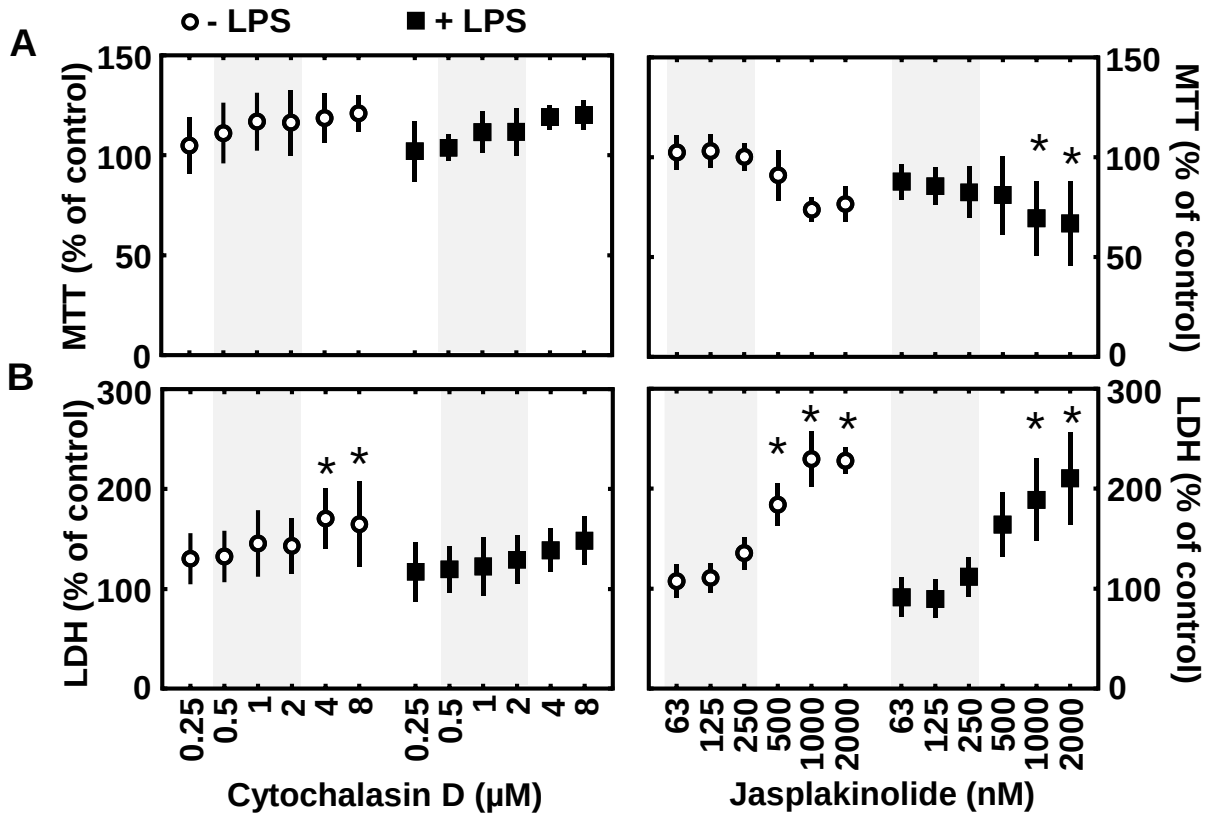

Figure 6 Viability of primary mouse microglia.
MTT dye assay (A) and LDH release (B), were not affected by treatment with either cytochalasin D or jasplakinolide for 24 hours at the concentrations used in subsequent experiments (highlighted by grey bars). However, at higher concentrations, toxic effects were observed for both cytoskeletal drugs. LPS was applied at 1 µg/ml for 24 hours as indicated. One-way ANOVA followed by Dunnett's multiple comparisons test. *$p<0.05$ relative to respective controls (i.e. cells not treated with cytochalasin D or jasplakinolide). N=3-5 independent measurements per data point.

4.2 Expression of actin-regulating proteins after classical activation with LPS and disruption of actin filament dynamics

4.2.1 Analysis of actin-regulating proteins in BV-2 murine microglial cells

To test the microglial expression of pre-selected actin-regulating proteins in the following treatment paradigm, BV-2 cells were stimulated in the absence (-LPS) or presence (+LPS) of LPS for 6 h (Figure 7A) and 24 h (Figure 7B) under three different conditions: For the control (Ctrl) condition, the solvent DMSO was used in equal dilution to the cytochalasin D treatment, cytochlasin D (Cyt) was used at a concentration of 2 µM and jasplakinolide (Jasp) at a concentration of 250 nM. Whole microglia protein extracts were probed by Western blotting with antibodies against gelsolin, serum-response factor (SRF), phospho-cofilin (P-

CFL) and cofilin (CFL). A comparable loading of protein was confirmed by glyceraldehyde-3-phosphate dehydrogenase (GAPDH) staining. After 6 h, gelsolin expression was already upregulated by cytochalsin D and jasplakinolide treatment with and without LPS activation compared to the corresponding control. This effect was even more pronounced after 24 h, especially for the jasplakinolide condition. After 24 h, SRF and P-CFL protein levels were clearly downregulated for jasplakinolide and cytochalasin treatment compared to the control condition. Cofilin expression was not influenced by any treatment tested in this thesis. Interestingly, LPS treatment per se did not influence the expression of the probed proteins.

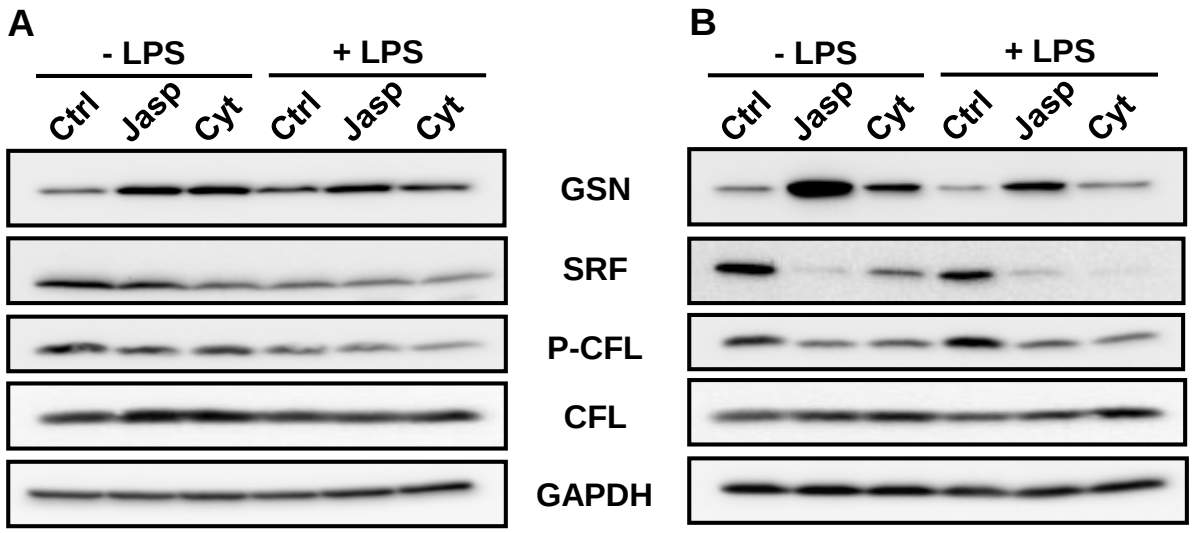

Figure 7 Actin-regulating proteins of classically activated microglia cells.
Western blot of protein extracts of non-LPS (-LPS) and LPS (+LPS) exposed BV-2 microglial cells after 6 h (A) and 24 h (B) probed with antibodies against gelsolin (GSN), serum-response factor (SRF), phospho-cofilin (P-CFL) and cofilin (CFL). Note downregulation of SRF and P-CFL in the presence of both cytoskeletal drugs (cytochalasin D: 2 µM; jasplakinolide: 250 nM) as well as strong upregulation of gelsolin in the presence of jasplakinolide (B). By contrast, activation of cells with LPS did not result in upregulation of actin-binding proteins. Comparable loading of protein was confirmed by glyceraldehyde-3-phosphate dehydrogenase (GAPDH).

4.2.2 Analysis of actin-regulating genes in primary postnatal microglia cells

To test the expression of key genes involved in actin cytoskeleton organization in postnatal primary microglia cells, quantitative real-time PCR was performed after 6 h of treatment (Figure 8). The treatment paradigm was similar to what has been described under 4.2.1. LPS treatment (1 µg/ ml) did not lead to any upregulated mRNA transcription of the tested genes. Expression of gelsolin was also not influenced by disruption of actin filament remodeling with either cytochalasin D or jasplakinolide. In contrast, all the other genes showed increased mRNA transcription after disruption of actin filament remodeling.

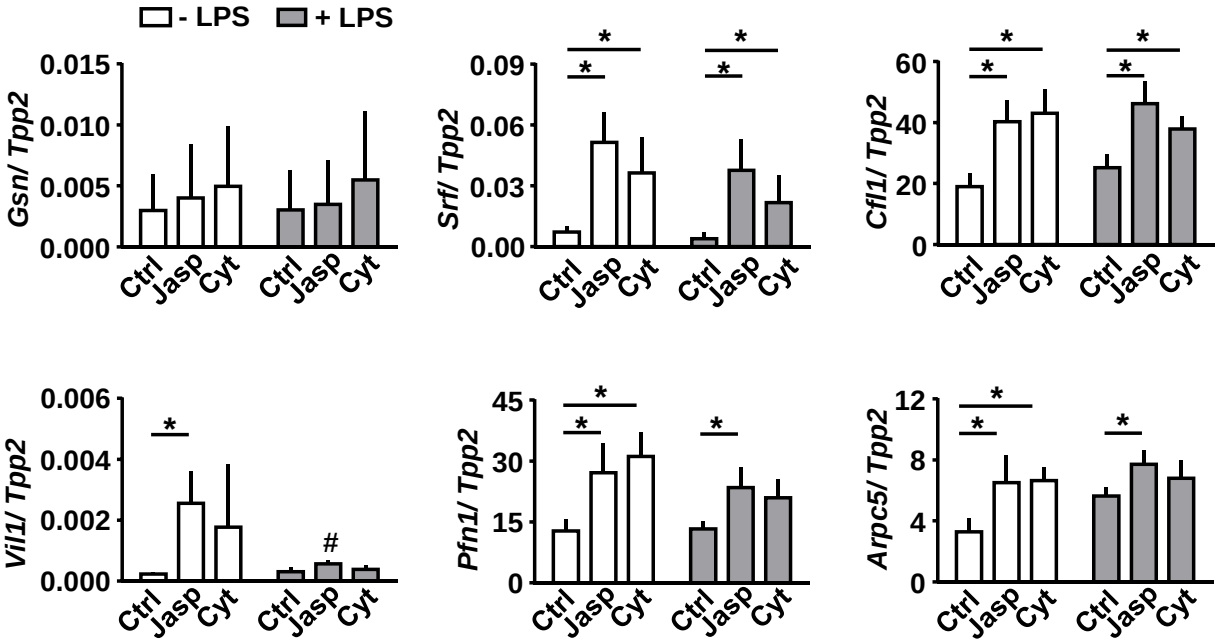

Figure 8 Analysis of mRNA expression of key genes involved in actin cytoskeleton organization.
Primary microglia were exposed to cytochalasin D (2 µM) and jasplakinolide (250 nM) for six hours. Note that activation of microglia with LPS did not increase mRNA transcription of any of the genes investigated. By contrast, disruption of actin filament dynamics resulted in an overall pattern characterized by increased gene transcription independent of activation status. gelsolin (*Gsn*), serum response factor (*Srf*), cofilin 1 (*Cfl1*), vilin 1 (*Vil1*), profilin 1 (*Pfn1*), actin related protein 2/3 complex, subunit 5 (*Arpc5)*, tripeptidyl peptidase 2 (*Tpp2*). Two-way ANOVA followed by Tukey's multiple comparisons test. *p<0.05 within +LPS/ -LPS treatment condition. #p<0.05 between +LPS and -LPS treatment condition. N=4-5 independent measurements per data point.

4.3 Pro-inflammatory phenotype after classical activation of microglia cells with LPS

4.3.1 Release of nitric oxide from microglia cells of postnatal mice is impaired *in vitro*

One hallmark of classical microglia activation is the production and release of high amounts of nitric oxide (NO). Via Griess assay, nitrite (NO_2^-), a breakdown product of NO, can be detected in the cell culture supernatant. On average, 20-24 µM NO_2^- accumulated after 24 hours LPS activation (+LPS) in the cell culture supernatant of primary postnatal cells (Figure 9A). For the control conditions without LPS (-LPS), virtually no nitrite accumulation was detectable. If cytoskeleton remodeling was disrupted with either cytochalasin D (1 µM, 2 µM) or jasplakinolide (125 nM, 250 nM), less nitrite was measured in a concentration-dependent manner (Figure 9A). Primary microglia cells derived from adult and aged $Gsn^{+/+}$ and $Gsn^{-/-}$

mice also responded to LPS challenge with NO release. Here, only a trend towards an attenuated response for *Gsn*$^{-/-}$ microglia of both ages was observed (Figure 9B).

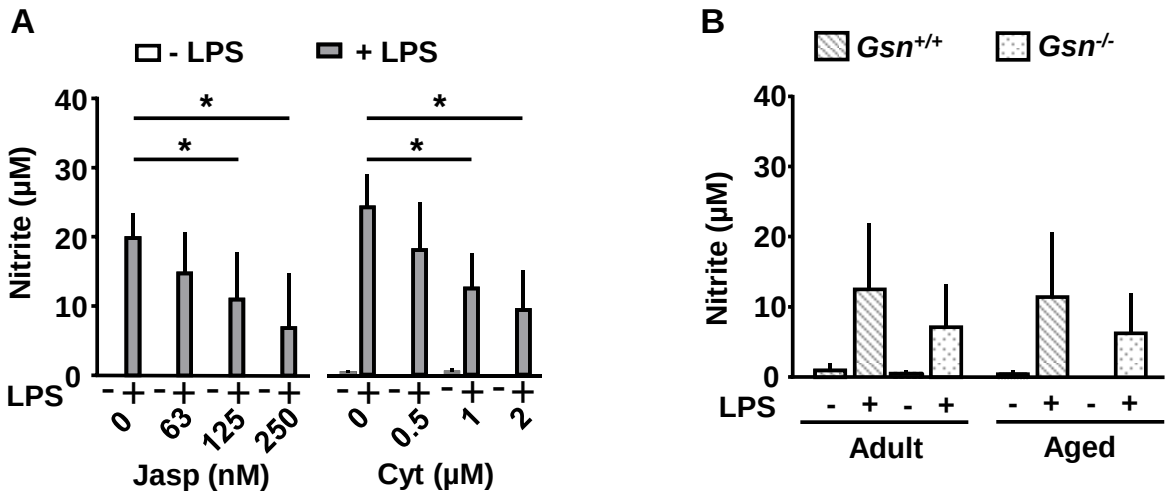

Figure 9 Griess assay after classical microglia activation.
Primary postnatal mouse microglia (A) and microglia cultured from adult (< 6 months, "young") and aged (> 16 months, "old") *Gsn*$^{+/+}$ and *Gsn*$^{-/-}$ mice (B) were stimulated with LPS (1 µg/ml; +) or vehicle (-) for 24 h. (A) In the presence of both cytoskeletal drugs, NO release as measured by the Griess reaction was significantly impaired. (B) At least descriptively, gelsolin deficiency also impaired NO release from adult-derived microglia with no further discernible effect of the factor age. Two-way ANOVA followed by Tukey's multiple comparisons test. *p<0.05 within +LPS/ -LPS treatment condition. N=3-5 independent measurements per data point.

4.3.2. Expression of *iNos* and genes involved in LPS-induced arginine transport and turnover are not regulated on the transcriptional level in response to disruption of actin filament dynamics

In order to dissect the molecular mechanisms underlying decreased NO release with cytoskeletal drugs seen in Figure 9, quantitative gene expression analyses were performed (Figure 10). In microglia cells, production of NO is catalyzed via the enzyme inducible Nitric oxide synthase (iNOS). The substrate for iNOS is the amino acid arginine, which is transported via cationic amino acid transporter 2 (CAT2) across the membrane into the microglia cell. Arginine is not only a substrate for iNOS, it is also a substrate for arginase 1 (ARG1), an enzyme upregulated after "alternative" microglia activation and known to be involved in the urea cycle. Argininosuccinate lyase (ASL) and argininosuccinate synthase 1 (ASS1) are further enzymes involved in the urea cycle.

Expression of *iNos* and *Cat2* was highly upregulated after six hours LPS treatment, but was not influenced by cotreatment with either cytochalasin D (2 µM) and jasplakinolide (250 nM) (Figure 10A). In contrast, *Asl* and *Arg1* are significantly downregulated after LPS treatment. Both genes are not directly involved in the iNOS pathway but play a role for arginine turnover. Again, cotreatment with actin filament destabilizer and stabilizer does not affect expression of these genes (Figure 10B). Expression of *Cat1*, *Cat3* and *Ass1* was not influenced by LPS treatment at all (Figure 10C).

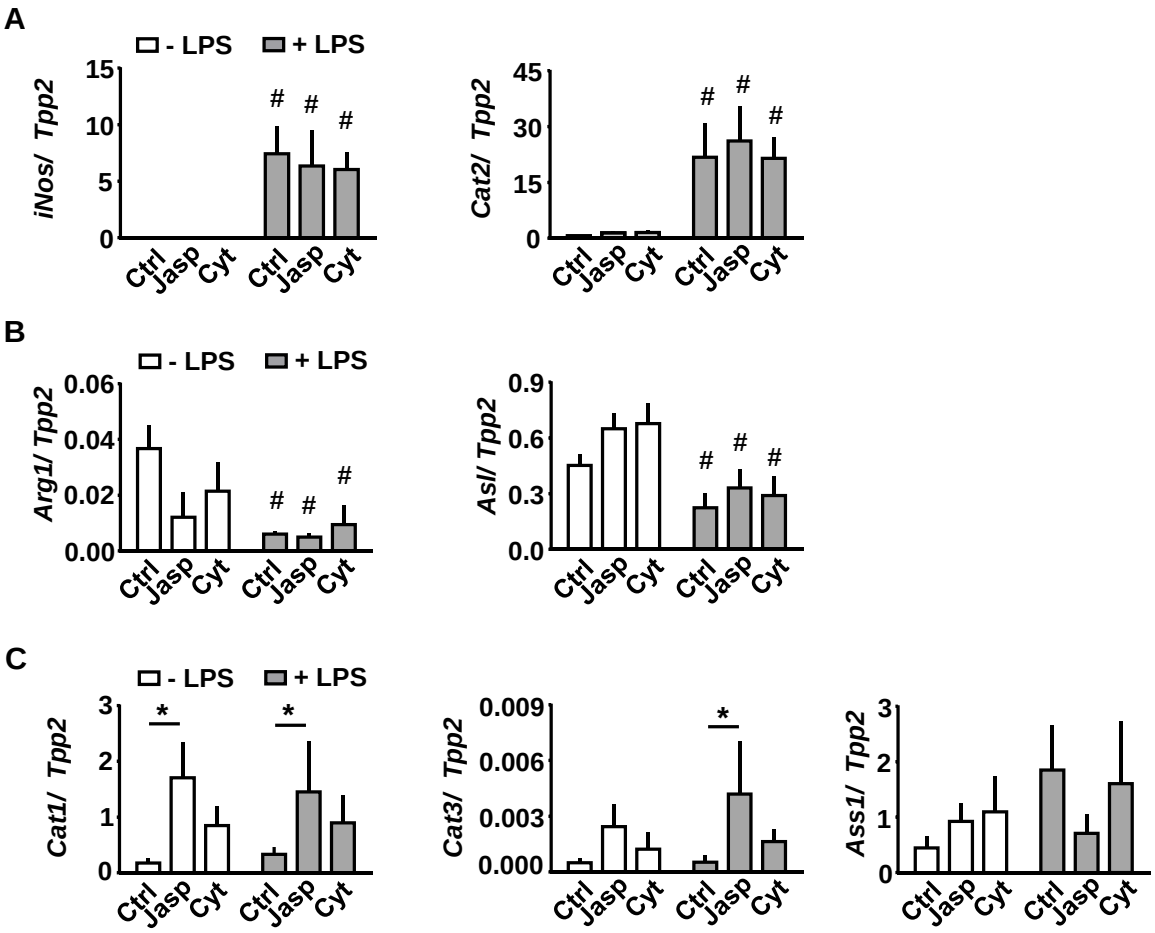

Figure 10 Regulation of genes involved in arginine transport and turnover in primary postnatal microglia at six hours after LPS stimulation.
While LPS significantly induced *iNos* and *Cat2* mRNA expression (A), *Arg1* and *Asl* mRNA levels were reduced (B). No significant effect of either cytoskeletal drug was observed (A, B). *Cat1*, *Cat3* and *Ass1* mRNA expression is not influenced by LPS treatment (C). *iNos* (inducible nitric oxide synthase), *Cat1/2/3* (cationic amino acid transporter 1/2/3), *Arg1* (arginase 1), *Asl* (argininosuccinate lyase), *Ass1* (argininosuccinate synthase 1). Two-way ANOVA followed by Tukey's multiple comparisons test. *p<0.05 within +LPS/ -LPS treatment condition. #p<0.05 between +LPS and -LPS treatment condition. N=4-5 independent measurements per data point.

4.3.3 Protein expression of iNOS after LPS challenge

LPS-challenged microglia showed reduced release of NO in the presence of cytoskeletal drugs (Figure 9). However, gene levels of *iNos* are not influenced by treatment with actin toxins (Figure 10). In order to clarify the causes for this NO reduction (Figure 9) and since the regulation of the transcriptional and translational levels are not necessarily directly related, iNOS protein levels were analyzed via Western Blot. LPS challenge led to an upregulation of iNOS in BV-2 (Figure 11A) and primary postnatal cells (Figure 11B). The protein was detected in the membrane as well as in the cytosolic fraction. Very interestingly, iNOS expression levels clearly decrease after jasplakinolide treatment, as well as after cytochalasin D treatment, occurring in both cell types (BV-2 and primary postnatal). G-actin levels did not change with type of treatment, while F-Actin levels increased under jasplakinolide conditions.

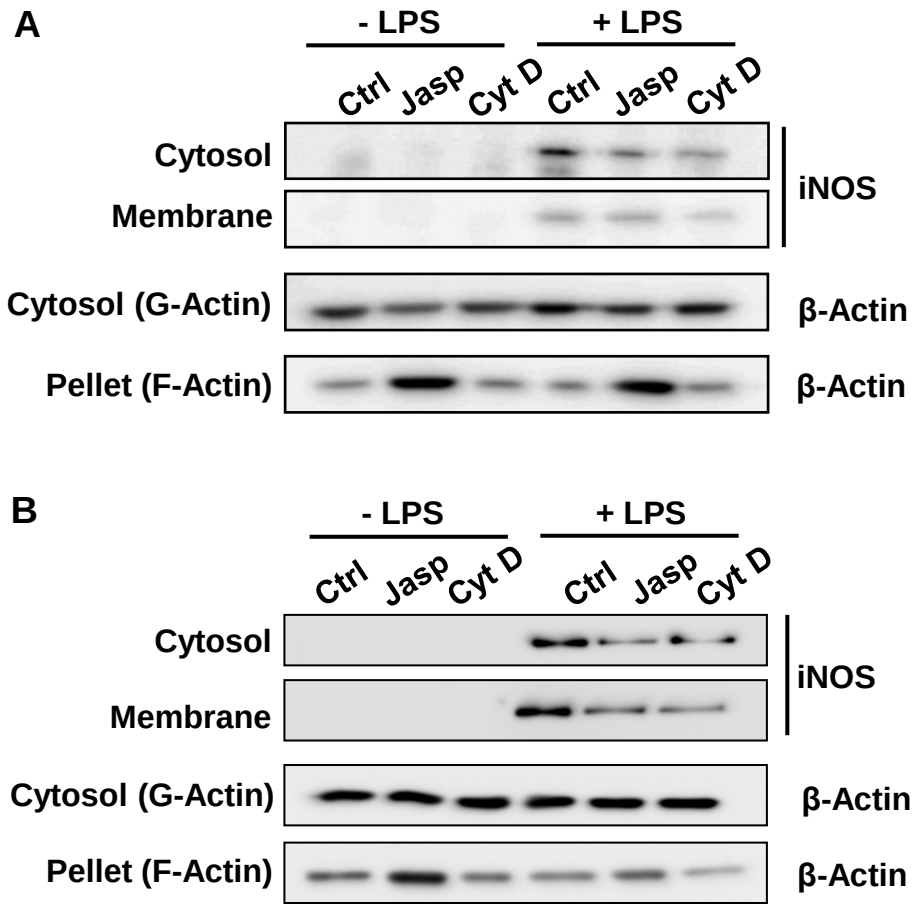

Figure 11 Western blot of protein extracts of non-LPS and LPS-exposed BV-2 microglial cells (A) and postnatal primary cells (B) after six hours incubation.
Note the strong LPS-induced upregulation of iNOS in the cytosolic fraction which is attenuated by both jasplakinolide (250 nM) and cytochalasin D (2 µM). In the corresponding cytoskeletal ("pellet") fractions, the actin polymerizing and stabilizing effects of jasplakinolide are reflected by increased filamentous (F)-actin levels.

4.3.4 Increased L-(^{14}C)-arginine uptake into LPS activated primary postnatal microglia cells

Decreased levels of NO release may also be associated with limited availability of substrate. As regards arginine, it may be linked with changes in arginine uptake. One sensitive approach for measuring the uptake of arginine into the cell is based on radioactively labeled arginine. As shown in Figure 10, expression of *iNos* and *Cat2* is upregulated after LPS activation. Also, iNOS protein levels increase after LPS stimulation (Figure 11). This already indicates that the substrate of iNOS (namely arginine) may be needed in higher amounts. This would result in higher uptake of arginine. As expected, the uptake of arginine was significantly increased after LPS stimulation compared to non LPS stimulation (#p<0.05, Figure 12). Moreover, jasplakinolide treatment also led to a decrease (*p<0.05, Figure 12) of arginine uptake after LPS treatment.

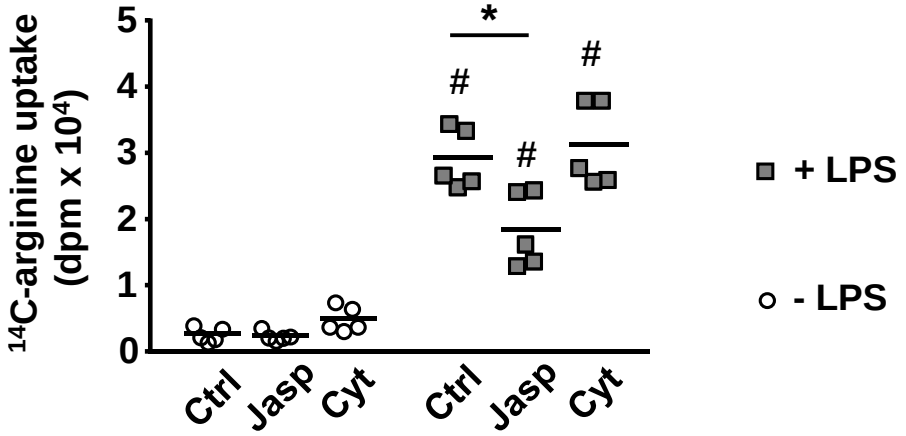

Figure 12 Arginine uptake assay.
Measurement of the uptake of ^{14}C-L-arginine (disintegrations per minute; dpm) into primary postnatal microglia after 6 hours preincubation with LPS, jasplakinolide (250 nM) and cytochalasin D (2 µM). Two-way ANOVA followed by Tukey's multiple comparisons test. *p<0.05 within LPS/non-LPS treatment condition. #p<0.05 between LPS and non-LPS treatment condition. N=5 independent measurements per data point.

4.3.5 Cytokine release after LPS treatment is differentially affected after disruption of actin filament dynamics

To characterize the LPS-induced release pattern of cytokines after cytoskeletal deregulation, cell culture supernatant of primary microglia cells was analyzed after 6 hours post activation (Figure 13A, B) and after 24 hours post activation (Figure 13C, D). An attenuated secretion of tumor necrosis factor (TNF-α) from primary postnatal microglia cultures was observed after treatment with 125 nM and 250 nM jasplakinolide and 1 µM and 2 µM cytochalasin D. Gelsolin deficiency also led to decreased release of TNF-α after LPS activation from microglia cells of aged mice (Figure 13B). Like TNF-α, interleukin-6 (IL-6) also follows the classical secretion pathway via entering the endoplasmic reticulum - Golgi complex. Disruption with jasplakinolide (250 nM) led to decreased release of IL-6 while cytochalasin D treatment did not significantly impair IL-6 release from microglia cells (Figure 13C). In contrast to IL-6 and TNF-α, IL-1β is secreted via an unconventional pathway, without entering the ER and Golgi apparatus. As expected, LPS activation increased IL-1β levels in the cell culture supernatant. Jasplakinolide treatment (63, 125, 250 nM), but not cytochalasin D, led to increased secretion of IL-1β (Figure 13D). This effect does not seem to be regulated on the transcriptional level. Although all the tested "M1" pro-inflammatory genes (*Il-6*, *Il-1β*, *Il-12*, *Nfkb*, *Tnf-α*) are upregulated after LPS treatment in primary postnatal microglia cells, disruption of the actin filament with cytochalsin D (2 µM) or jasplakinolide (250nM) did not alter gene transcription significantly 6 hours post treatment (Figure 13E). *Adam17* and *p230* are genes encoding for proteins involved in processing and trafficking of TNF-α. Both are not affected by LPS activation or actin cytoskeletal disruption with Jasp/ Cyt (Figure 13E).

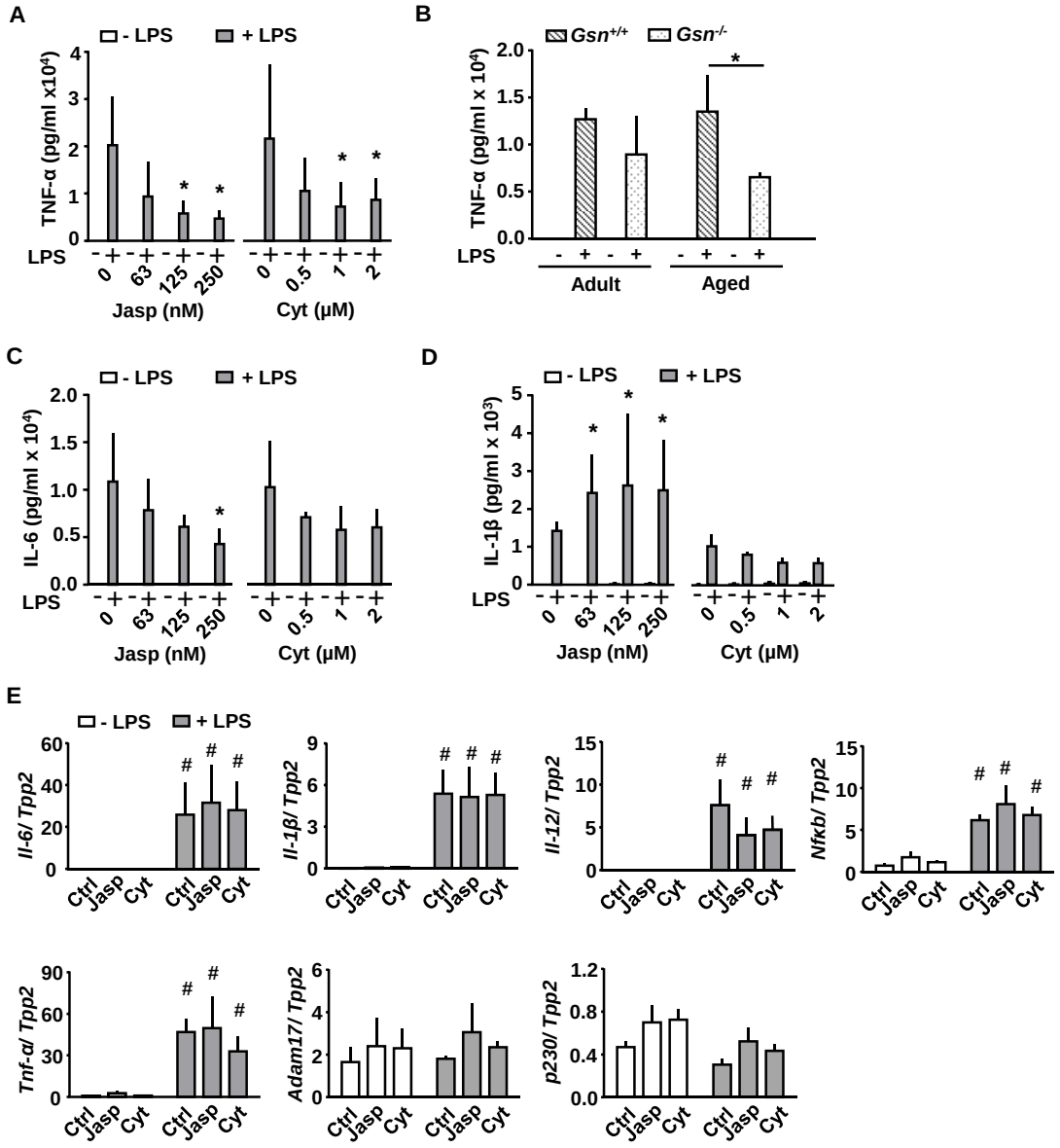

Figure 13 Cytokine release and transcription from classically activated microglia. Disruption of actin filament dynamics differentially affects conventional and unconventional cytokine release from 1 μg/ml LPS-activated microglia (A-D) TNF-α release from primary postnatal microglia (A) as well as from primary adult (~ 6 months) and aged (~16 months) microglia derived from *Gsn*$^{+/+}$ and *Gsn*$^{-/-}$ mice (B) was measured after six hours incubation with LPS. IL6 release (C) and IL-1β release (D) from primary postnatal microglia was measured after six and 24 hours incubation with LPS, respectively. Actin filament stabilization with jasplakinolide significantly increases IL-1β release ("unconventional" pathway of cytokine release) (D). Expression of genes associated with classical microglia activation (*Il-6, Il-1b, Il-12, Nfκb, Tnf-α*) and maturation of TNF-α (*Adam17, p230*) after 6 hours incubation with LPS and/or cytoskeletal drugs (cytochalasin D: 2 μM; jasplakinolide: 250 nM) (E). While LPS strongly induced transcription of M1 genes, we did not observe any significant effect of either cytoskeletal drug (E). Two-way ANOVA followed by Tukey's multiple comparisons test. *p<0.05 within LPS/ non-LPS treatment condition. #p<0.05 between LPS and non-LPS treatment condition. N=3-5 independent measurements per data point. *Nfκb* (nuclear factor of kappa light polypeptide gene enhancer in B cells 1), *Tnf* (tumor necrosis factor), *Il-6* (interleukin 6), *Il-1β* (interleukin 1 beta), *Adam17* (a disintegrin and metallopeptidase domain 17), *p230* (trans-golgi p230), *Tpp2* (tripeptidyl peptidase 2)

4.4 Alternative activation of microglia cells with IL4

4.4.1 Disruption of actin filament dynamics impairs IGF-1 secretion and expression of IL-4 responsive genes

The neurotrophic insulin-like growth factor 1 (IGF-1) is released *in vivo* from activated or proliferating mouse microglia after ischemic injury (95). IL-4 (10 ng/ml) stimulation for 24 h of primary postnatal microglia *in vitro* led to a twofold increase of IGF-1 levels (Figure 14A) and up to twofold higher gene expression (Figure 14B) with p-values less than 0.05 (between – IL-4 and + IL-4 treatment condition). When comparing the secretion and expression levels between absence and presence of toxins (cytochalsain D 2 µM, jasplakinolide 250 nM), the amount of secreted IGF-1 (Figure 14A) and the mRNA levels of *Igf-1* (Figure 14B) is significantly smaller after impairment of cytoskeleton remodeling. When investigating other IL-4 responsive genes described in alternative microglia activation *in vivo* and *in vitro,* such as *Ym1*, *Fizz1*, *Mrc1* and *Arg1*, the attenuating effect of the toxins on alternative activation is also visible (Figure 14C). In line with mRNA expression data of cationic amino acid transporters 1-3 after classical microglia activation (Figure 10A, C), only *Cat2* is upregulated after IL-4 treatment (Figure 14D). Toxins (Jasp, Cyt) did not lead to downregulated *Cat* mRNA expression (Figure 14D) as seen for IL-4 responsive genes (Figure 14B, C).

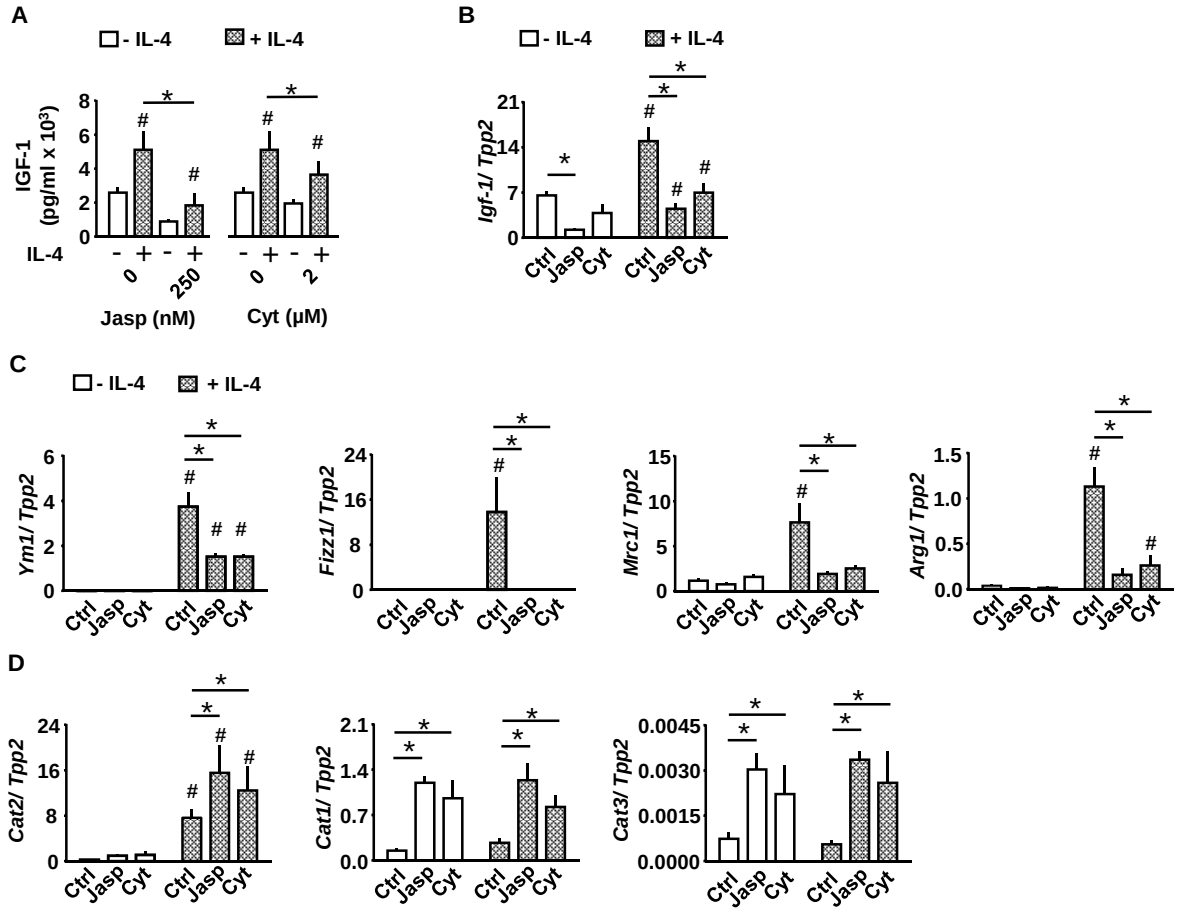

Figure 14 ELISA (A) and quantitative Real-Time PCR (B, C, D) of 24 h alternative activated postnatal primary microglia.
IGF-1 release is impaired after disruption of actin filament dynamics (A). Cytoskeletal drugs (jasplakinolide: 250 nM; cytochalasin D: 2 µM) significantly inhibit transcription of *Igf-1* (B) and key genes implicated in alternative activation of microglia (C). IL-4 treatment leads to upregulation of *Cat2* but does not influence *Cat1* and *Cat3* mRNA expression (D). IGF-1, *Igf-1* (insulin-like growth factor 1); *Ym1* (chitinase-3-like protein 3); *Fizz1* (found in inflammatory zone 1); *Mrc1* (macrophage mannose receptor 1), *Arg1* (arginase 1), *Cat1-3* (cationic amino acid transporter 1-3) Two-way ANOVA followed by Tukey's multiple comparisons test. *$p<0.05$ within – IL-4/ + IL-4 treatment condition. #$p<0.05$ between – IL-4 and + IL-4 treatment condition. N=4-5 independent measurements per data point.

4.4.2 Transcriptional inhibition after cytoskeletal disruption is regulated by the IL-4/ STAT6 pathway

In order to examine the molecular mechanism involved in decreased expression of IL-4 induced genes (Figure 14B, C), the IL-4/ STAT6 signalling pathway was analyzed by monitoring i) STAT6 phosphorylation in the cytoplasm and ii) the accumulation of pSTAT6 in the nucleus (Figure 15). Compared to the control condition, neither treatment with cytochalasin D (2 µM) nor jasplakinolide (250 nM) influenced the phosphorylation process of STAT6 in the cytoplasm after 60 minutes of IL-4 activation (Figure 15, "Cytosol+IL-4"). The accumulation of pSTAT6 clearly increases IL-4 activation in the nucleus, and cytoskeletal

disruption leads to the appearance of reduced abundance of the transcriptional activator pSTAT6 (cp. Figure 15, "Nucleus+IL-4"). GAPDH and HDAC1 were blotted as loading controls for the cytosolic and nuclear fractions, respectively. Protein levels of both did not differ within and between the treatments.

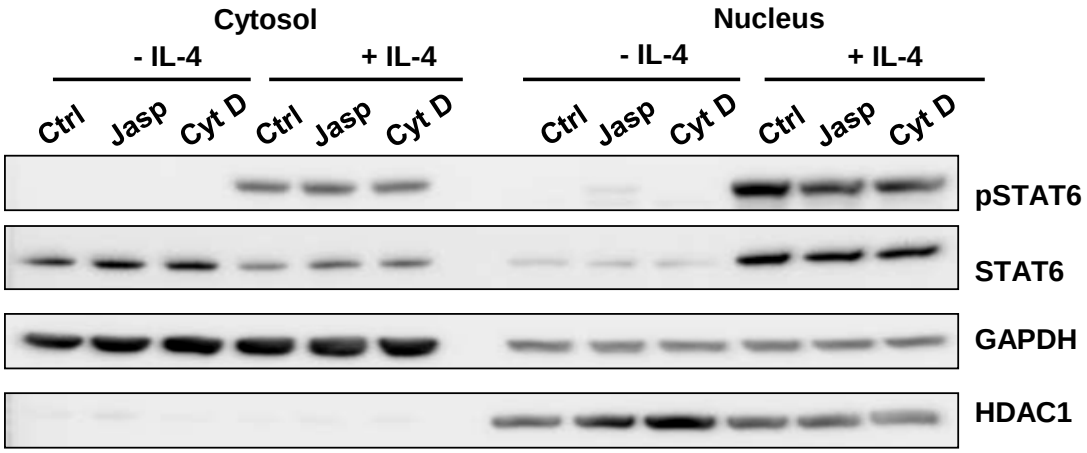

Figure 15 Western Blot of fractionated BV-2 microglia lysates after 60 minutes absence or presence of IL4.
IL-4 treatment induces the cytoplasmic phosphorylation of STAT6 and the transport into the nucleus. The nuclear IL-4 dependent increase of pSTAT6 levels is attenuated in the presence of cytoskeletal drugs (cytochalasin D 2 µM, jasplakinolide 250 nM). GAPDH and HDAC1 serve as loading controls for the cytosolic and nuclear fraction, respectively. IL-4 (interleukin-4); pSTAT6 (phosphorylated signal transducer and activator of transcription 6); STAT6 (signal transducer and activator of transcription 6); GAPDH (glyceraldehyde-3-phosphate dehydrogenase); HDAC1 (histone deacetylase1)

4.5 Migration, phagocytosis and proliferation of microglia cells after disrupting actin remodeling

The actin cytoskeleton is the key component involved in regulation of migration, phagocytosis and proliferation. These features are important for immune cells, i.e. migration towards an injury site, phagocytosis of cell debris or pathogens and proliferation in response to stimuli.

The migration towards ADP was assessed by a modified Boyden chamber assay in primary postnatal cells treated with either vehicle (Ctrl), jasplakinolide (250 nM) or cytochalasin D (2 µM) (Figure 16A). Migration towards ADP was reduced by > 50% after treatment with actin toxins when compared to the control condition. Also, phagocytosis of bacterial particles was reduced after treatment with these toxins at the above mentioned concentrations (Figure 16B).

While cytochalasin showed a strong effect already at a very low concentration (0.5 µM), jasplakinolide reduced phagocytosis only at high concentrations (250 nM) - but not at lower concentrations (63, 125 nM). Migration of *ex vivo* isolated $CD11b^+$ cells obtained from adult and aged mouse brains yielded similar effects. Reduced migration towards ADP was observed in $Gsn^{-/-}$ relative to $Gsn^{+/+}$ microglia, but no difference was detected between adult and aged animals (Figure 16C). Similar to primary postnatal microglia treated with cytoskeletal drugs (Figure 16B), gelsolin-deficiency reduced phagocytosis of bacterial particles by primary microglia cultured from adult and aged mice (Figure 16D). *In vitro* proliferation was assessed by counting and comparing the $Gsn^{+/+}$ and $Gsn^{-/-}$ cells after harvest from the astrocytic layer. Gelsolin deficient cells proliferate at a lower rate compared to $Gsn^{+/+}$ cells. Once more, no influence of age could be detected (Figure 16E).

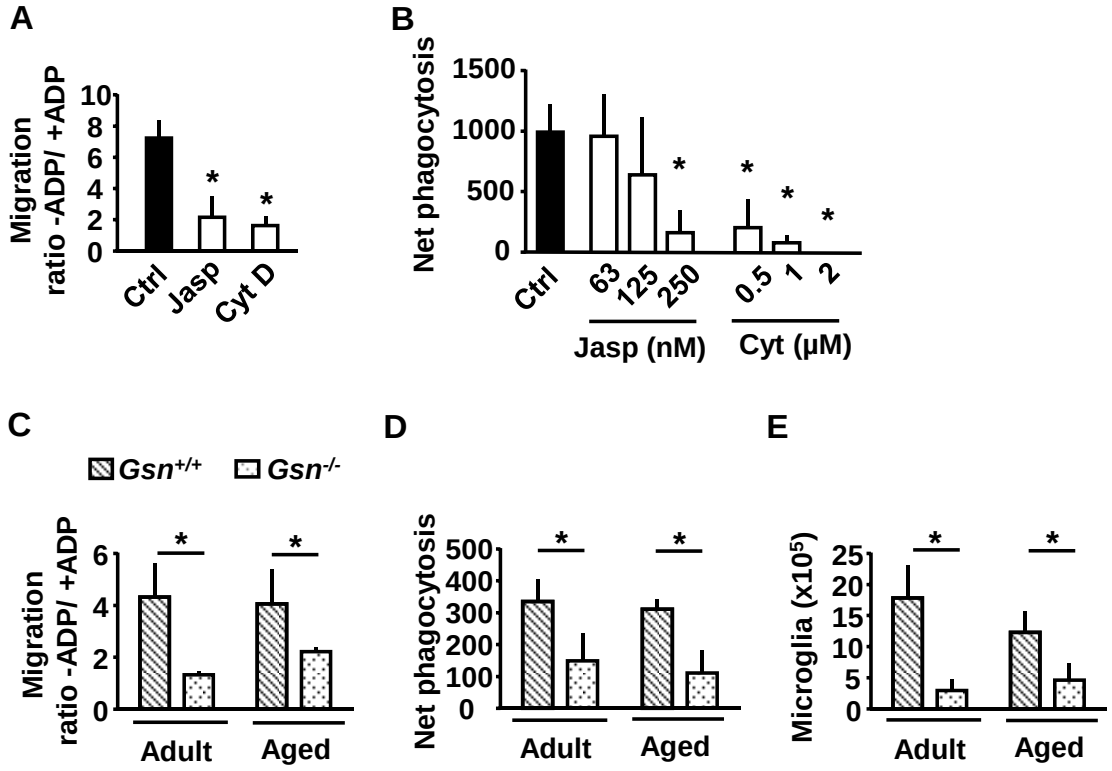

Figure 16 Migration, phagocytosis and proliferation of microglia cells after modulation of actin dynamics.
Primary postnatal microglia cells were treated with cytoskeletal drugs (jasplakinolide/ cytochalasin D) to study migration behavior towards ADP (A) and phagocytosis of bacterial particles (B). $Gsn^{+/+}$ and $Gsn^{-/-}$ microglia derived from mouse brains of different age show reduced migration (C), phagocytosis (D) and proliferation (E) independent of age. One-way ANOVA followed Dunnett´s multiple comparisons test, *$p<0.05$ in comparison to Ctrl condition (A, B). Two-way ANOVA followed by Tukey's multiple comparisons test, *$p<0.05$ (C, D, E). N=3-4 independent measurements per data point.

4.6 Cytoskeletal disruption in a disease context – Amyloid ß treatment *in vitro*

It is widely accepted among scientists that microglia play an important role in the process and pathological outcomes of Alzheimer's disease. Several roles of microglia affecting the outcomes of Alzheimer`s disease have been described so far, but it is not even clear to date, whether microglia have a positive or negative overall impact on the disease. Activated microglia trigger the chronic inflammation observed in Alzheimer's brains and have been found to surround senile amyloid plaques. The soluble oligomeric amyloid β (oAβ) is a precursor of the senile plaque and can be found in the brain and the CSF. Levels of oAβ correlate with cognitive decline (132). Oligomeric Aβ can also induce M1-like microglial activation (133).

The *in vitro* experimental setup employed here was developed to test whether interference with actin dynamics influences the uptake of oligomeric amyloid ß (1-42) and is capable to alter the subsequent mRNA induction of pro-inflammatory proteins such as *iNos*.

The *in vitro* uptake of FITC coupled oAß is shown in Figure 17A. Compared to non-treated cells (100 % uptake of oAß-FITC; dashed line), incubation with jasplakinolide and cytochalasin D led to impaired uptake of oAß-FITC as measured in a plate reader. Importantly, extracellular fluorescence was quenched with trypan blue solution before each measurement and additional Hoechst nuclear staining was applied. No different Hoechst fluorescence intensities between treatments were observed, indicating equal seeding densities. Treatment with cytochalasin D and jasplakinolide reduced the uptake of the oligomeric Aß over 40% for jasplakinolide and over 60% for cytochalasin D on average (Figure 17A). Expression of pro-inflammatory *iNos* in primary postnatal mouse microglia was assessed by quantitative Real-Time PCR. A slight upregulation was detected after treatment with 10 µM oAβ for six hours only in the control condition (Ctrl, +Aβ). Treatment with jasplakinolide and cytochalsain D, on the other hand, impeded the upregulation of *iNos* after oAβ treatment (Figure 17B).

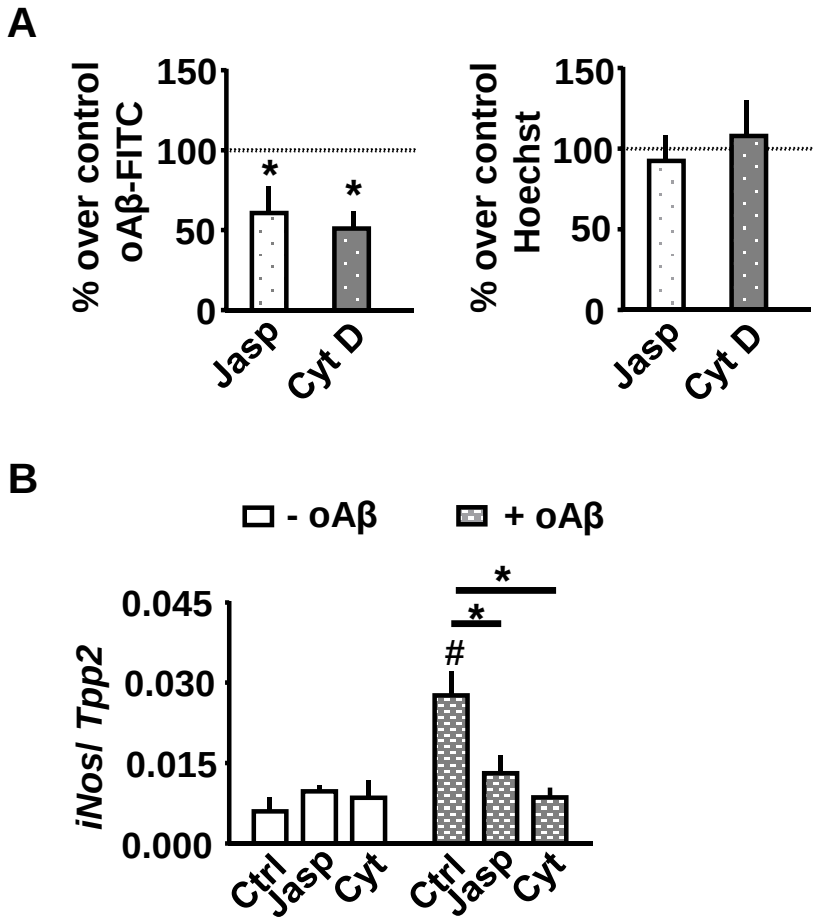

Figure 17 Uptake of oligomeric FITC-amyloid β and *iNos* gene expression by postnatal primary microglia.
The uptake of oAβ is reduced with treatment of cytoskeletal drugs jasplakinolide and cytochalasin D. Equal microglia seeding densities were confirmed by Hoechst-staining. Dashed lines indicate 100% uptake of oAβ (A). Oligomeric amyloid β influences mRNA expression of *iNos* only in the absence of jasplakinolide and cytochalasin D, as measured by qRT-PCR (B). One-way ANOVA followed Dunnett´s multiple comparisons test, *p<0.05 in comparison to 100 % uptake of oAß condition (dashed line) (A). Two-way ANOVA followed by Tukey's multiple comparisons test. *p<0.05 within +LPS/ -LPS treatment condition. #p<0.05 between +LPS and -LPS treatment condition (B). N=3 independent measurements per data point.

4.7 Increase of proliferating IBA-1 (ionized calcium binding adaptor protein 1) labeled cells in the peri-ischemic area after experimental stroke

Previous studies already showed increased infarct size and neuronal vulnerability after oxygen and glucose depriviation (OGD) in gelsolin deficient mice (26). The peri-infarct area ("penumbra") is a region surrounding the ischemic core. It includes reperfused tissue consisting of metabolically active cells. Within this area, microglia and invading macrophages (both IBA-1^+) are "activated", highly proliferative and trigger post-stroke inflammation. The *in vitro/ ex vivo* studies on *Gsn*$^{+/+}$ and *Gsn*$^{-/-}$ microglia described earlier in this thesis (Chapter 4.5) revealed reduced migration and proliferation of microglia (Figure 16C, E). Here, we observed less BrdU$^+$IBA-1^+ (proliferating) cells 3 days after 30 min MCAo, depicted in Figure 18A with representative pictures. After normalizing to all IBA-1^+ cells in the peri-infarct area, less proliferating microglia cells (BrdU$^+$IBA-1^+) are counted in *Gsn*$^{-/-}$ brains (Mean ± SEM 35 ± 7, n=4) three days after a 30 min MCAo compared to the analyzed *Gsn*$^{+/+}$ brains (Mean ± SEM 55 ± 4, n=5) (unpaired student's t-test, $p<0.03$; Figure 18B).

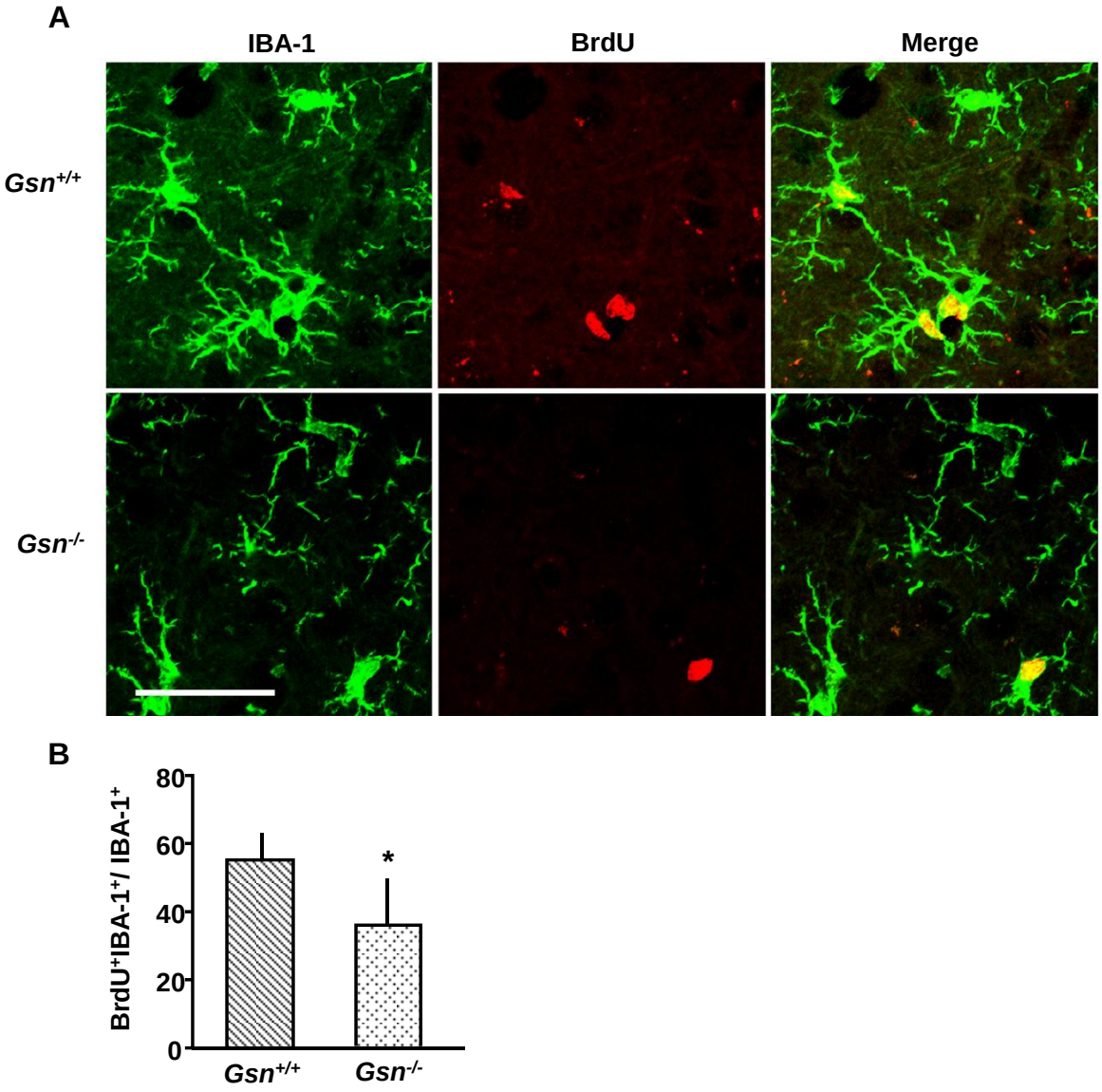

Figure 18 IBA-1$^+$ cells within the peri-ischemic area differently proliferate (BrdU$^+$) in *Gsn*$^{+/+}$ and *Gsn*$^{-/-}$ mice.
Representative pictures showing IBA-1$^+$/ BrdU$^+$ cells in the peri-infarct area after 30 min MCAO (72 hours of recovery) (A). Cell counting analysis evidence the reduced proliferative capacity of IBA-1$^+$ in gelsolin deficient mice (B) *p<0.05 unpaired student's t-test. N=4-5 independent measurements per data point. Scale bar 40µm.

4.8 Gelsolin deficiency leads to increased intracellular Ca^{2+} levels in *ex vivo* microglia cells from adult and aged mice

Gelsolin is a calcium dependent protein and plays a key role in calcium homeostasis. Primary *Gsn*$^{-/-}$ neurons are characterized by increased calcium levels compared to controls. The protective action of Gelsolin in neurons is associated to the maintenance of the intracellular Ca^{2+} homeostasis by modulation of calcium channel and NMDA receptor activities (54). Disturbed calcium homeostasis has implications for proliferation, migration and phagocytosis as well as for many other characteristics of a living cell, because calcium is a common and versatile second messenger in cells. We monitored intracellular microglia Ca^{2+} levels using the Ca^{2+}-sensitive dye Fluo-2/acetoxymethylester (AM). Already at baseline, *Gsn*$^{-/-}$ microglia exhibited higher intracellular Ca^{2+} levels compared to *Gsn*$^{+/+}$ microglia (Figure 19A, B). No interaction with age was found (Figure 19B). After application of 100 µM ATP, microglia cells responded with increased intracellular calcium levels, which was significantly higher in "aged" *Gsn* deficient cells (Figure 19A, C). To confirm the responsiveness of the cells and the detection system, at the end of each experiment, cells were exposed to 10 µM of the calcium ionophore Ionomycin (Figure 19A).

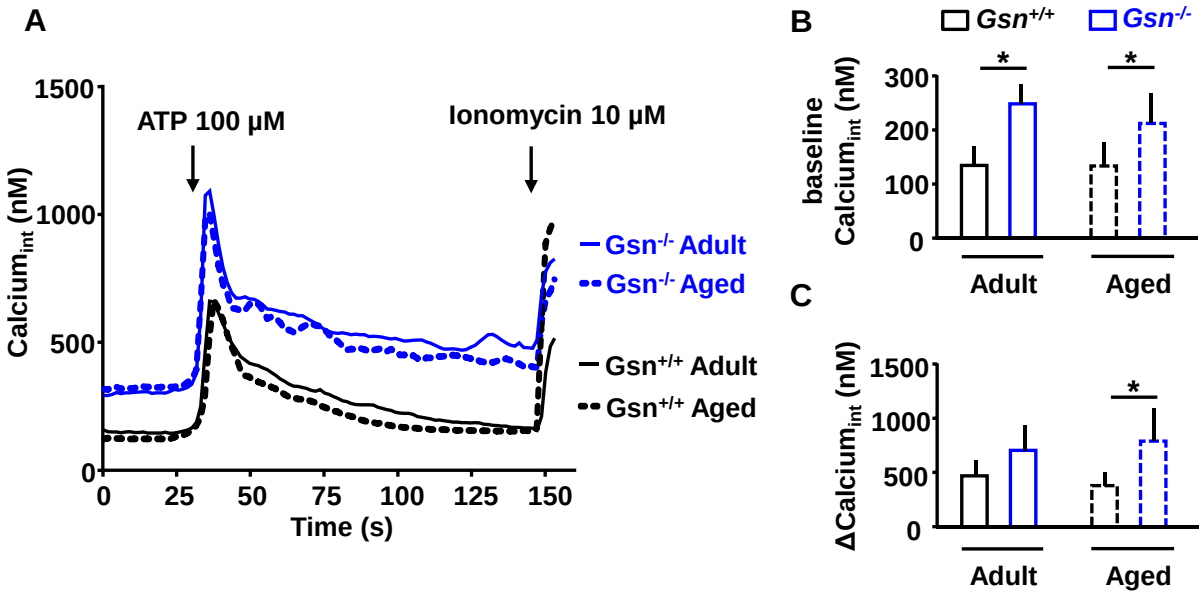

Figure 19 Calcium imaging of *ex vivo* isolated microglia cells from adult or aged *Gsn*$^{+/+}$ and *Gsn*$^{-/-}$ mouse brains.
Representative curves of intracellular Ca^{2+} and the response after ATP and Ionomycin application (A). Compared to *Gsn*$^{+/+}$, baseline intracellular calcium levels are significantly higher in *Gsn*$^{-/-}$ microglia cells (B). The average response amplitude is significantly higher in *Gsn* deficient microglia cells from aged animals (C). Two-way ANOVA followed by Tukey's multiple comparisons test, *$p<0.05$. N=5-8 independent measurements (wells) per data point.

4.9 Microglia density increases with age but is not influenced by *Gsn*$^{-/-}$ genotype

It has been shown that microglia biology changes with age (134, 135). Hence, the interaction of *Gsn*$^{+/+}$ and *Gsn*$^{-/-}$ microglia with the factor age was tested by determination of the microglia density under physiological/ non-pathological conditions. Therefore, IBA-1^{+} cells were immunohistochemically stained and then quantified according to a semi-quantitative counting analysis (Figure 20). IBA-1^{+} microglia are scattered all over the brain, including the striatum and hippocampus of both, *Gsn*$^{+/+}$ and *Gsn*$^{-/-}$ animals, with higher densities associated with aged animals (Figure 20A, B). Within the hippocampus of *Gsn*$^{+/+}$ animals, an increase from 208 ± 7 cells to 269 ± 7 cells/mm^2 was found (Mean ± SEM, n=12). The number of cells within the hippocampus of *Gsn*$^{-/-}$ animals increased from 215 ± 6 cells to 258 ± 6 cells/mm^2 (Figure 20A). IBA-1^{+} microglia of the striatum increased from 257 ± 10 cells to 309 ± 9 cells/mm^2 for *Gsn*$^{+/+}$ animals and from 249 ± 11 cells to 288 ± 10 cells/mm^2 for *Gsn*$^{-/-}$ animals (Mean ± SEM, n=12). No interaction of age could be detected between *Gsn* deficient and wildtype mice (Figure 20B).

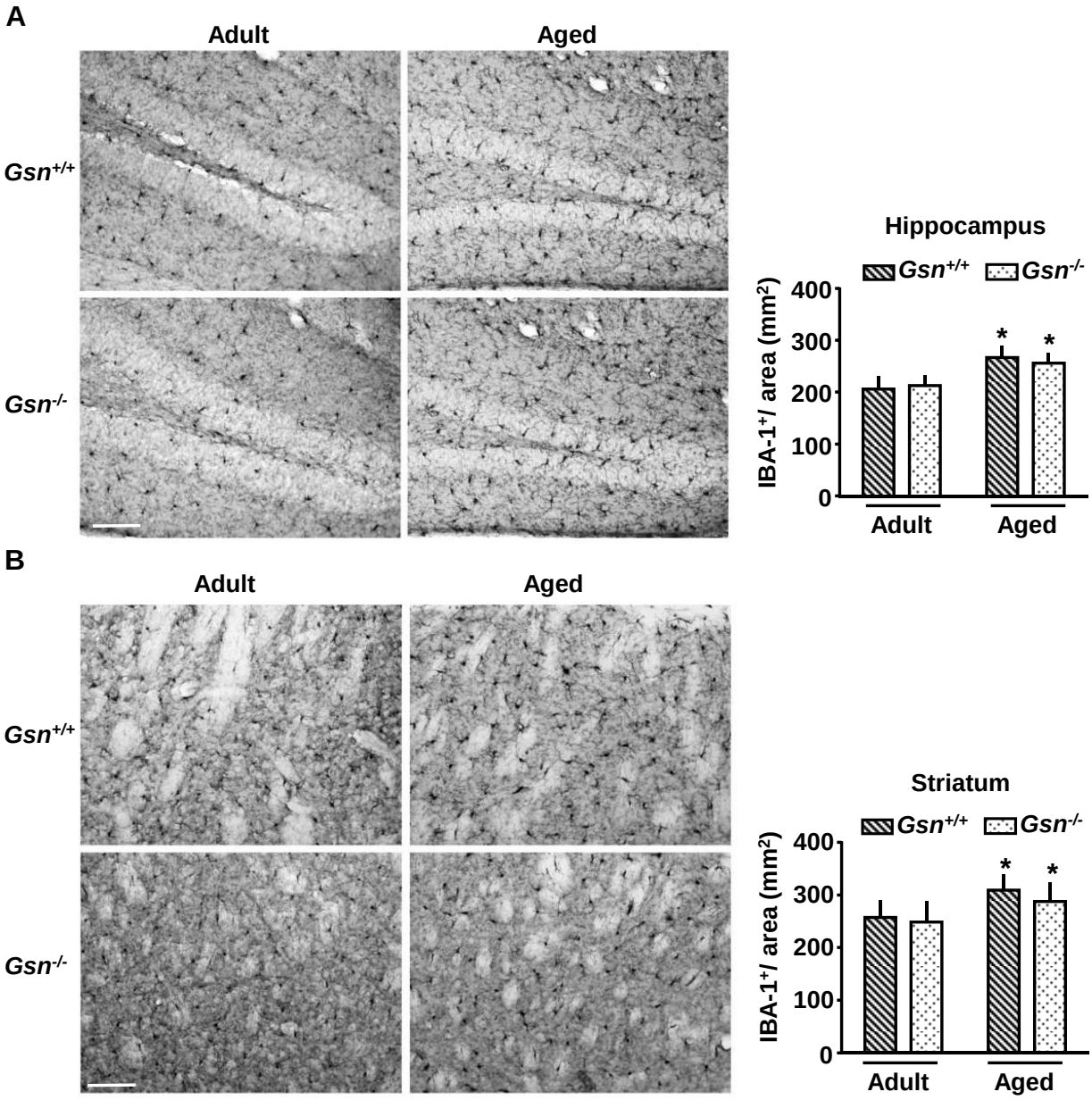

Figure 20 Microglia density in *Gsn*$^{+/+}$ and *Gsn*$^{-/-}$ mouse brains of different age as assessed with IBA-1^{+} staining.
IBA1^{+} cells are depicted and counted in two different brain regions, hippocampus (A) and striatum (B). *p<0.05, two-way ANOVA followed by Tukey's multiple comparisons test. N=12 independent measurements per data point. Scale bar 100µM.

4.10 Microglia density within the *nucleus facialis* is reduced in *Gsn*$^{-/-}$ mice after facial nerve axotomy

After axotomy, *in vivo* proliferation of microglia cells was assessed within the contralateral and ipsilateral *nucleus motorius nervi facialis* of brain stem sections stained with IBA-1. Data is represented as increase (%) of counted IBA-1^{+} cells in the *nucleus facialis* on the ipsilateral side over cells counted on the contralateral side (= 100%). Three days after axotomy, both genotypes showed typical signs of microglia activation in the ipsilateral facial nucleus. Gelsolin deficiency significantly reduced the increase in activated microglia (Figure 21).

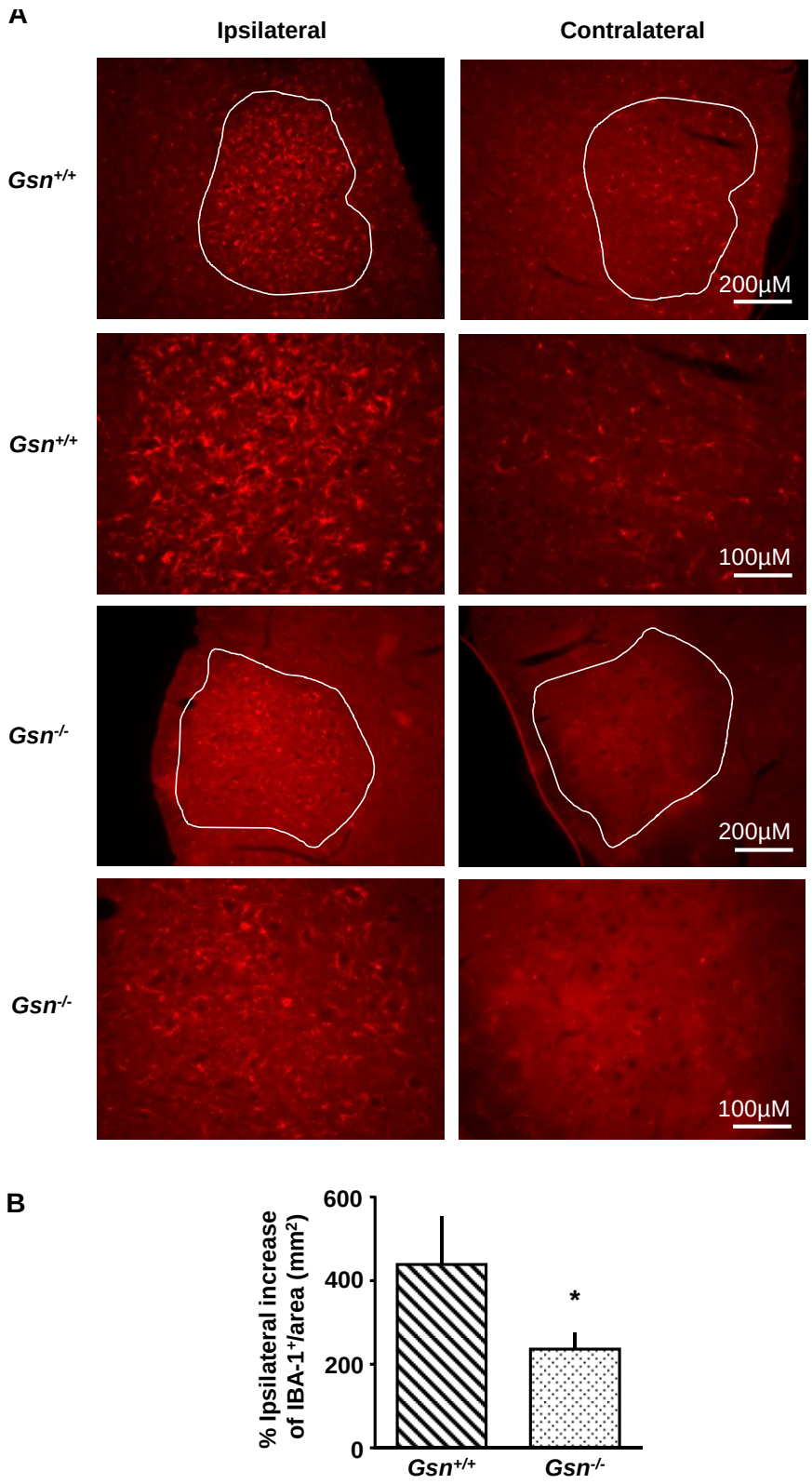

Figure 21 Microglia density in the contralateral and ipsilateral *nucleus facialis* of *Gsn*$^{+/+}$ and *Gsn*$^{-/-}$ was assessed with IBA-1 staining and cell counting after axotomy. Representative pictures of IBA-1 staining at two different magnifications. Delineated are the contralateral and ipsilateral region of the *nucleus facialis* (A). Results of cell counting are presented as mean percentage increase of counted IBA-1^{+} cells in the *nucleus facialis* on the ipsilateral side over cells counted on the contralateral side (=100%) (B). *p<0.05, unpaired student's t-test. N=5 mice per genotype.

5. DISCUSSION

5.1 Viability of postnatal primary microglial cells is influenced by actin toxins in a concentration-dependent manner

As part of the exogenous experimental approach applied in this thesis, cytoskeleton rearrangement was disturbed by application of substances acting in the opposite way: Jasplakinolide stabilizes whereas cytochalasin D destabilizes actin filaments (45, 49). Initially, subtoxic concentrations of the two substances regarding microglia viability had to be determined. A dose that elicits effects on microglia phenotypes (such as phagocytosis, migration or cytokine release) but that does not influence standard toxicological parameters (such as MTT assay and LDH release) falls within a range between 63 nM and 500 nM for jasplakinolide and 0.5 µM and 2 µM for cytochalasin D.

5.2 "Classical" microglia activation and regulation of actin binding proteins (ABPs)

Activation of microglia cells leads to a change in morphology *in vitro* and *in vivo*. *In vitro*, unstimulated cells are mostly unipolar with fan-shaped lamellum, whereas LPS activated cells are rounded up and exhibit amoeboid morphology (136, 137). *In vivo*, activated cells, as in the ipsilateral peri-ischemic area after experimental stroke, reveal increased soma sizes, de-ramification and decreased process movement when compared to cells of the contralateral hemisphere (138).

These phenotypic transitions are accompanied by actin remodeling. In macrophages, the proportion of F-actin changes in LPS stimulated cells after 20 to 60 min post activation (139). The Western Blot analysis performed here did not reveal differences in F and G-actin levels between unstimulated and stimulated microglia cells after 6 hours of LPS treatment (Figure 11, "Cytosol", "Pellet"). In contrast to LPS stimulation, treatment with jasplakinolide, which is an actin filament stabilizing drug, clearly increases F-actin levels (Figure 11, "Pellet"). G-actin levels were apparently not as strongly influenced by treatment with cytochalasin D as F-actin levels by jasplakinolide. This result can be explained by the fact that cells retain a large pool of G-actin to respond immediately in case of environmental stimuli (140). Thus, the

Western Blot technique may not be the adequate method to measure subtle changes of G-actin levels generated by cytochalasin D treatment, which is a blocker of actin filament elongation.

Appropriate actin filament remodeling is based on actin binding proteins (ABP), enabling the actin strand to polymerize, depolymerize or link with another strand. Interestingly, none of the actin binding proteins that were tested in this thesis showed different levels of mRNA and protein expression after 6 hours of LPS treatment (Figure 7, 8). A possible explanation could be the transient switch of actin related cellular responses to LPS, as reported in the literature (12, 139). Kleveta and colleagues (2012) have shown that in macrophages, 60 min post LPS stimulation, F/G actin ratios already reached baseline levels (prior stimulation levels) and the phosphorylation of the tested actin-regulating proteins paxilline and N-WASP peaked already after 20-30 min post-stimulation (139). Abd-el-Basset and Fedoroff (1994) found in LPS stimulated microglia that it takes 2 hours to re-establish the pre-phagocytosis pattern of the actin filament network (12). Apparently, even though as a consequence of activation the phenotype of the microglia cell appears different, LPS stimulation leads only to transient expression of ABPs and actin in a narrow time frame before a stable pattern of the actin filament network is re-established.

In contrast to LPS activation, chronic administration of jasplakinolide and cytochalasin D differently influenced ABP expression. Protein levels of gelsolin, the key player of Ca^{2+} dependent actin depolymerization in the mammalian brain (20), were compensatorily upregulated after jasplakinolide and cytochalasin D treatment in BV-2 microglia cells (Figure 7). This gelsolin upregulation was not reflected on the level of gene expression after the same treatment paradigm in primary postnatal cells. With regards to the remaining ABPs tested as part of this thesis (*Cfl, Pfn, Arpc5, Vil*), a counterregulatory upregulation of gene expression in primary postnatal microglia cells can be observed (Figure 8). Gelsolin protein overexpression after disruption of actin dynamics could not easily be explained by counterregulatory upregulation of the transcriptional activator SRF, because SRF protein levels are reduced after 24 hours cytochalasin D and jasplakinolide treatment (Figure 7B) (141). The reduced SRF protein levels are also contrary to findings in fibroblast cells, where both, jasplakinolide and cytochalasin D, activate SRF (142). Interestingly, SRF is not only a transcriptional regulator, it is also able to regulate the activity of the actin severing protein cofilin via a post-translational mechanism (143). After disruption of actin dynamics with cytochalasin D and jasplakinolide, a decrease of phosphorylated cofilin (= dephosphorylation

= activation) for BV-2 microglia cells - but no different total Cofilin levels were found in this thesis (Figure 7). This supports findings of Kronenberg et al. (2010), whereafter a knockout of gelsolin, such as the jasplakinolide treatment on microglia in the present thesis, led to an activation (= dephosphorylation) of Cofilin without influencing total cofilin (144). In contrast to the results of the thesis in hand, SRF levels were not influenced by gelsolin deficiency in the previously mentioned study (144). However, recent experimental approaches enabled the detection of a direct interaction between cytoplasmic SRF levels and cofilin dephosphorylation in neurons (145). The "SRF-cofilin-actin signaling axis" (146) describes the regulatory loop of cytoplasmic SRF, Cofilin dephosphorylation and resulting actin dynamics. So far, there is no data available if these mechanisms apply in microglia, but according to my data, disruption of actin dynamics could somehow influences this axis. Another potential factor influencing cofilin expression is the activity of slingshot phosphatase that was not investigated during this thesis. Slingshot phosphatase (SSH1) elevates the cofilin activity and damage of the actin cytoskeleton with cucurbitacins leads to increased cofilin dephosphorylation in a slingshot phosphatase dependent manner (147). A further Western blot probed with specific antibodies, such as SSH1, would give more insights to the molecular mechanism of ABPs expression after actin dynamic disruption.

5.3 Release of NO from "classically" activated microglia cells is impaired *in vitro*

The release of pro-inflammatory substances from primary microglia after manipulation of actin dynamics has not been studied so far. My work demonstrates reduced NO release after actin cytoskeletal disruption, by either actin filament stabilization or destabilization (Figure 9). In macrophages, cytochalasin D treatment leads to decreased NO release after LPS activation without influencing gene and protein expression levels of inducible nitric oxide synthase (iNOS) (148). The authors of that study suggest a post-translational regulation of iNOS by the actin cytoskeleton (148). No such influence on the gene expression of *iNos* nor the cationic amino acid transporter 2 (*Cat2)*, the membrane channel that shuttles arginine into the cell, was observed here (Figure 10A). Contrary to expectations deriving from the transcriptional data collected and analyzed as part of the present thesis, a clear downregulation of iNOS protein after treatment with the toxins in BV-2 and primary postnatal microglia cells could be shown (Figure 11). Since *Cat2* was not regulated on the transcriptional level, the transport efficiency for arginine after actin filament damage was

measured. As expected and previously shown concerning macrophages (149, 150), arginine transport through the microglial cell membrane increased after LPS stimulation (Figure 12). Interestingly, my work shows that arginine transport is robustly decreased after jasplakinolide treatment. So far, no relationship between actin filament stabilization/ destabilization and NO production has been found in macrophages or microglia. For pulmonary artery endothelial cells, a relationship between actin filament stabilization and L-arginine transport with influence on NO release has been shown, but with results opposite to the results reported here (151). The authors found a stimulatory effect of jasplakinolide on NO production of endothelial cells. But at this point it should be considered that three different isoforms of nitric oxide synthases do exist in the brain, whose activation and signaling pathways are differentially regulated. Unlike iNOS in microglia, eNos is the NO producing enzyme in endothelial cells, wheres nNOS is the NO producing enzyme in neurons (152). "Neuroprotective" nanomolar concentrations of NO are produced by eNos and nNOS, activated via Ca^{2+}/ calmodolin whereas "neurotoxic" micromolar concentrations of NO is produced by iNOS, which is activated via cytokines or pathogenic stimuli (153). Furthermore, the subcellular localization of the enzymes differs in a cell dependent way, e.g. eNOS in endothelial cells is primarily membrane bound (154), wheras iNOS in microglia is enriched in the cytosol (155). Besides different locations of the NOS isofomes, a mechanism that regulates the enzymatic activity of eNos by controlling intracellular translocation of this enzyme has been discovered via nitric oxide synthase-interacting protein (NOSIP), a mechanism that does not seem to apply for iNOS (156). Thus, mechanisms that influence the activity of the enzymes by actin dynamics might operate differently for the different NOS isoforms in different cell types. The current thesis suggests a role for actin filament stabilization in NO production and release. Actin filament stabilization with jasplakinolide reduces the transport of L-arginine into the cell and actin filament destabilization with cytochalasin D as well as stabilization with jasplakinolide leads to reduced iNOS levels.

5.4. Cytokine release for "classical" activation is differentially affected after disruption of actin filament dynamics

After disruption of actin dynamics, a differential release pattern of cytokines could be observed following LPS induced cell activation (Figure 13). On the one hand, the constitutive cytokine release (TNF-α, IL-6) is impaired by exogenous (jasp/ cyt) and endogenous (*Gsn*$^{-/-}$) disruption of actin filament dynamics (Figure 13A, B, C). On the other hand, non-classical secretion of IL-1β is increased after actin polymerization with jasplakinolide (Figure 13D). IL-1β release is not comparable to the constitutive pathway that is characterized by packaging of cytokines through endoplasmic reticulum and Golgi apparatus and further transport to the plasma membrane (157). It is rather comparable to neurotransmitter release, defined by exocytosis, independent of ER and Golgi apparatus. After cleavage of pro-IL-1β by caspase 1, mature IL-1β is released into the extracellular space (158). The increased release of IL-1β after jasplakinolide treatment that has been observed in the present thesis, is in line with findings of Kronenberg et al. (2010) who showed that gelsolin deficiency confers increased exocytotic neurotransmitter release in neurons (144).

Since the differential release pattern is obviously not the result of transcriptional regulation of cytokine mRNA expression (Figure 13E), the following two post-transcriptional processes are hypothesized to influence the constitutive cytokine (IL-6, TNF-α) release after disruption of actin filament remodeling:

1. Impaired cytokine mRNA translation, which was shown by van den Berg and colleagues (2006) in terms of IL-6 after cytochalasin D treatment (159).
2. Dysfunction of the release pathway/ intracellular trafficking of cytokines, as it was shown by Shurety and collegues (2000) for TNF-α (160).

Additional experiments that have not been conducted as part of this thesis, such as immunoblotting of fractionated cell lysates as well as a comprehensive histological investigation with specific antibodies against key proteins involved in intracellular transport, might provide important information in order to verify or falsify the above mentioned hypotheses concerning post-transcriptional processes affecting the constitutive cytokine (IL-6, TNF-α) release after interruption of actin filament remodeling. This knowledge would be an important milestone to achieve an effective modulation of cytokine release after injury or during disease towards "neuroprotection".

5.5 "Alternative" activation of microglia cells with IL-4

Alternative "M2" activation of microglia leads to increased expression and release of anti-inflammatory factors that contribute to tissue repair and remodeling. Therefore, alternatively activated microglia are supposed to be "neuroprotective" (161, 162). IGF-1 is an important microglia-derived neuroprotective factor influencing the proliferation of microglia cells after stroke but also is important in the developing brain to maintain neuronal survival (163, 164). By using IL-4 as alternative activator in experiments from chaper 4.4 (Figure 14, 15), IGF-1 release from microglia cells increases and is reduced by actin filament disruption (Figure 14A). Interestingly, in contrast to LPS stimulation, actin filament disruption influences gene expression not only of *Igf*, but also other alternative activation markers (*Ym1*, *Fizz1*, *Mrc1*, *Arg1*) (Figure 14B, C). Of the cationic amino acid transporters 1 to 3, only *Cat2* is upregulated after IL-4 treatment, but not influenced by actin cytoskeletal drugs (Figure 14D). This suggests that Cat2, but not Cat1 or Cat3, is the transporter in microglial cells that shuttles L-arginine into the cell, which is in line with the results for classical (LPS) activation (Figure 10A, C) and previously published data obtained with a microglia cell line (165). Actin cytoskeletal drugs do not decrease the expression levels of *Cat2* (Figure 14D) as they do the IL-4 responsive genes (Figure 14C), implying a selective effect for jasplakinolide and cytochalasin D on microglia signaling pathways. An influence on actin dynamics in the regulation of the IL-4 regulated gene transcription has not yet been described in the literature. To further dissect the site of action of the actin agents (jasplakinolide/ cytochalasin D), the IL-4 signaling pathway upstream of the transcription of IL-4 responsive genes was investigated. It is known that Stat6 (signal transducer and activator of transcription 6) is the key player involved in IL-4 receptor mediated signaling (166). After phosphorylation of Stat6 by janus kinases (Jak), pStat6 is transported into the nucleus to act as a transcriptional activator (73, 167, 168). Accordingly, the immunoblot from fractionated IL-4 stimulated microglia cells, as conducted as part of the present thesis, reveals decreased transport of phosphorylated Stat6 after actin cytoskeleton stabilization / destabilization (Figure 15). These results provide first evidence that the IL-4 signaling pathway is linked to actin filament dynamics in microglia. Modulation of actin filament dynamics interferes with the activation of IL-4 responsive gene transcription via pStat6 transport into the nucleus.

5.6 *In vitro* migration, phagocytosis and proliferation of microglia cells after disrupting actin remodeling – *in vivo* stroke approach and facial nerve axotomy

Neurodegenerative disease or brain injury is often accompanied by activation of the brain innate immune system, helping to restore a physiologic homeostasis by triggering inflammation and by removing cell debris and producing anti- and pro-inflammatory stimuli (169). Therefore, under pathophysiological conditions, microglia cells need to proliferate, migrate towards the site of injury or phagocytose cell debris. The dynamic remodeling of actin is the key mechanism enabling the microglia cell to fulfill all these duties (12, 137, 170, 171). As expected, microglia cells with exogenously disrupted actin dynamics or gelsolin deficiency investigated over the course of this thesis are different in respect to the above mentioned parameters *in vitro* and *in vivo (*after MCAo and facial nerve axotomy) compared to untreated or wildtype microglia.

Kronenberg et al. (2010) reported reduced migration of newly generated cells through the rostral migratory stream in $Gsn^{-/-}$ mice *in vivo* and decreased migration of gelsolin deficient neural progenitor cells (NPCs) *in vitro* (144). Additionally, several previous studies emphasize impaired migratory capacity of $Gsn^{-/-}$ fibroblasts, neutrophils and macrophages (51, 122, 172). The current study shows that gelsolin deficiency leads to reduced migration of microglia cells towards ADP *in vitro* (Figure 16C). Reduced *in vitro* microglia migration is possibly associated with the interesting finding that less proliferating microglia was observed *in vivo* three days after stroke within the peri-ischemic area (Figure 18). Extracellular ADP, an ATP derivative leaked from damaged cells after injury, is an important signaling molecule and can be found in high levels in the extracellular space after MCAo (173). The interplay of ATP sensing purinergic receptors on microglia, such as $P2X_7$, $P2Y_{12}$ and $P2Y_6$, regulate activation of the cells, migration towards the penumbral region and phagocytosis post-stroke (174). It is still discussed if activated microglia is beneficial or detrimental after stroke. Compared to wildtype controls, *Gsn* deficient mice have bigger infarct sizes (26). The data of the current thesis suggests that worse stroke outcome in gelsolin deficient mice is not only a result of increased neuronal excitotoxicity but rather an additional mismatch of IBA-1 cells in the penumbral region.

The experiments on microglia proliferation performed in this thesis (Figure16 E, Figure 21) are not in line with previous data on NPCs (144). Gelsolin deficiency but not age had an attenuating effect on microglia proliferation *in vitro* (Figure 16E). The effect of the actin filament stabilization on microglia proliferation was reproduced *in vivo* by application of the facial nerve axotomy model in $Gsn^{-/-}$ and $Gsn^{+/+}$ mice (Figure 21). At this point it should be considered that NPC proliferation was assessed under physiological conditions, whereas experiments on microglia proliferation were assessed under stimulative conditions (addition of growth factors *in vitro*; nerve axotomy *in vivo*). Therefore, the "mild" effect of gelsolin deficiency probably has more impact on high proliferation rates after a pathological insult then for cells proliferating under non-diseased/ developmental aspects (NPCs).

Cytochalasin D and jasplakinolide, as previously reported, are capable to inhibit the process of phagocytosis (175, 176). The experiments of this thesis yielded results in line with the existing literature (Figure 16B). However, the role of gelsolin in microglia phagocytosis had not been investigated so far. There is data available only in respect to collagen phagocytosis, which is reduced in $Gsn^{-/-}$ fibroblasts compared to $Gsn^{+/+}$ cells (177). A reduced phagocytosis of bacterial particles by gelsolin deficient microglia was discovered during the experiments on the engulfment of bacterial particles (Figure 16D). The experimental setup is based on particles from the gram-positive bacterial strain *S. aureus* that are conjugated to a pH sensitive dye. The particles expose PAMPs (peptidoglycan, lipoteichoic acid) that bind to the surface of the phagocyte on PRRs (pathogen recognition receptors) (178). PRRs control diverse downstream signaling pathways leading amongst others to actin filament remodeling. Since gelsolin deficiency and treatment with jasplakinolide and cytochalasin D disrupts the remodeling of the actin cytoskeleton, the reduced engulfment of particles is probably due to an interruption of pseudopodia extension and efficient particle internalization.

5.7 *Gsn* deficiency leads to increased intracellular Ca^{2+} levels in adult and aged *ex vivo* isolated microglia cells

Ca^{2+} as an important second messenger triggers various functions in microglia cells under physiological and pathophysiological conditions, such as enzyme and release activities, regulation of channels and receptor mediated signaling (55). Gelsolin, a Ca^{2+} dependent protein, is able to prevent neuronal death under pathophysiological conditions by regulating

actin dynamics and calcium channels (26, 54). A plethora of calcium channels, pumps and exchangers regulate intracellular calcium levels in microglia (55).

Imaging of microglia cells incubated with calcium sensitive dye, as performed during this thesis, revealed that *Gsn*$^{-/-}$ microglia possess elevated intracellular Ca^{2+} levels already at baseline (Figure 19). Elevated Ca^{2+} levels have been described for LPS activated microglia and microglia from Alzheimer's disease patients (179, 180). Actin filament remodeling is disturbed in *Gsn*$^{-/-}$ cells, resulting in stabilized actin fibers (51). Stabilized actin fibers are known to influence Ca^{2+} channel activity (181). In turn, calcium signaling is important for the regulation of the actin cytoskeleton, as a basis for migration or proliferation (182-184). Recently, it was found that activation of small-conductance calcium-activated potassium (KCNN3/SK3/K_{Ca}2.3) channels are able to influence intracellular calcium levels and as a consequence, modulate proliferation and cytokine release from microglia cells (185).

Extracellular ATP is an important intercellular signaling molecule ("danger signal") and can activate specific receptors on microglia (55). In accordance with already published data, this thesis reveals that stimulation of microglia with ATP leads to increased intracellular Ca^{2+} levels (Figure 19A) (186). The calcium imaging of gelsolin deficient microglia indicates a more pronounced peak of intracellular Ca^{2+} levels after ATP stimulation compared to gelsolin-bearing cells (Figure 19A, C). The mechanism behind this finding remains yet unclear; a probable explanation is that the threshold (concentration of intracellular Ca^{2+}) for switching on a signal cascade in gelsolin deficient microglia is shifted. Thus, signal cascades in *Gsn*$^{-/-}$ deficient microglia are differently affected by stimulation of intracellular Ca^{2+} compared to *Gsn*$^{+/+}$ microglia. As a consequence, it is likely that disturbed calcium signaling by gelsolin deficiency alters microglia behaviors as evidenced by the altered parameters (migration, proliferation etc.) tested during the present thesis.

The results of this thesis demonstrated that gelsolin is an important protein not only involved in actin filament remodeling but also in regulating calcium homeostasis. The extent, however, to which intracellular or extracellular calcium pools are responsible for this phenomenon, cannot be quantified on the basis of the present results. Further calcium imaging experiments testing specific calcium channel inhibitors for dissecting between intra- and extra-cellular calcium pools as well as calcium from different cellular compartments could provide further insights into this question.

5.8 Cytoskeletal disruption in a disease context – oligomeric Amyloid-β treatment *in vitro*

The pathological hallmark of Alzheimer's disease (AD) is the major loss of neurons. According to the "amyloid cascade hypothesis", amyloid β or its oligomeric forms crucially contributes to the pathogenesis of AD (187, 188). Soluble oligomeric Amyloid-ß (oAβ) is related to neuronal synaptic dysfunction (189) and is capable to induce the release of inflammatory substances from microglia (190-192). Sondag et al. (2009) showed that $A\beta_{1-42}$ oligomers were only neurotoxic in neuron-microglia co-cultures under *in vitro* conditions (193).

The experiments studying FITC-coupled oAβ uptake and subsequent *iNOS* mRNA expression show the interrelation of impaired oAβ uptake by actin filament stabilization/ destabilization and the resulting failure to induce the transcription of *iNos* (Figure 17). Cathepsin B was found to be one important factor in microglial mediated neuronal death after Aβ stimulation (194). Yang et al. (2011) could show an interaction of oAβ with scavenger receptor type-A (SR-A) and a mediated degradation of oAβ by lysosomal cathepsin B (195). It is known that cathepsin B is capable to trigger inflammasome NRLP3 activity that mediates inflammation in microglia cells and induction of genes such as *iNOS* (196, 197). Although a molecular signaling pathway from uptake of oAβ towards transcriptional activation in microglia is still unknown, it is likely that the reduced uptake of oAß results in a "non-inflammatory" microglia phenotype, which is lacking *iNos* induction.

5.9 Microglia density increases with age but is not influenced by genotype

Clinical and experimental data suggest that brain inflammation increases with age. By comparing the morphology, a "dystrophy" of microglia from aged humans has been described (116). The concept of "dystrophic" microglia that are primed by age, distinguishes these cells from "hypertrophic" microglia activated by injury or disease (198). Several studies concerning dystrophic microglia or microglial senescence showed an altered reactivity of murine microglial cells associated with age in terms of cytokine release, phagocytosis, motility and migration (120, 134, 199). Thus, dystrophic microglia also affect neuronal

plasticity, behavior and cognition (200). These findings lead to the question, whether altered microglia reactivity is a component that correlates with microglia density. Published studies dealing with the relationship between microglia density and age-effects revealed different and partly contradictory results. Long et al. (1998) and Rodriguez et al. (2013) reported increasing numbers of microglia cells in mouse models of disease but not in control animals, a study conducted by Mouton et al. (2002) revealed gender-specific differences (201-203). There are also studies supporting a decrease of microglia density with age (204, 205). These different findings may be associated with the diversity of animal strains, markers for microglia, stereological methods and different ages investigated. However, microglia staining with IBA-1 followed by stereology as conducted in this thesis clearly indicates microglia density to increase with age in two brain regions for both, $Gsn^{+/+}$ and $Gsn^{-/-}$ animals (Figure 20). Other experiments conducted during this thesis revealed no age-related alterations of microglia reactivity to LPS in respect to NO (Figure 9B) and TNF-α (Figure 13B) release. Also, migration towards ADP, phagocytosis of bacterial particles, intracellular calcium levels and *in vitro* proliferation was not influenced by age (Figure 16C-E, 19). The primary adult cells used in the experiments of this thesis were cultivated according to an already published methodology (124). It is likely that during the cultivation procedure, age-related effects disappear, because cells massively proliferate after isolation under non-physiological conditions in response to growth factors. It should also be considered that microglia from adult (< 6 months) mice were compared with microglia from aged (> 16 months) mice. Most certainly, an age-related effect would be even more distinguished when microglia cells of adult mice are compared with those of newborns.

5.10 Actin dynamics in microglia activation and its impact on neurodegenerative diseases and age

This thesis gives evidence that actin dynamics are not only important for microglia functions like phagocytosis, migration and proliferation but also influence pro- and anti-inflammatory responses of microglia cells after classical and alternative activation. These findings may have impact on further research, particularly with regard to age-related neurodegenerative diseases such as stroke or Alzheimer's dementia. Neuroinflammation as a concomitant phenomenon of neurodegenerative diseases and its manipulation by pharmacological intervention via actin dynamics could be a promising approach towards improved disease outcome.

Gelsolin knock out mouse as an animal model representing age?

The challenge of mouse models is the translation of scientific results from bench to bedside (206). Multiple factors avert clinical translation. One striking point is the diverse natural lifespan of human and mice and the preference to use young and healthy animals for experimental paradigms. Aging, and especially human aging, is associated with increased rigidity of cytoskeletal structures. With increasing cellular senescence, the equilibrium between monomeric, non-aggregated G-actin ("globular actin") and fibrillar F-actin shifts toward the filamentous state (112-115). Because of increased actin filament stabilization in gelsolin deficient mice, the $Gsn^{-/-}$ mouse could represent an animal model for age. In this thesis, microglia of $Gsn^{-/-}$ mice were compared to microglia from $Gsn^{+/+}$ controls in terms of:

i) pro-inflammatory release of NO (Figure 9B) and TNF-α (Figure 13B).

ii) migration, phagocytosis, proliferation (Figure 16C-E, 18, 21).

iii) calcium response (Figure 19).

iv) density in the healthy brain (Figure 20).

Overall, the redundancy of the actin filament severing protein leads to no phenotype of the gelsolin knock out in mice under physiological conditions (microglia density), with major effects under pathophysiological conditions (migration, proliferation, phagocytosis). Hence, using the gelsolin mouse model for experiments in neurodegenerative diseases would be suitable to bring the relevant factor "age" into account.

6. CONCLUSION

The major findings of my PhD thesis can be summarized as following:

1. Long-term administration of LPS (6 and 24 hr) does not influence ABP expression in microglia cells. Modulation of actin dynamics with toxins leads to counter-regulatory differential ABP expression and differences in F/G actin ratio.

2. Disruption of actin dynamics affects the response to classical microglia activation by reducing the release of pro-inflammatory NO, TNF-α and IL-6. Increased release of IL-1β was observed after pathological actin filament stabilization. This differential response is not regulated on a transcriptional level. Reduced NO release after actin cytoskeletal disruption results from interplay of reduced substrate (arginine) supply and reduced iNOS protein expression.

3. Disruption of actin dynamics affects the response to alternative microglia activation by reduced gene expression of typical M2 genes (*Igf-1, Ym1, Mrc1, and Arg1*) and attenuates release of the neurotrophic factor IGF-1. The reduced gene expression of M2 genes is due to impaired transcriptional activation via Stat6. As evidenced by Western blot, pStat6 transport into the nucleus is impaired by actin cytoskeletal disruption.

4. Modulation of actin dynamics affects microglia proliferation, migration and phagocytosis. Except for microglia densities measured in hippocampus and striatum, no effect of age was observed throughout the experiments. Two explanations seem plausible: the culturing method of primary adult microglia abolishes age effects or the time span between the two investigated ages is too short.

7. REFERENCES

1. Mostowy, S., and Cossart, P. (2012) Septins: the fourth component of the cytoskeleton. *Nat Rev Mol Cell Biol* **13**, 183-194

2. Moseley, J. B. (2013) An expanded view of the eukaryotic cytoskeleton. *Mol Biol Cell* **24**, 1615-1618

3. Rubenstein, P. A. (1990) The functional importance of multiple actin isoforms. *Bioessays* **12**, 309-315

4. Bunnell, T. M., Burbach, B. J., Shimizu, Y., and Ervasti, J. M. (2011) beta-Actin specifically controls cell growth, migration, and the G-actin pool. *Mol Biol Cell* **22**, 4047-4058

5. Bergeron, S. E., Zhu, M., Thiem, S. M., Friderici, K. H., and Rubenstein, P. A. (2010) Ion-dependent polymerization differences between mammalian beta- and gamma-nonmuscle actin isoforms. *J Biol Chem* **285**, 16087-16095

6. Shawlot, W., Deng, J. M., Fohn, L. E., and Behringer, R. R. (1998) Restricted beta-galactosidase expression of a hygromycin-lacZ gene targeted to the beta-actin locus and embryonic lethality of beta-actin mutant mice. *Transgenic Res* **7**, 95-103

7. Belyantseva, I. A., Perrin, B. J., Sonnemann, K. J., Zhu, M., Stepanyan, R., McGee, J., Frolenkov, G. I., Walsh, E. J., Friderici, K. H., Friedman, T. B., and Ervasti, J. M. (2009) Gamma-actin is required for cytoskeletal maintenance but not development. *Proc Natl Acad Sci U S A* **106**, 9703-9708

8. Di Donato, N., Rump, A., Koenig, R., Der Kaloustian, V. M., Halal, F., Sonntag, K., Krause, C., Hackmann, K., Hahn, G., Schrock, E., and Verloes, A. (2014) Severe forms of Baraitser-Winter syndrome are caused by ACTB mutations rather than ACTG1 mutations. *Eur J Hum Genet* **22**, 179-183

9. Cingolani, L. A., and Goda, Y. (2008) Actin in action: the interplay between the actin cytoskeleton and synaptic efficacy. *Nat Rev Neurosci* **9**, 344-356

10. Wegner, A., and Isenberg, G. (1983) 12-fold difference between the critical monomer concentrations of the two ends of actin filaments in physiological salt conditions. *Proc Natl Acad Sci U S A* **80**, 4922-4925

11. Neuhaus, J. M., Wanger, M., Keiser, T., and Wegner, A. (1983) Treadmilling of actin. *J Muscle Res Cell Motil* **4**, 507-527

12. Abd-el-Basset, E. M., and Fedoroff, S. (1994) Dynamics of actin filaments in microglia during Fc receptor-mediated phagocytosis. *Acta Neuropathol* **88**, 527-537

13. Vincent, C., Siddiqui, T. A., and Schlichter, L. C. (2012) Podosomes in migrating microglia: components and matrix degradation. *J Neuroinflammation* **9**, 190

14. Imai, Y., and Kohsaka, S. (2002) Intracellular signaling in M-CSF-induced microglia activation: role of Iba1. *Glia* **40**, 164-174

15. Muessel, M. J., Harry, G. J., Armstrong, D. L., and Storey, N. M. (2013) SDF-1alpha and LPA modulate microglia potassium channels through rho gtpases to regulate cell morphology. *Glia* **61**, 1620-1628

16. Blanchoin, L., Boujemaa-Paterski, R., Sykes, C., and Plastino, J. (2014) Actin dynamics, architecture, and mechanics in cell motility. *Physiol Rev* **94**, 235-263

17. Spiering, D., and Hodgson, L. (2011) Dynamics of the Rho-family small GTPases in actin regulation and motility. *Cell Adh Migr* **5**, 170-180

18. Winder, S. J., and Ayscough, K. R. (2005) Actin-binding proteins. *J Cell Sci* **118**, 651-654

19. Silacci, P., Mazzolai, L., Gauci, C., Stergiopulos, N., Yin, H. L., and Hayoz, D. (2004) Gelsolin superfamily proteins: key regulators of cellular functions. *Cell Mol Life Sci* **61**, 2614-2623

20. Sun, H. Q., Yamamoto, M., Mejillano, M., and Yin, H. L. (1999) Gelsolin, a multifunctional actin regulatory protein. *J Biol Chem* **274**, 33179-33182

21. Yin, H. L., and Stossel, T. P. (1979) Control of cytoplasmic actin gel-sol transformation by gelsolin, a calcium-dependent regulatory protein. *Nature* **281**, 583-586

22. Kwiatkowski, D. J., Stossel, T. P., Orkin, S. H., Mole, J. E., Colten, H. R., and Yin, H. L. (1986) Plasma and cytoplasmic gelsolins are encoded by a single gene and contain a duplicated actin-binding domain. *Nature* **323**, 455-458

23. Janmey, P. A., and Stossel, T. P. (1987) Modulation of gelsolin function by phosphatidylinositol 4,5-bisphosphate. *Nature* **325**, 362-364

24. Ditsch, A., and Wegner, A. (1994) Nucleation of actin polymerization by gelsolin. *Eur J Biochem* **224**, 223-227

25. Kothakota, S., Azuma, T., Reinhard, C., Klippel, A., Tang, J., Chu, K., McGarry, T. J., Kirschner, M. W., Koths, K., Kwiatkowski, D. J., and Williams, L. T. (1997) Caspase-3-generated fragment of gelsolin: effector of morphological change in apoptosis. *Science* **278**, 294-298

26. Endres, M., Fink, K., Zhu, J., Stagliano, N. E., Bondada, V., Geddes, J. W., Azuma, T., Mattson, M. P., Kwiatkowski, D. J., and Moskowitz, M. A. (1999) Neuroprotective effects of gelsolin during murine stroke. *J Clin Invest* **103**, 347-354

27. Antequera, D., Vargas, T., Ugalde, C., Spuch, C., Molina, J. A., Ferrer, I., Bermejo-Pareja, F., and Carro, E. (2009) Cytoplasmic gelsolin increases mitochondrial activity and reduces Abeta burden in a mouse model of Alzheimer's disease. *Neurobiol Dis* **36**, 42-50

28. Ahn, J. S., Jang, I. S., Kim, D. I., Cho, K. A., Park, Y. H., Kim, K., Kwak, C. S., and Chul Park, S. (2003) Aging-associated increase of gelsolin for apoptosis resistance. *Biochem Biophys Res Commun* **312**, 1335-1341

29. Ono, S. (2007) Mechanism of depolymerization and severing of actin filaments and its significance in cytoskeletal dynamics. *Int Rev Cytol* **258**, 1-82

30. Hadas, S., Spira, M., Hanisch, U. K., Reichert, F., and Rotshenker, S. (2012) Complement receptor-3 negatively regulates the phagocytosis of degenerated myelin through tyrosine kinase Syk and cofilin. *J Neuroinflammation* **9**, 166

31. Kwan, W., Trager, U., Davalos, D., Chou, A., Bouchard, J., Andre, R., Miller, A., Weiss, A., Giorgini, F., Cheah, C., Moller, T., Stella, N., Akassoglou, K., Tabrizi, S. J., and Muchowski, P. J. (2012) Mutant huntingtin impairs immune cell migration in Huntington disease. *J Clin Invest* **122**, 4737-4747

32. Maciver, S. K., and Hussey, P. J. (2002) The ADF/cofilin family: actin-remodeling proteins. *Genome Biol* **3**, reviews3007

33. Bravo-Cordero, J. J., Magalhaes, M. A., Eddy, R. J., Hodgson, L., and Condeelis, J. (2013) Functions of cofilin in cell locomotion and invasion. *Nat Rev Mol Cell Biol* **14**, 405-415

34. Vartiainen, M. K., Mustonen, T., Mattila, P. K., Ojala, P. J., Thesleff, I., Partanen, J., and Lappalainen, P. (2002) The three mouse actin-depolymerizing factor/cofilins evolved to fulfill cell-type-specific requirements for actin dynamics. *Mol Biol Cell* **13**, 183-194

35. Yang, N., Higuchi, O., Ohashi, K., Nagata, K., Wada, A., Kangawa, K., Nishida, E., and Mizuno, K. (1998) Cofilin phosphorylation by LIM-kinase 1 and its role in Rac-mediated actin reorganization. *Nature* **393**, 809-812

36. Huang, T. Y., DerMardirossian, C., and Bokoch, G. M. (2006) Cofilin phosphatases and regulation of actin dynamics. *Curr Opin Cell Biol* **18**, 26-31

37. Yonezawa, N., Nishida, E., Iida, K., Yahara, I., and Sakai, H. (1990) Inhibition of the interactions of cofilin, destrin, and deoxyribonuclease I with actin by phosphoinositides. *J Biol Chem* **265**, 8382-8386

38. Kullmann, J. A., Neumeyer, A., Gurniak, C. B., Friauf, E., Witke, W., and Rust, M. B. (2012) Profilin1 is required for glial cell adhesion and radial migration of cerebellar granule neurons. *EMBO Rep* **13**, 75-82

39. Dong, J. H., Ying, G. X., and Zhou, C. F. (2004) Entorhinal deafferentation induces the expression of profilin mRNA in the reactive microglial cells in the hippocampus. *Glia* **47**, 102-108

40. Carlsson, L., Nystrom, L. E., Sundkvist, I., Markey, F., and Lindberg, U. (1977) Actin polymerizability is influenced by profilin, a low molecular weight protein in non-muscle cells. *J Mol Biol* **115**, 465-483

41. Witke, W. (2004) The role of profilin complexes in cell motility and other cellular processes. *Trends Cell Biol* **14**, 461-469

42. Miano, J. M., Long, X., and Fujiwara, K. (2007) Serum response factor: master regulator of the actin cytoskeleton and contractile apparatus. *Am J Physiol Cell Physiol* **292**, C70-81

43. Arsenian, S., Weinhold, B., Oelgeschlager, M., Ruther, U., and Nordheim, A. (1998) Serum response factor is essential for mesoderm formation during mouse embryogenesis. *EMBO J* **17**, 6289-6299

44. Vartiainen, M. K., Guettler, S., Larijani, B., and Treisman, R. (2007) Nuclear actin regulates dynamic subcellular localization and activity of the SRF cofactor MAL. *Science* **316**, 1749-1752

45. Goddette, D. W., and Frieden, C. (1986) Actin polymerization. The mechanism of action of cytochalasin D. *J Biol Chem* **261**, 15974-15980

46. Brown, S. S., and Spudich, J. A. (1979) Cytochalasin inhibits the rate of elongation of actin filament fragments. *J Cell Biol* **83**, 657-662

47. Casella, J. F., Flanagan, M. D., and Lin, S. (1981) Cytochalasin D inhibits actin polymerization and induces depolymerization of actin filaments formed during platelet shape change. *Nature* **293**, 302-305

48. Cooper, J. A. (1987) Effects of cytochalasin and phalloidin on actin. *J Cell Biol* **105**, 1473-1478

49. Holzinger, A. (2001) Jasplakinolide. An actin-specific reagent that promotes actin polymerization. *Methods Mol Biol* **161**, 109-120

50. Holzinger, A. (2009) Jasplakinolide: an actin-specific reagent that promotes actin polymerization. *Methods Mol Biol* **586**, 71-87

51. Witke, W., Sharpe, A. H., Hartwig, J. H., Azuma, T., Stossel, T. P., and Kwiatkowski, D. J. (1995) Hemostatic, inflammatory, and fibroblast responses are blunted in mice lacking gelsolin. *Cell* **81**, 41-51

52. Yildirim, F., Gertz, K., Kronenberg, G., Harms, C., Fink, K. B., Meisel, A., and Endres, M. (2008) Inhibition of histone deacetylation protects wildtype but not gelsolin-deficient mice from ischemic brain injury. *Exp Neurol* **210**, 531-542

53. Harms, C., Bosel, J., Lautenschlager, M., Harms, U., Braun, J. S., Hortnagl, H., Dirnagl, U., Kwiatkowski, D. J., Fink, K., and Endres, M. (2004) Neuronal gelsolin prevents apoptosis by enhancing actin depolymerization. *Mol Cell Neurosci* **25**, 69-82

54. Furukawa, K., Fu, W., Li, Y., Witke, W., Kwiatkowski, D. J., and Mattson, M. P. (1997) The actin-severing protein gelsolin modulates calcium channel and NMDA receptor activities and vulnerability to excitotoxicity in hippocampal neurons. *J Neurosci* **17**, 8178-8186

55. Kettenmann, H., Hanisch, U. K., Noda, M., and Verkhratsky, A. (2011) Physiology of microglia. *Physiol Rev* **91**, 461-553

56. Ueno, M., and Yamashita, T. (2014) Bidirectional tuning of microglia in the developing brain: from neurogenesis to neural circuit formation. *Curr Opin Neurobiol* **27C**, 8-15

57. Walker, F. R., Beynon, S. B., Jones, K. A., Zhao, Z., Kongsui, R., Cairns, M., and Nilsson, M. (2014) Dynamic structural remodelling of microglia in health and disease: A review of the models, the signals and the mechanisms. *Brain Behav Immun* **37C**, 1-14

58. Perry, V. H., Nicoll, J. A., and Holmes, C. (2010) Microglia in neurodegenerative disease. *Nat Rev Neurol* **6**, 193-201

59. Hanisch, U. K., and Kettenmann, H. (2007) Microglia: active sensor and versatile effector cells in the normal and pathologic brain. *Nat Neurosci* **10**, 1387-1394

60. Ginhoux, F., Greter, M., Leboeuf, M., Nandi, S., See, P., Gokhan, S., Mehler, M. F., Conway, S. J., Ng, L. G., Stanley, E. R., Samokhvalov, I. M., and Merad, M. (2010) Fate mapping analysis reveals that adult microglia derive from primitive macrophages. *Science* **330**, 841-845

61. Kierdorf, K., Erny, D., Goldmann, T., Sander, V., Schulz, C., Perdiguero, E. G., Wieghofer, P., Heinrich, A., Riemke, P., Holscher, C., Muller, D. N., Luckow, B., Brocker, T., Debowski, K., Fritz, G., Opdenakker, G., Diefenbach, A., Biber, K., Heikenwalder, M., Geissmann, F., Rosenbauer, F., and Prinz, M. (2013) Microglia emerge from erythromyeloid precursors via Pu.1- and Irf8-dependent pathways. *Nat Neurosci* **16**, 273-280

62. Schulz, C., Gomez Perdiguero, E., Chorro, L., Szabo-Rogers, H., Cagnard, N., Kierdorf, K., Prinz, M., Wu, B., Jacobsen, S. E., Pollard, J. W., Frampton, J., Liu, K. J., and Geissmann, F. (2012) A lineage of myeloid cells independent of Myb and hematopoietic stem cells. *Science* **336**, 86-90

63. Ajami, B., Bennett, J. L., Krieger, C., Tetzlaff, W., and Rossi, F. M. (2007) Local self-renewal can sustain CNS microglia maintenance and function throughout adult life. *Nat Neurosci* **10**, 1538-1543

64. Shechter, R., and Schwartz, M. (2013) Harnessing monocyte-derived macrophages to control central nervous system pathologies: no longer 'if' but 'how'. *J Pathol* **229**, 332-346

65. Olah, M., Biber, K., Vinet, J., and Boddeke, H. W. (2011) Microglia phenotype diversity. *CNS Neurol Disord Drug Targets* **10**, 108-118

66. Hanisch, U. K. (2013) Functional diversity of microglia - how heterogeneous are they to begin with? *Front Cell Neurosci* **7**, 65

67. Ziebell, J. M., Taylor, S. E., Cao, T., Harrison, J. L., and Lifshitz, J. (2012) Rod microglia: elongation, alignment, and coupling to form trains across the somatosensory cortex after experimental diffuse brain injury. *J Neuroinflammation* **9**, 247

68. Boche, D., Perry, V. H., and Nicoll, J. A. (2013) Review: activation patterns of microglia and their identification in the human brain. *Neuropathol Appl Neurobiol* **39**, 3-18

69. Goldmann, T., and Prinz, M. (2013) Role of microglia in CNS autoimmunity. *Clin Dev Immunol* **2013**, 208093

70. Park, K. W., Lee, H. G., Jin, B. K., and Lee, Y. B. (2007) Interleukin-10 endogenously expressed in microglia prevents lipopolysaccharide-induced neurodegeneration in the rat cerebral cortex in vivo. *Exp Mol Med* **39**, 812-819

71. Yu, H. H., Wu, F. L., Lin, S. E., and Shen, L. J. (2008) Recombinant arginine deiminase reduces inducible nitric oxide synthase iNOS-mediated neurotoxicity in a coculture of neurons and microglia. *J Neurosci Res* **86**, 2963-2972

72. Qin, L., Liu, Y., Hong, J. S., and Crews, F. T. (2013) NADPH oxidase and aging drive microglial activation, oxidative stress, and dopaminergic neurodegeneration following systemic LPS administration. *Glia* **61**, 855-868

73. Zhou, X., Spittau, B., and Krieglstein, K. (2012) TGFbeta signalling plays an important role in IL4-induced alternative activation of microglia. *J Neuroinflammation* **9**, 210

74. Kobayashi, K., Imagama, S., Ohgomori, T., Hirano, K., Uchimura, K., Sakamoto, K., Hirakawa, A., Takeuchi, H., Suzumura, A., Ishiguro, N., and Kadomatsu, K. (2013) Minocycline selectively inhibits M1 polarization of microglia. *Cell Death Dis* **4**, e525

75. Wang, G., Zhang, J., Hu, X., Zhang, L., Mao, L., Jiang, X., Liou, A. K., Leak, R. K., Gao, Y., and Chen, J. (2013) Microglia/macrophage polarization dynamics in white matter after traumatic brain injury. *J Cereb Blood Flow Metab* **33**, 1864-1874

76. Zhao, W., Xie, W., Xiao, Q., Beers, D. R., and Appel, S. H. (2006) Protective effects of an anti-inflammatory cytokine, interleukin-4, on motoneuron toxicity induced by activated microglia. *J Neurochem* **99**, 1176-1187

77. Kreutzberg, G. W. (1996) Microglia: a sensor for pathological events in the CNS. *Trends Neurosci* **19**, 312-318

78. Harry, G. J. (2013) Microglia during development and aging. *Pharmacol Ther* **139**, 313-326

79. Streit, W. J., Mrak, R. E., and Griffin, W. S. (2004) Microglia and neuroinflammation: a pathological perspective. *J Neuroinflammation* **1**, 14

80. Tanaka, R., Komine-Kobayashi, M., Mochizuki, H., Yamada, M., Furuya, T., Migita, M., Shimada, T., Mizuno, Y., and Urabe, T. (2003) Migration of enhanced green fluorescent protein expressing bone marrow-derived microglia/macrophage into the mouse brain following permanent focal ischemia. *Neuroscience* **117**, 531-539

81. Ifuku, M., Farber, K., Okuno, Y., Yamakawa, Y., Miyamoto, T., Nolte, C., Merrino, V. F., Kita, S., Iwamoto, T., Komuro, I., Wang, B., Cheung, G., Ishikawa, E., Ooboshi, H., Bader, M., Wada, K., Kettenmann, H., and Noda, M. (2007) Bradykinin-induced microglial migration mediated by B1-bradykinin receptors depends on Ca2+ influx via reverse-mode activity of the Na+/Ca2+ exchanger. *J Neurosci* **27**, 13065-13073

82. Davalos, D., Grutzendler, J., Yang, G., Kim, J. V., Zuo, Y., Jung, S., Littman, D. R., Dustin, M. L., and Gan, W. B. (2005) ATP mediates rapid microglial response to local brain injury in vivo. *Nat Neurosci* **8**, 752-758

83. Walter, L., Franklin, A., Witting, A., Wade, C., Xie, Y., Kunos, G., Mackie, K., and Stella, N. (2003) Nonpsychotropic cannabinoid receptors regulate microglial cell migration. *J Neurosci* **23**, 1398-1405

84. Ifuku, M., Okuno, Y., Yamakawa, Y., Izumi, K., Seifert, S., Kettenmann, H., and Noda, M. (2011) Functional importance of inositol-1,4,5-triphosphate-induced intracellular Ca2+ mobilization in galanin-induced microglial migration. *J Neurochem* **117**, 61-70

85. Rivers-Auty, J. R., Smith, P. F., and Ashton, J. C. (2014) The cannabinoid CB receptor agonist GW405833 does not ameliorate brain damage induced by hypoxia-ischemia in rats. *Neurosci Lett*

86. Savill, J., Dransfield, I., Gregory, C., and Haslett, C. (2002) A blast from the past: clearance of apoptotic cells regulates immune responses. *Nat Rev Immunol* **2**, 965-975

87. Sierra, A., Abiega, O., Shahraz, A., and Neumann, H. (2013) Janus-faced microglia: beneficial and detrimental consequences of microglial phagocytosis. *Frontiers in cellular neuroscience* **7**, 6

88. Brown, G. C., and Neher, J. J. (2014) Microglial phagocytosis of live neurons. *Nature reviews. Neuroscience* **15**, 209-216

89. Neumann, H., Kotter, M. R., and Franklin, R. J. (2009) Debris clearance by microglia: an essential link between degeneration and regeneration. *Brain : a journal of neurology* **132**, 288-295

90. Koizumi, S., Shigemoto-Mogami, Y., Nasu-Tada, K., Shinozaki, Y., Ohsawa, K., Tsuda, M., Joshi, B. V., Jacobson, K. A., Kohsaka, S., and Inoue, K. (2007) UDP acting at P2Y6 receptors is a mediator of microglial phagocytosis. *Nature* **446**, 1091-1095

91. Cardona, A. E., Pioro, E. P., Sasse, M. E., Kostenko, V., Cardona, S. M., Dijkstra, I. M., Huang, D., Kidd, G., Dombrowski, S., Dutta, R., Lee, J. C., Cook, D. N., Jung, S., Lira, S. A., Littman, D. R., and Ransohoff, R. M. (2006) Control of microglial neurotoxicity by the fractalkine receptor. *Nat Neurosci* **9**, 917-924

92. Dustin, M. L. (2012) Signaling at neuro/immune synapses. *J Clin Invest* **122**, 1149-1155

93. Lawson, L. J., Perry, V. H., Dri, P., and Gordon, S. (1990) Heterogeneity in the distribution and morphology of microglia in the normal adult mouse brain. *Neuroscience* **39**, 151-170

94. Gomez-Nicola, D., Fransen, N. L., Suzzi, S., and Perry, V. H. (2013) Regulation of microglial proliferation during chronic neurodegeneration. *J Neurosci* **33**, 2481-2493

95. Lalancette-Hebert, M., Gowing, G., Simard, A., Weng, Y. C., and Kriz, J. (2007) Selective ablation of proliferating microglial cells exacerbates ischemic injury in the brain. *J Neurosci* **27**, 2596-2605

96. Li, T., Pang, S., Yu, Y., Wu, X., Guo, J., and Zhang, S. (2013) Proliferation of parenchymal microglia is the main source of microgliosis after ischaemic stroke. *Brain* **136**, 3578-3588

97. Kamphuis, W., Orre, M., Kooijman, L., Dahmen, M., and Hol, E. M. (2012) Differential cell proliferation in the cortex of the APPswePS1dE9 Alzheimer's disease mouse model. *Glia* **60**, 615-629

98. Ding, Z., Mathur, V., Ho, P. P., James, M. L., Lucin, K. M., Hoehne, A., Alabsi, H., Gambhir, S. S., Steinman, L., Luo, J., and Wyss-Coray, T. (2014) Antiviral drug ganciclovir is a potent inhibitor of microglial proliferation and neuroinflammation. *J Exp Med* **211**, 189-198

99. Yamamoto, S., Nakajima, K., and Kohsaka, S. (2010) Macrophage-colony stimulating factor as an inducer of microglial proliferation in axotomized rat facial nucleus. *J Neurochem* **115**, 1057-1067

100. Raivich, G., Haas, S., Werner, A., Klein, M. A., Kloss, C., and Kreutzberg, G. W. (1998) Regulation of MCSF receptors on microglia in the normal and injured mouse central nervous system: a quantitative immunofluorescence study using confocal laser microscopy. *J Comp Neurol* **395**, 342-358

101. Graeber, M. B., Tetzlaff, W., Streit, W. J., and Kreutzberg, G. W. (1988) Microglial cells but not astrocytes undergo mitosis following rat facial nerve axotomy. *Neurosci Lett* **85**, 317-321

102. Streit, W. J., and Kreutzberg, G. W. (1988) Response of endogenous glial cells to motor neuron degeneration induced by toxic ricin. *J Comp Neurol* **268**, 248-263

103. Kettenmann, H. (2007) Neuroscience: the brain's garbage men. *Nature* **446**, 987-989

104. Nimmerjahn, A., Kirchhoff, F., and Helmchen, F. (2005) Resting microglial cells are highly dynamic surveillants of brain parenchyma in vivo. *Science* **308**, 1314-1318

105. Kettenmann, H., Kirchhoff, F., and Verkhratsky, A. (2013) Microglia: new roles for the synaptic stripper. *Neuron* **77**, 10-18

106. Krabbe, G., Halle, A., Matyash, V., Rinnenthal, J. L., Eom, G. D., Bernhardt, U., Miller, K. R., Prokop, S., Kettenmann, H., and Heppner, F. L. (2013) Functional impairment of microglia coincides with Beta-amyloid deposition in mice with Alzheimer-like pathology. *PLoS One* **8**, e60921

107. Gandy, S., and Heppner, F. L. (2013) Microglia as dynamic and essential components of the amyloid hypothesis. *Neuron* **78**, 575-577

108. Taylor, R. A., and Sansing, L. H. (2013) Microglial responses after ischemic stroke and intracerebral hemorrhage. *Clin Dev Immunol* **2013**, 746068

109. Bishop, N. A., Lu, T., and Yankner, B. A. (2010) Neural mechanisms of ageing and cognitive decline. *Nature* **464**, 529-535

110. Kukull, W. A., Higdon, R., Bowen, J. D., McCormick, W. C., Teri, L., Schellenberg, G. D., van Belle, G., Jolley, L., and Larson, E. B. (2002) Dementia and Alzheimer disease incidence: a prospective cohort study. *Arch Neurol* **59**, 1737-1746

111. Macciocchi, S. N., Diamond, P. T., Alves, W. M., and Mertz, T. (1998) Ischemic stroke: relation of age, lesion location, and initial neurologic deficit to functional outcome. *Arch Phys Med Rehabil* **79**, 1255-1257

112. Van Gansen, P., Pays, A., and Malherbe, L. (1985) Actin content and organization of microfilaments in primary cultures of mouse embryonic fibroblasts (in vitro ageing). *Biol Cell* **54**, 251-260

113. Wang, E., and Gundersen, D. (1984) Increased organization of cytoskeleton accompanying the aging of human fibroblasts in vitro. *Exp Cell Res* **154**, 191-202

114. Rattan, S. I. (1998) Repeated mild heat shock delays ageing in cultured human skin fibroblasts. *Biochem Mol Biol Int* **45**, 753-759

115. Trougakos, I. P., Saridaki, A., Panayotou, G., and Gonos, E. S. (2006) Identification of differentially expressed proteins in senescent human embryonic fibroblasts. *Mech Ageing Dev* **127**, 88-92

116. Streit, W. J., Sammons, N. W., Kuhns, A. J., and Sparks, D. L. (2004) Dystrophic microglia in the aging human brain. *Glia* **45**, 208-212

117. Streit, W. J., Braak, H., Xue, Q. S., and Bechmann, I. (2009) Dystrophic (senescent) rather than activated microglial cells are associated with tau pathology and likely precede neurodegeneration in Alzheimer's disease. *Acta Neuropathol* **118**, 475-485

118. Streit, W. J., and Xue, Q. S. (2012) Alzheimer's disease, neuroprotection, and CNS immunosenescence. *Front Pharmacol* **3**, 138

119. Sheng, J. G., Mrak, R. E., and Griffin, W. S. (1998) Enlarged and phagocytic, but not primed, interleukin-1 alpha-immunoreactive microglia increase with age in normal human brain. *Acta Neuropathol* **95**, 229-234

120. Damani, M. R., Zhao, L., Fontainhas, A. M., Amaral, J., Fariss, R. N., and Wong, W. T. (2011) Age-related alterations in the dynamic behavior of microglia. *Aging Cell* **10**, 263-276

121. Floden, A. M., and Combs, C. K. (2011) Microglia demonstrate age-dependent interaction with amyloid-beta fibrils. *J Alzheimers Dis* **25**, 279-293

122. Azuma, T., Witke, W., Stossel, T. P., Hartwig, J. H., and Kwiatkowski, D. J. (1998) Gelsolin is a downstream effector of rac for fibroblast motility. *EMBO J* **17**, 1362-1370

123. Hellmann-Regen, J., Kronenberg, G., Uhlemann, R., Freyer, D., Endres, M., and Gertz, K. (2013) Accelerated degradation of retinoic acid by activated microglia. *J Neuroimmunol* **256**, 1-6

124. Scheffel, J., Regen, T., Van Rossum, D., Seifert, S., Ribes, S., Nau, R., Parsa, R., Harris, R. A., Boddeke, H. W., Chuang, H. N., Pukrop, T., Wessels, J. T., Jurgens, T., Merkler,

D., Bruck, W., Schnaars, M., Simons, M., Kettenmann, H., and Hanisch, U. K. (2012) Toll-like receptor activation reveals developmental reorganization and unmasks responder subsets of microglia. *Glia* **60**, 1930-1943

125. Chromy, B. A., Nowak, R. J., Lambert, M. P., Viola, K. L., Chang, L., Velasco, P. T., Jones, B. W., Fernandez, S. J., Lacor, P. N., Horowitz, P., Finch, C. E., Krafft, G. A., and Klein, W. L. (2003) Self-assembly of Abeta(1-42) into globular neurotoxins. *Biochemistry* **42**, 12749-12760

126. Fa, M., Orozco, I. J., Francis, Y. I., Saeed, F., Gong, Y., and Arancio, O. (2010) Preparation of oligomeric beta-amyloid 1-42 and induction of synaptic plasticity impairment on hippocampal slices. *J Vis Exp*

127. Koh, J. Y., and Choi, D. W. (1987) Quantitative determination of glutamate mediated cortical neuronal injury in cell culture by lactate dehydrogenase efflux assay. *J Neurosci Methods* **20**, 83-90

128. Moore, D. (2001) Purification and concentration of DNA from aqueous solutions. *Curr Protoc Immunol* **Chapter 10**, Unit 10 11

129. Nishida, Y., Sugahara-Kobayashi, M., Takahashi, Y., Nagata, T., Ishikawa, K., and Asai, S. (2006) Screening for control genes in mouse hippocampus after transient forebrain ischemia using high-density oligonucleotide array. *J Pharmacol Sci* **101**, 52-57

130. Pannasch, U., Farber, K., Nolte, C., Blonski, M., Yan Chiu, S., Messing, A., and Kettenmann, H. (2006) The potassium channels Kv1.5 and Kv1.3 modulate distinct functions of microglia. *Mol Cell Neurosci* **33**, 401-411

131. Kronenberg, G., Wang, L. P., Synowitz, M., Gertz, K., Katchanov, J., Glass, R., Harms, C., Kempermann, G., Kettenmann, H., and Endres, M. (2005) Nestin-expressing cells divide and adopt a complex electrophysiologic phenotype after transient brain ischemia. *J Cereb Blood Flow Metab* **25**, 1613-1624

132. Santos, A. N., Ewers, M., Minthon, L., Simm, A., Silber, R. E., Blennow, K., Prvulovic, D., Hansson, O., and Hampel, H. (2012) Amyloid-beta oligomers in cerebrospinal fluid are associated with cognitive decline in patients with Alzheimer's disease. *J Alzheimers Dis* **29**, 171-176

133. Michelucci, A., Heurtaux, T., Grandbarbe, L., Morga, E., and Heuschling, P. (2009) Characterization of the microglial phenotype under specific pro-inflammatory and anti-inflammatory conditions: Effects of oligomeric and fibrillar amyloid-beta. *J Neuroimmunol* **210**, 3-12

134. Sierra, A., Gottfried-Blackmore, A. C., McEwen, B. S., and Bulloch, K. (2007) Microglia derived from aging mice exhibit an altered inflammatory profile. *Glia* **55**, 412-424

135. Njie, E. G., Boelen, E., Stassen, F. R., Steinbusch, H. W., Borchelt, D. R., and Streit, W. J. (2010) Ex vivo cultures of microglia from young and aged rodent brain reveal age-related changes in microglial function. *Neurobiol Aging*

136. Lively, S., and Schlichter, L. C. (2013) The microglial activation state regulates migration and roles of matrix-dissolving enzymes for invasion. *J Neuroinflammation* **10**, 75

137. abd-el-Basset, E., and Fedoroff, S. (1995) Effect of bacterial wall lipopolysaccharide (LPS) on morphology, motility, and cytoskeletal organization of microglia in cultures. *J Neurosci Res* **41**, 222-237

138. Morrison, H. W., and Filosa, J. A. (2013) A quantitative spatiotemporal analysis of microglia morphology during ischemic stroke and reperfusion. *J Neuroinflammation* **10**, 4

139. Kleveta, G., Borzecka, K., Zdioruk, M., Czerkies, M., Kuberczyk, H., Sybirna, N., Sobota, A., and Kwiatkowska, K. (2012) LPS induces phosphorylation of actin-regulatory proteins leading to actin reassembly and macrophage motility. *J Cell Biochem* **113**, 80-92

140. Ballestrem, C., Wehrle-Haller, B., and Imhof, B. A. (1998) Actin dynamics in living mammalian cells. *J Cell Sci* **111 (Pt 12)**, 1649-1658

141. Alberti, S., Krause, S. M., Kretz, O., Philippar, U., Lemberger, T., Casanova, E., Wiebel, F. F., Schwarz, H., Frotscher, M., Schutz, G., and Nordheim, A. (2005) Neuronal migration in the murine rostral migratory stream requires serum response factor. *Proc Natl Acad Sci U S A* **102**, 6148-6153

142. Sotiropoulos, A., Gineitis, D., Copeland, J., and Treisman, R. (1999) Signal-regulated activation of serum response factor is mediated by changes in actin dynamics. *Cell* **98**, 159-169

143. Mokalled, M. H., Johnson, A., Kim, Y., Oh, J., and Olson, E. N. (2010) Myocardin-related transcription factors regulate the Cdk5/Pctaire1 kinase cascade to control neurite outgrowth, neuronal migration and brain development. *Development* **137**, 2365-2374

144. Kronenberg, G., Gertz, K., Baldinger, T., Kirste, I., Eckart, S., Yildirim, F., Ji, S., Heuser, I., Schrock, H., Hortnagl, H., Sohr, R., Djoufack, P. C., Juttner, R., Glass, R., Przesdzing, I., Kumar, J., Freyer, D., Hellweg, R., Kettenmann, H., Fink, K. B., and Endres, M. (2010) Impact of actin filament stabilization on adult hippocampal and olfactory bulb neurogenesis. *J Neurosci* **30**, 3419-3431

145. Stern, S., Haverkamp, S., Sinske, D., Tedeschi, A., Naumann, U., Di Giovanni, S., Kochanek, S., Nordheim, A., and Knoll, B. (2013) The Transcription Factor Serum Response Factor Stimulates Axon Regeneration through Cytoplasmic Localization and Cofilin Interaction. *J Neurosci* **33**, 18836-18848

146. Beck, H., Flynn, K., Lindenberg, K. S., Schwarz, H., Bradke, F., Di Giovanni, S., and Knoll, B. (2012) Serum Response Factor (SRF)-cofilin-actin signaling axis modulates mitochondrial dynamics. *Proc Natl Acad Sci U S A* **109**, E2523-2532

147. Zhang, Y. T., Ouyang, D. Y., Xu, L. H., Zha, Q. B., and He, X. H. (2013) Formation of cofilin-actin rods following cucurbitacin-B-induced actin aggregation depends on Slingshot homolog 1-mediated cofilin hyperactivation. *J Cell Biochem* **114**, 2415-2429

148. Eswarappa, S. M., Pareek, V., and Chakravortty, D. (2008) Role of actin cytoskeleton in LPS-induced NF-kappaB activation and nitric oxide production in murine macrophages. *Innate Immun* **14**, 309-318

149. Yeramian, A., Martin, L., Serrat, N., Arpa, L., Soler, C., Bertran, J., McLeod, C., Palacin, M., Modolell, M., Lloberas, J., and Celada, A. (2006) Arginine transport via cationic amino acid transporter 2 plays a critical regulatory role in classical or alternative activation of macrophages. *J Immunol* **176**, 5918-5924

150. Baydoun, A. R., Bogle, R. G., Pearson, J. D., and Mann, G. E. (1993) Arginine uptake and metabolism in cultured murine macrophages. *Agents Actions* **38 Spec No**, C127-129

151. Zharikov, S. I., Sigova, A. A., Chen, S., Bubb, M. R., and Block, E. R. (2001) Cytoskeletal regulation of the L-arginine/NO pathway in pulmonary artery endothelial cells. *Am J Physiol Lung Cell Mol Physiol* **280**, L465-473

152. Paakkari, I., and Lindsberg, P. (1995) Nitric oxide in the central nervous system. *Ann Med* **27**, 369-377

153. Forstermann, U., and Sessa, W. C. (2012) Nitric oxide synthases: regulation and function. *Eur Heart J* **33**, 829-837, 837a-837d

154. Tomimoto, H., Akiguchi, I., Wakita, H., Nakamura, S., and Kimura, J. (1994) Histochemical demonstration of membranous localization of endothelial nitric oxide synthase in endothelial cells of the rat brain. *Brain Res* **667**, 107-110

155. Htain, W. W., Leong, S. K., and Ling, E. A. (1997) In vivo expression of inducible nitric oxide synthase in supraventricular amoeboid microglial cells in neonatal BALB/c and athymic mice. *Neurosci Lett* **223**, 53-56

156. Schleicher, M., Brundin, F., Gross, S., Muller-Esterl, W., and Oess, S. (2005) Cell cycle-regulated inactivation of endothelial NO synthase through NOSIP-dependent targeting to the cytoskeleton. *Mol Cell Biol* **25**, 8251-8258

157. Stanley, A. C., and Lacy, P. (2010) Pathways for cytokine secretion. *Physiology (Bethesda)* **25**, 218-229

158. Eder, C. (2009) Mechanisms of interleukin-1beta release. *Immunobiology* **214**, 543-553

159. van den Berg, A., Freitas, J., Keles, F., Snoek, M., van Marle, J., Jansen, H. M., and Lutter, R. (2006) Cytoskeletal architecture differentially controls post-transcriptional processing of IL-6 and IL-8 mRNA in airway epithelial-like cells. *Exp Cell Res* **312**, 1496-1506

160. Shurety, W., Merino-Trigo, A., Brown, D., Hume, D. A., and Stow, J. L. (2000) Localization and post-Golgi trafficking of tumor necrosis factor-alpha in macrophages. *J Interferon Cytokine Res* **20**, 427-438

161. Gordon, S. (2003) Alternative activation of macrophages. *Nat Rev Immunol* **3**, 23-35

162. Aguzzi, A., Barres, B. A., and Bennett, M. L. (2013) Microglia: scapegoat, saboteur, or something else? *Science* **339**, 156-161

163. Lalancette-Hebert, M., Swarup, V., Beaulieu, J. M., Bohacek, I., Abdelhamid, E., Weng, Y. C., Sato, S., and Kriz, J. (2012) Galectin-3 is required for resident microglia activation and proliferation in response to ischemic injury. *J Neurosci* **32**, 10383-10395

164. Ueno, M., Fujita, Y., Tanaka, T., Nakamura, Y., Kikuta, J., Ishii, M., and Yamashita, T. (2013) Layer V cortical neurons require microglial support for survival during postnatal development. *Nature neuroscience* **16**, 543-551

165. Kawahara, K., Gotoh, T., Oyadomari, S., Kajizono, M., Kuniyasu, A., Ohsawa, K., Imai, Y., Kohsaka, S., Nakayama, H., and Mori, M. (2001) Co-induction of argininosuccinate synthetase, cationic amino acid transporter-2, and nitric oxide synthase in activated murine microglial cells. *Brain Res Mol Brain Res* **90**, 165-173

166. Maier, E., Duschl, A., and Horejs-Hoeck, J. (2012) STAT6-dependent and -independent mechanisms in Th2 polarization. *Eur J Immunol* **42**, 2827-2833

167. Nelms, K., Keegan, A. D., Zamorano, J., Ryan, J. J., and Paul, W. E. (1999) The IL-4 receptor: signaling mechanisms and biologic functions. *Annu Rev Immunol* **17**, 701-738

168. Gordon, S., and Martinez, F. O. (2010) Alternative activation of macrophages: mechanism and functions. *Immunity* **32**, 593-604

169. Schwartz, M., Kipnis, J., Rivest, S., and Prat, A. (2013) How do immune cells support and shape the brain in health, disease, and aging? *J Neurosci* **33**, 17587-17596

170. Cross, A. K., and Woodroofe, M. N. (1999) Chemokines induce migration and changes in actin polymerization in adult rat brain microglia and a human fetal microglial cell line in vitro. *J Neurosci Res* **55**, 17-23

171. Ohsawa, K., Imai, Y., Kanazawa, H., Sasaki, Y., and Kohsaka, S. (2000) Involvement of Iba1 in membrane ruffling and phagocytosis of macrophages/microglia. *J Cell Sci* **113 (Pt 17)**, 3073-3084

172. Goncalves, A. F., Dias, N. G., Moransard, M., Correia, R., Pereira, J. A., Witke, W., Suter, U., and Relvas, J. B. (2010) Gelsolin is required for macrophage recruitment during remyelination of the peripheral nervous system. *Glia* **58**, 706-715

173. Fields, R. D., and Burnstock, G. (2006) Purinergic signalling in neuron-glia interactions. *Nat Rev Neurosci* **7**, 423-436

174. Patel, A. R., Ritzel, R., McCullough, L. D., and Liu, F. (2013) Microglia and ischemic stroke: a double-edged sword. *Int J Physiol Pathophysiol Pharmacol* **5**, 73-90

175. Ribes, S., Ebert, S., Regen, T., Agarwal, A., Tauber, S. C., Czesnik, D., Spreer, A., Bunkowski, S., Eiffert, H., Hanisch, U. K., Hammerschmidt, S., and Nau, R. (2010) Toll-like receptor stimulation enhances phagocytosis and intracellular killing of nonencapsulated and encapsulated Streptococcus pneumoniae by murine microglia. *Infect Immun* **78**, 865-871

176. Flannagan, R. S., Harrison, R. E., Yip, C. M., Jaqaman, K., and Grinstein, S. (2010) Dynamic macrophage "probing" is required for the efficient capture of phagocytic targets. *J Cell Biol* **191**, 1205-1218

177. Arora, P. D., Glogauer, M., Kapus, A., Kwiatkowski, D. J., and McCulloch, C. A. (2004) Gelsolin mediates collagen phagocytosis through a rac-dependent step. *Mol Biol Cell* **15**, 588-599

178. Kielian, T., Mayes, P., and Kielian, M. (2002) Characterization of microglial responses to Staphylococcus aureus: effects on cytokine, costimulatory molecule, and Toll-like receptor expression. *J Neuroimmunol* **130**, 86-99

179. Hoffmann, A., Kann, O., Ohlemeyer, C., Hanisch, U. K., and Kettenmann, H. (2003) Elevation of basal intracellular calcium as a central element in the activation of brain macrophages (microglia): suppression of receptor-evoked calcium signaling and control of release function. *J Neurosci* **23**, 4410-4419

180. McLarnon, J. G., Choi, H. B., Lue, L. F., Walker, D. G., and Kim, S. U. (2005) Perturbations in calcium-mediated signal transduction in microglia from Alzheimer's disease patients. *J Neurosci Res* **81**, 426-435

181. Nakamura, M., Sunagawa, M., Kosugi, T., and Sperelakis, N. (2000) Actin filament disruption inhibits L-type Ca(2+) channel current in cultured vascular smooth muscle cells. *Am J Physiol Cell Physiol* **279**, C480-487

182. Siddiqui, T. A., Lively, S., Vincent, C., and Schlichter, L. C. (2012) Regulation of podosome formation, microglial migration and invasion by Ca(2+)-signaling molecules expressed in podosomes. *J Neuroinflammation* **9**, 250

183. Monif, M., Reid, C. A., Powell, K. L., Smart, M. L., and Williams, D. A. (2009) The P2X7 receptor drives microglial activation and proliferation: a trophic role for P2X7R pore. *J Neurosci* **29**, 3781-3791

184. Luongo, L., Guida, F., Imperatore, R., Napolitano, F., Gatta, L., Cristino, L., Giordano, C., Siniscalco, D., Di Marzo, V., Bellini, G., Petrelli, R., Cappellacci, L., Usiello, A., de Novellis, V., Rossi, F., and Maione, S. (2014) The A1 adenosine receptor as a new player in microglia physiology. *Glia* **62**, 122-132

185. Dolga, A. M., Letsche, T., Gold, M., Doti, N., Bacher, M., Chiamvimonvat, N., Dodel, R., and Culmsee, C. (2012) Activation of KCNN3/SK3/K(Ca)2.3 channels attenuates enhanced calcium influx and inflammatory cytokine production in activated microglia. *Glia* **60**, 2050-2064

186. Light, A. R., Wu, Y., Hughen, R. W., and Guthrie, P. B. (2006) Purinergic receptors activating rapid intracellular Ca increases in microglia. *Neuron Glia Biol* **2**, 125-138

187. Hardy, J. A., and Higgins, G. A. (1992) Alzheimer's disease: the amyloid cascade hypothesis. *Science* **256**, 184-185

188. Rosenblum, W. I. (2013) Why Alzheimer trials fail: removing soluble oligomeric beta amyloid is essential, inconsistent, and difficult. *Neurobiol Aging*

189. Shankar, G. M., Li, S., Mehta, T. H., Garcia-Munoz, A., Shepardson, N. E., Smith, I., Brett, F. M., Farrell, M. A., Rowan, M. J., Lemere, C. A., Regan, C. M., Walsh, D. M., Sabatini, B. L., and Selkoe, D. J. (2008) Amyloid-beta protein dimers isolated directly from Alzheimer's brains impair synaptic plasticity and memory. *Nat Med* **14**, 837-842

190. Lindberg, C., Selenica, M. L., Westlind-Danielsson, A., and Schultzberg, M. (2005) Beta-amyloid protein structure determines the nature of cytokine release from rat microglia. *J Mol Neurosci* **27**, 1-12

191. Pan, X. D., Zhu, Y. G., Lin, N., Zhang, J., Ye, Q. Y., Huang, H. P., and Chen, X. C. (2011) Microglial phagocytosis induced by fibrillar beta-amyloid is attenuated by oligomeric beta-amyloid: implications for Alzheimer's disease. *Mol Neurodegener* **6**, 45

192. Maezawa, I., Zimin, P. I., Wulff, H., and Jin, L. W. (2011) Amyloid-beta protein oligomer at low nanomolar concentrations activates microglia and induces microglial neurotoxicity. *J Biol Chem* **286**, 3693-3706

193. Sondag, C. M., Dhawan, G., and Combs, C. K. (2009) Beta amyloid oligomers and fibrils stimulate differential activation of primary microglia. *J Neuroinflammation* **6**, 1

194. Gan, L., Ye, S., Chu, A., Anton, K., Yi, S., Vincent, V. A., von Schack, D., Chin, D., Murray, J., Lohr, S., Patthy, L., Gonzalez-Zulueta, M., Nikolich, K., and Urfer, R. (2004) Identification of cathepsin B as a mediator of neuronal death induced by Abeta-activated microglial cells using a functional genomics approach. *J Biol Chem* **279**, 5565-5572

195. Yang, C. N., Shiao, Y. J., Shie, F. S., Guo, B. S., Chen, P. H., Cho, C. Y., Chen, Y. J., Huang, F. L., and Tsay, H. J. (2011) Mechanism mediating oligomeric Abeta clearance by naive primary microglia. *Neurobiol Dis* **42**, 221-230

196. Halle, A., Hornung, V., Petzold, G. C., Stewart, C. R., Monks, B. G., Reinheckel, T., Fitzgerald, K. A., Latz, E., Moore, K. J., and Golenbock, D. T. (2008) The NALP3 inflammasome is involved in the innate immune response to amyloid-beta. *Nat Immunol* **9**, 857-865

197. Heneka, M. T., Kummer, M. P., Stutz, A., Delekate, A., Schwartz, S., Vieira-Saecker, A., Griep, A., Axt, D., Remus, A., Tzeng, T. C., Gelpi, E., Halle, A., Korte, M., Latz, E., and Golenbock, D. T. (2013) NLRP3 is activated in Alzheimer's disease and contributes to pathology in APP/PS1 mice. *Nature* **493**, 674-678

198. Streit, W. J., and Xue, Q. S. (2013) Microglial senescence. *CNS Neurol Disord Drug Targets* **12**, 763-767

199. Njie, E. G., Boelen, E., Stassen, F. R., Steinbusch, H. W., Borchelt, D. R., and Streit, W. J. (2012) Ex vivo cultures of microglia from young and aged rodent brain reveal age-related changes in microglial function. *Neurobiol Aging* **33**, 195 e191-112

200. Yirmiya, R., and Goshen, I. (2011) Immune modulation of learning, memory, neural plasticity and neurogenesis. *Brain Behav Immun* **25**, 181-213

201. Long, J. M., Kalehua, A. N., Muth, N. J., Calhoun, M. E., Jucker, M., Hengemihle, J. M., Ingram, D. K., and Mouton, P. R. (1998) Stereological analysis of astrocyte and microglia in aging mouse hippocampus. *Neurobiol Aging* **19**, 497-503

202. Rodriguez, J. J., Noristani, H. N., Hilditch, T., Olabarria, M., Yeh, C. Y., Witton, J., and Verkhratsky, A. (2013) Increased densities of resting and activated microglia in the dentate gyrus follow senile plaque formation in the CA1 subfield of the hippocampus in the triple transgenic model of Alzheimer's disease. *Neurosci Lett* **552**, 129-134

203. Mouton, P. R., Long, J. M., Lei, D. L., Howard, V., Jucker, M., Calhoun, M. E., and Ingram, D. K. (2002) Age and gender effects on microglia and astrocyte numbers in brains of mice. *Brain Res* **956**, 30-35

204. Hayakawa, N., Kato, H., and Araki, T. (2007) Age-related changes of astorocytes, oligodendrocytes and microglia in the mouse hippocampal CA1 sector. *Mech Ageing Dev* **128**, 311-316

205. Adachi, M., Abe, M., Sasaki, T., Kato, H., Kasahara, J., and Araki, T. (2010) Role of inducible or neuronal nitric oxide synthase in neurogenesis of the dentate gyrus in aged mice. *Metab Brain Dis* **25**, 419-424

206. Dirnagl, U. (2006) Bench to bedside: the quest for quality in experimental stroke research. *J Cereb Blood Flow Metab* **26**, 1465-1478

8. EIDESSTATTLICHE VERSICHERUNG

„Ich, Ria Uhlemann, versichere an Eides statt durch meine eigenhändige Unterschrift, dass ich die vorgelegte Dissertation mit dem Thema: „Essential role of actin filament dynamics in microglia activation“ selbstständig und ohne nicht offengelegte Hilfe Dritter verfasst und keine anderen als die angegebenen Quellen und Hilfsmittel genutzt habe.

Alle Stellen, die wörtlich oder dem Sinne nach auf Publikationen oder Vorträgen anderer Autoren beruhen, sind als solche in korrekter Zitierung (siehe „Uniform Requirements for Manuscripts (URM)“ des ICMJE -*www.**icmje**.org*) kenntlich gemacht. Die Abschnitte zu Methodik (insbesondere praktische Arbeiten, Laborbestimmungen, statistische Aufarbeitung) und Resultaten (insbesondere Abbildungen, Graphiken und Tabellen) entsprechen den URM (s.o) und werden von mir verantwortet.

Meine Anteile an etwaigen Publikationen zu dieser Dissertation entsprechen denen, die in der untenstehenden gemeinsamen Erklärung mit dem/der Betreuer/in, angegeben sind. Sämtliche Publikationen, die aus dieser Dissertation hervorgegangen sind und bei denen ich Autor bin, entsprechen den URM (s.o) und werden von mir verantwortet.

Die Bedeutung dieser eidesstattlichen Versicherung und die strafrechtlichen Folgen einer unwahren eidesstattlichen Versicherung (§156,161 des Strafgesetzbuches) sind mir bekannt und bewusst.“

_____ _____

Datum Dipl.-Biol. Ria Uhlemann

9. ANTEILSERKLÄRUNG AN ERFOLGTEN PUBLIKATIONEN

Während ihrer Doktorarbeit hatte Ria Uhlemann Anteil an folgenden Publikationen:

Publikation 1:

Autoren:	Julian Hellmann-Regen, Golo Kronenberg, Ria Uhlemann, Dorette Freyer, Matthias Endres, Karen Gertz
Titel:	Accelerated degradation of retinoic acid by activated microglia.
Zeitschrift:	Journal of Neuroimmunology
Erscheinungsjahr:	2013, 256(1-2):1-6.
Beitrag:	25% eigener Anteil Neben der Isolation und Kultivierung der primären postnatalen Mikrogliazellen wurden diese vom Promovenden gemäß dem Behandlungsschema aktiviert und für nachfolgende Experimente geerntet.

Publikation 2:

Autoren:	Julian Hellmann-Regen, Karen Gertz, Ria Uhlemann, Michael Colla, Matthias Endres, Golo Kronenberg
Titel:	Retinoic acid as target for local pharmacokinetic interaction with modafinil in neural cells.
Zeitschrift:	European Archives of Psychiatry and Clinical Neuroscience
Erscheinungsjahr:	2012, 262(8):697-704
Beitrag:	20% eigener Anteil Neben der Kultur der Zelllinie GL261 wurden die Interventionen gemäß dem Behandlungsschema sowie die Untersuchung zum Proliferationsverhalten der Zellen vom Promovenden durchgeführt.

_____

Unterschrift, Datum und Stempel Prof. Dr. Golo Kronenberg

_____

Unterschrift Ria Uhlemann

10. RÉSUMÉ

Mein Lebenslauf wird aus datenschutzrechtlichen Gründen in der elektronischen Version meiner Arbeit nicht veröffentlicht.

11. ACKNOWLEDGEMENTS

I would like to sincerely thank:

- My supervisor Prof. Dr. Golo Kronenberg. I am grateful for his support, advice and many discussions throughout the project.

- Prof. Dr. Matthias Endres for giving me the opportunity to work in his group on this exciting topic.

- My colleagues Dr. Karen Gertz, Dr. Tobias Schwarz, Dr. Wolfgang Böhmerle, Dr. Dorette Freyer, Ingo Przesdzing, Bettina Herrmann, Melanie Kroh, Susann Eigel, Stefanie Balz, Valerié Boujon, who at various stages have supported me in technical and scientific matters.

- Our collaborators Dr. Christiane Nolte and Prof. Dr. Helmut Kettenmann, Max Delbrück Center for Molecular Medicine, Berlin-Buch.

- Prof. Dr. Uwe-Karsten Hanisch at the University Medical Center Göttingen for providing me the protocol of primary adult microglia cultivation.

- The International Graduate Program "Medical Neurosciences" of the Charité-Universitätsmedizin Berlin.

I am very grateful to Theodor and Thomas for their patience to endure all the challenging periods during the last years. I would like to express my gratitude to my parents Lothar and Heidrun Uhlemann, who always supported me and my small family. I am obliged to Christine and Dr. Roland Göttert for flexible childcare throughout my doctoral thesis.

This list would grow even larger, if I were to include every single person who has been helpful during my doctoral thesis. Thanks to all of you.